Title

Microbial Interactions with Water Contaminants and Surfaces: Applications Ranging from Bioremediation to Biofouling Prevention

Author

Polasko, Alexandra LaPat

Publication Date

2021

Peer reviewed|Thesis/dissertation

UNIVERSITY OF CALIFORNIA

Los Angeles

Microbial Interactions with Water Contaminants and Surfaces: Applications Ranging from Bioremediation to Biofouling Prevention

A dissertation submitted in partial satisfaction of the

requirements for the degree Doctor of Philosophy

in Civil Engineering

by

Alexandra LaPat Polasko

2021

ABSTRACT OF THE DISSERTATION

Microbial Interactions with Water Contaminants and Surfaces: Applications Ranging from Bioremediation to Biofouling Prevention

by

Alexandra LaPat Polasko

Doctor of Philosophy in Civil Engineering

University of California, Los Angeles, 2021

Professor Shaily Mahendra, Chair

While microorganisms drive nearly all of the Earth's major biogeochemical cycles, a subset of those microorganisms exert a spectrum of deleterious effects on health, environmental, and industrial processes. This broad range of potential benefits and pitfalls, makes it critical to properly characterize and manage this microbial world. This dissertation describes original research on the treatment of contaminated water using biodegradation by bacterial cultures as well as visualizing and quantifying pathogenic biofilms on surfaces.

Solvent stabilizers, such as 1,4-dioxane, are frequently detected in water resources and often co-occur with chlorinated volatile organic compounds (CVOCs). Both classes of trace organic compounds (TrOCs) are persistent in the environment and have carcinogenic properties.

First, a microbial community comprised of the anaerobic chlorinated ethene-degrading consortium (KB-1) and aerobic bacterial strain, *Pseudonocardia dioxanivorans* CB1190, was formulated in a defined medium and verified to biodegrade mixtures of chlorinated ethenes and 1,4-dioxane under varying redox conditions. Further, CB1190 was shown to survive 100 continuous days of anaerobic incubation and multiple anaerobic-aerobic cycles. After aeration, it biodegraded 1,4-dioxane rapidly because minimal loss or lag occurred in the induction of the genes, *dxmB* and *aldH*, which code for key enzymes in the 1,4-dioxane degradation pathway.

While vinyl chloride (VC) and cis-1,2-dichloroethene (cDCE) are inhibitors of 1,4-dioxane biodegradation, surprisingly both compounds were degraded by CB1190. Increasing concentrations of VC decreased 1,4-dioxane biodegradation rates, whereas increasing 1,4-dioxane did not have as significant of an effect on VC biodegradation. VC was found to be the strongest inhibitory CVOC with respect to 1,4-dioxane biodegradation, but it was also utilized as a source of carbon and energy to support CB1190's growth. Metabolic flux analyses confirmed that VC-derived intermediates were incorporated into CB1190's central metabolism.

A pilot-scale project utilizing *in situ* aerobic biostimulation and bioaugmentation with CB1190 demonstrated successful removal of CVOCs and 1,4-dioxane from groundwater. Biostimulation (e.g., air sparging) resulted in a significant CVOC removal, but limited 1,4-dioxane removal. When CB1190 culture was added along with air sparging, the concentrations of 1,4-dioxane and CVOCs, such as cDCE and VC, substantially decreased. This signifies the

importance of establishing appropriate microorganisms in the subsurface for the remediation of contaminated environments.

Contrastingly, microbial adhesion to medical tubing surfaces is undesirable due to adverse patient health outcomes. To mitigate biofilm formation, polysiloxane materials coated with a hydrophilic, zwitterionic polysulfobetaine polymer were designed. These samples were systematically tested against bacterial and fungal agents in static and flow conditions. Additionally, a non-strain-specific protocol combining four microbiological assays was developed to accurately quantify cellular and extracellular components attached to catheter surfaces. The efficacy of this multipronged approach was demonstrated using four pathogenic, clinical isolates, two types of silicone catheters *in vitro*, and indwelling patient catheters.

A quantitative understanding of microbial interactions with chemicals and materials will be valuable for improved environmental bioremediation systems as well as limiting biofilms on medically relevant surfaces.

The dissertation of Alexandra LaPat Polasko is approved.

Patrick Allard

Sanjay K. Mohanty

Jennifer Ayla Jay

Shaily Mahendra, Committee Chair

University of California, Los Angeles

2021

Table of Contents

List of Figures

List of Tables

Acknowledgements

First, I would like to express my deep and sincere gratitude to my advisor and committee chair, Dr. Shaily Mahendra. I remember the first time I met Dr. Mahendra in Boelter Hall and the combination of her enthusiasm, compassion, and immense knowledge was inspiring then and is still to this day. Her guidance has opened my eyes and mind to parts of the microbial world I didn't know existed all the while being incredibly patient and motivating. I could not have dreamed of having a better mentor and advisor during my PhD and can honestly say that I would not be an engineer without her continued support.

I would like to also thank my committee members Professor Patrick Allard, Professor Sanjay Mohanty, and Professor Jennifer A. Jay. Each of them was an integral part of my PhD and provided valuable insights for my research and future career. From developing gas chromatography analytical methods with Dr. Allard, to bacterial enumeration methods with Dr. Mohanty's, to sharing my teaching successes and challenges in Dr. Jay's office, I treasure each memory and lesson learned.

I would like to thank Dr. Richard Kaner and his students for introducing me to the work of surface modifications and polymer science. What I thought would be a 2-month collaboration has turned into a two-year collaboration with two publications. Your guidance has been helpful in my research as well as my professional development. Also, I will never look at a catheter the same again.

The world of metabolomics was a faraway land before I met Dr. Junyoung Park and his doctoral student Keunseok Park. Thank you for your guidance on how to best design experiments for metabolomics as well as conducting the metabolomics analytical analyses. I

truly believe that this exciting technology will have lasting impacts on the environmental engineering field.

I would like to thank Drs. Phillip Gedalanga, Shu Zhang, and Peerapong Pornwongthong who began exploring the impact of chlorinated solvents on 1,4-dioxane biodegradation, which was foundational for the research presented in Chapter 2 and 4.

The work presented in this dissertation would not have happened without the tremendous time and energy provided by my incredible undergraduate researchers. Thank you, Sophia Wang, for being my first undergraduate research student and being an integral part of revealing CB1190's unique ability to survive under low oxygen conditions. Alessandro Zulli and Dominic Robolino, without you, we would not know that CB1190 can withstand 100 days of anaerobic incubation and anaerobic-aerobic cycling. Thank you for all those hours at the gas chromatograph flame ionize detector and mass spectrometer. Thank you, Ivy Kwok and Katherine Tsai, you both were my co-pilots in identifying CB1190's ability to biodegrade vinyl chloride and honestly, my lifeline during the pandemic. I am so grateful.

I truly believe it takes a village to complete a PhD and I am so thankful to my lab members for providing the support to get through the many challenges of lab work and life. I would like to thank Drs. Yu Miao and Nicholas Johnson for the constant support and willingness to analyze data with me any time, day or night. Also, I will never forget how to clean an ion source for the rest of my life! I am so grateful also to Dr. Victoria Whitener, Dr. Shashank Kalra, Dr. Megan Rugh, Anjali Lothe, Yifan Gao, Catherine Clark, and Christina Najm for their valuable discussion and insights for approaching my research obstacles as they arose. I would also like to give a special thanks to Vera Smirnova, Annesh Borthakur, Katherine Tsai, and Sara Alkidim for

being integral to our research on contaminants in Lake Baikal. I never dreamed of getting so far on this project and it is because of you all.

I would like to thank everyone in the Department of Civil and Environmental Engineering who have guided me through all of the less glamorous, but nonetheless crucial administrative tasks necessary to conduct research at UCLA as a doctoral student. Jesse Dieker, Dr. Vanessa Thulsiraj, Mimi Baik, Stacey Tran Fong, Reba Glover, Dr. Eric Ahlberg, Dr. Ben Rossi, Helen Weary, Dylan Giron, and Paula Columbia.

I would like to thank Dr. Elizabeth Erin Mack of Corteva Agriscience, Dr. Claudia Walecka-Hutchison of The Dow Chemical Company, and Dr. Rula Deeb of Geosyntec Consultants for their input and championing my co-culture research. I would also like to thank Professor Jens Blotevogel of Colorado State University, Fort Collins for his guidance and suggestions with respect to measuring chlorinated solvents. I am also sincerely grateful to Dr. Sandra Dworatzek of SiREM and Professor Elizabeth Edwards of the University of Toronto for providing KB-1 and *Geobacter lovleyi*, respectively.

This research was supported by Strategic Environmental Research and Development Program (SERDP) Contracts ER-2300, ER-2713, and ER-2718. National Science Foundation (NSF) Faculty Early Career Development (CAREER) award to Professor Mahendra, Dow Chemical Company [contract #244633], DuPont Corporate Remediation Group [contract #MA-03653-13], DuPont Young Professor Award to Professor Mahendra, Paul L. Busch Award to Professor Mahendra, Matrix New World Engineering, Geosyntec, UCLA Sustainable Grand Challenges, and UCLA Civil and Environmental Engineering Department. Studies in this research were performed in a renovated collaboratory funded by the NSF Grant Number 0963183, which was awarded under the American Recovery and Reinvestment Act of 2009

(ARRA). Additionally, I would like to thank all the companies and organizations that provided scholarships to help me through graduate school including, Eugene V. Cota-Robles, Brown and Caldwell, American Water Works Association, Hydrophilix, New England Biolabs and UCLA's Center for the Advancement of Teaching.

Lastly, I would like to thank my husband, Michael Todd, who listened to my lab woes and victories every day and championed me every step of the way. Thank you to all my friends who have become family over these years and supported me through my journey to UCLA and now beyond. Mom, not a day goes by that I don't thank the heavens for having the gift of being able to share a passion for environmental engineering and bioremediation. Dad, thank you for introducing me to the world of cycling, which was the main way I stayed sane through my PhD. And to Grandma Jackie, I wouldn't be here today if wasn't for your constant encouragement and unconditional love. "When the long road is the right road." Love you all, always.

Vita

EDUCATION

M.S., Civil & Environmental Engineering, University of California, Los Angeles	2017
B.S., Environmental Science, University of California, Berkeley	2015

PUBLICATIONS

*Polasko, A., *Ramos, P., Kaner, R. B., and S. Mahendra. A multipronged approach for systematic *in vitro* quantification of catheter-associated biofilms. *Journal of Hazardous Materials*, 2021, 100032. *authors contributed equally to this work.

Miao, Y., Heintz, M., Bell, C. H., Johnson, N. W., Polasko, A., Gedalanga, P. B., Favero, D. and Mahendra, S. Profiling microbial community structures in biostimulation and bioaugmentation strategies for treating 1,4-dioxane contaminated groundwater. *Journal of Hazardous Materials*, 2021, 124457.

Polasko, A., A. Zulli, P. Gedalanga, P. Pornwongthong, and S. Mahendra. A mixed microbial community for the biodegradation of chlorinated ethenes and 1,4-dioxane. *Environmental Science & Technology Letters,* 2019, 6: 49-54.

Zhao, L., Lu, X., Polasko, A., Johnson, N.W., Miao, Y., Yang, Z., Mahendra, S., and Gu, B. Co-contaminant effects on 1,4-dioxane biodegradation in packed soil column flow-through systems. *Environmental Pollution*, 2018, 243: 573-581.

Safdari, M.S., Kariminia, H.R., Rahmati, M., Fazlollahi, F., Polasko, A., Mahendra, S., Wilding, W.V. and Fletcher, T.H. Development of bioreactors for comparative study of natural attenuation, biostimulation, and bioaugmentation of petroleum-hydrocarbon contaminated soil. *Journal of Hazardous Materials*, 2018, 342: 270-278.

Mao, X., Polasko, A. and Alvarez-Cohen, L. The effects of sulfate reduction on TCE dechlorination by *Dehalococcoides* containing microbial communities. *Applied and Environmental Microbiology,* 2017, 83:1-28.

Mao, X., Stenuit, B., Polasko, A. and Alvarez-Cohen, L. Efficient metabolic exchange and electron transfer within a syntrophic TCE degrading co-culture of *Dehalococcoides mccartyi* 195 and *Syntrophomonas wolfei*. *Applied and Environmental Microbiology,* 2015, 81: 2015-2024.

Ziv-El, M., Popat, S.C., Parameswaran, P., Kang, D.-W. Polasko, A., Halden, R.U., Rittmann, B.E. and Krajmalnik-Brown, R. Using electron balances and molecular techniques to assess trichoroethene-induced shifts to a dechlorinating microbial community. *Biotechnology and Bioengineering*, 2012, 109: 2230-2239.

HONORS AND AWARDS

2021	UCLA Distinguished Teaching Award for Teaching Assistants
2015-2020	Eugene V. Cota Robles 4-year Grant ($50,000 + tuition/fees)
2019-2020	Hydrophilix Industry-Sponsored Research Fellowship ($4,500)
2019	Center for Advancement of Teaching Classroom Mini-Grant ($250)
2019	American Water Works Association Drinking Water Fellowship ($5,000)
2018	Emerging Contaminants Conference Poster Presentation Award, 1st Place
2017	UCLA Campus Wide Research Pitch Competition (GradSlam), 3rd Place
2017	American Society of Microbiology Agar Art Finalist
2016	Brown and Caldwell Women in Leadership Fellowship ($5,000)
2016	New England Biolabs National Passion in Science Fellowship ($1,000)
2016	National Science Foundation Graduate Research Fellowship, Honorable Mention
2015	Malcom R. Stacey Research Fellowship ($5,000)
2015	Charlene Conrad Liebau Prize for Undergraduate Research, Honorable Mention
2015	Len Assante National Groundwater Research Fellowship ($5,000)
2011	AMEC Consulting Firm Student Scholarship Award ($5,000)
2011	Stockholm Junior Water Prize, Arizona State Winner

PATENTS

Shaily Mahendra and Alexandra L. Polasko. Anaerobic-Aerobic Bioremediation of Contaminated Water. Filed November 21st, 2018 (US & International Patent Pending).

Richard B. Kaner, Dayong Chen, Brian T. McVerry, Ethan Rao, and Alexandra L. Polasko. The Regents of the University of California, Hydrophilix. Biofouling Resistant Coatings and Methods of Making and Using the Same. United States patent US 10,729822. 2020 Aug.

Chapter 1 Introduction and Objectives

1.1 Objectives and Scope

While microorganisms support the existence of all higher trophic life forms, approximately one in a billion have been identified as pathogenic to humans and produce deadly consequences. With such a broad range of potential benefits and pitfalls, it has become critical for humans to properly utilize and manage this microbial world.(1) My research focuses on two such techniques, using microorganisms to degrade harmful pollutants and preventing malignant ones from forming potentially detrimental biofilms on medical surfaces. Microbial interactions with pollutants can result in water purification via biodegradation processes. These processes are attractive for their sustainability, efficiency, low energy inputs, and low waste outputs. The contaminants, 1,4-dioxane and chlorinated volatile organic compounds (CVOCs) have been raising concerns over the past several decades because of increasing widespread detection in surface and groundwaters and an improved toxicological understanding of their impact on human health.(2) Removal of these industrial chemicals, which are human carcinogens, is possible via microbial degradation; but is complicated by the fact that these industrial pollutants often occur together at varying concentrations and in diverse sub-subsurface biogeochemical conditions such as oxygen levels, pH, salinity, organic carbon, and major nutrient availability.(3) It is critical to understand the impact of these factors as to build the most effective natural and engineered microbial systems for the removal of these harmful water pollutants. Microbial interactions with surfaces can result in undesirable biofilms that can lead to infections and biofouling. Biofilms form when replicating microbial cells secrete extracellular polymeric substances that contain an insoluble mixture of proteins and polysaccharides. This three-dimensional gelatinous matrix can provide pathogenic cells an enhanced environment via regulated pH, osmolarity, nutrients, and sheer force as well as reduce the diffusion rate of antimicrobials through the matrix, thus

rendering the cells within the biofilm significantly more resistant than their planktonic counterparts. Furthermore, biofilms are linked to recurring infections, and already-formed biofilms are extremely difficult to resolve. The biofilm formation cascade is initiated by planktonic bacterial cell adhesion to a surface. Without initial attachment, the biofilm formation could be prevented or reduced. As medical device surfaces are a nidus for biofilm growth, there is a need for a clinically relevant biofilm prevention that does not necessarily involve antibiotics and a quantification method to more comprehensively estimate these films.

The overall objective of this work was to characterize and engineer microbial cultures to biodegrade groundwater pollutants as well as quantify and prevent microbial adhesion to medically relevant surfaces. In this dissertation, bench-and field-scale systems as well as *in vitro* and flow through models were studied and are described below.

Objective 1: To engineer a microbial community composed of anaerobic and aerobic bacteria in modified medium to simultaneously or sequentially degrade CVOCs and 1,4-dioxane.

Objective 2: To evaluate *in situ* biostimulation and bioaugmentation for enhancing the removal of 1,4-dioxane and CVOCs.

Objective 3: To characterize *Pseudonocardia dioxanivorans* CB1190's ability to metabolize vinyl chloride along with co-occurring contaminants like 1,4-dioxane

Objective 4: To visualize and quantify microbial adhesion to polysiloxanes as well as formulate a multipronged quantification approach suitable for medical tubing.

1.2 Dissertation Overview

This dissertation is divided into six chapters. Chapter 1 contains a brief summary of the current literature that sets the stage for the research objectives. Chapter 2 contains the results of a mixed microbial community comprised of the aerobic pure strain, *Pseudonocardia dioxanivorans* CB1190 and anaerobic consortia, KB-1, that can biodegrade chlorinated ethenes and 1,4-dioxane. This chapter is included with permission from *Environmental Science and Technology Letters*.(4) An *in situ* field demonstration project with aerobic biostimulation and bioaugmentation with CB1190 for the removal of 1,4-dioxane and chlorinated volatile organic compounds is described in Chapter 3. The ability of CB1190 to metabolize both 1,4-dioxane and vinyl chloride is presented in Chapter 4. Lastly, the assessment and quantification of microbial adhesion to modified substrates and medical devices is presented in Chapter 5. A summary of the conclusions and significance to the field of environmental science, engineering, and medicine along with suggestions for future research directions is presented in Chapter 6. Supporting information for Chapters 2, 4, and 5 are included in Appendices A, B, and C.

1.3 References

(1) Balloux, F. and L. van Dorp. Q&A: What Are Pathogens, and What Have They Done to and for Us? *BMC Biol.*, 2017, 15, 91-91.

(2) Adamson, D.T., S. Mahendra, K.L. Walker, S.R. Rauch, S. Sengupta, and C.J. Newell. A Multisite Survey to Identify the Scale of the 1,4-Dioxane Problem at Contaminated Groundwater Sites. *Environ. Sci. & Technol. Lett.*, 2014, 1, 254-258.

(3) Vogel, T.M., *Natural Bioremediation of Chlorinated Solvents, in Handbook of Bioremediation*. 2017, CRC Press. p. 26.

(4) Polasko, A.L., A. Zulli, P.B. Gedalanga, P. Pornwongthong, and S. Mahendra. A Mixed Microbial Community for the Biodegradation of Chlorinated Ethenes and 1,4-Dioxane. *Environ. Sci. Technol. & Lett.*, **2019**, 6, 49-54.

Chapter 2 A Mixed Microbial Community for the Biodegradation of Chlorinated Ethenes and 1,4-Dioxane

2.1 Introduction

Chlorinated ethenes and 1,4-dioxane are probable human carcinogens and commonly co-occurring groundwater contaminants.(1-5) Biological treatment technologies for these compounds individually have become attractive remediation methods due to low implementation costs and minimal invasiveness.(6, 7) Members of the bacterial genus, *Dehalococcoides*, are the most widely reported bacteria capable of metabolically degrading chlorinated ethenes, such as trichloroethene (TCE) via reductive dechlorination.(8) However, a downside to this process is the formation and accumulation of intermediate transformation products, such as cis-1,2-dichoroethene (cDCE) and vinyl chloride (VC).(9) Aerobic cometabolism of TCE can be carried out using substrates such as methane, propane, methanol, toluene, phenol, and ammonia.(6) However, cometabolism-based remediation requires additional amendments, such as electron donors for inducing appropriate biodegradative enzymes in microbial populations.(10, 11)

A variety of microbial strains have been reported to metabolically or co-metabolically degrade 1,4-dioxane under aerobic conditions only.(7) A bacterial multicomponent monooxygenase responsible for initiating 1,4-dioxane degradation is the tetrahydrofuran (THF)/dioxane monooxygenase.(12) The genes coding for this enzyme, *thmADBC/dxmADBC*, along with the aldehyde dehydrogenase, *aldH*, serve as biomarkers to verify 1,4-dioxane biodegradation.(13) Some actinomycetes, especially, members of *Pseudonocardia*, are capable of mineralizing 1,4-dioxane via initial monooxygenase-catalyzed hydroxylation, followed by common cellular metabolic pathways.(12-16) 1,4-Dioxane-cometabolizing microorganisms are equipped with monooxygenases induced by multiple carbon sources such as methane, propane, phenol, tetrahydrofuran, and toluene.(17, 18) Decoupling cellular growth from 1,4-dioxane

degradation may allow for the removal of lower concentrations of 1,4-dioxane (13, 19-24) but might result in toxic products, such as 2-hydroxyethoxyacetic acid.(20) Conversely, minimum substrate concentrations are required to sustain microbial growth (25) but toxic intermediates are not expected to accumulate during 1,4-dioxane metabolizing processes.(12)

Numerous in-situ bioremediation projects have been performed that use biostimulation along with bioaugmentation to promote biodegradation of chlorinated ethenes.(26-29) Many of these projects have involved enhancing reductive dechlorination and have focused on promoting anaerobic conditions with very low redox environments (oxidation-reduction potential < -200 millivolts). If complete reduction to ethene is not achieved, there is a risk of cDCE or VC migrating downgradient from source zones. As the concern of 1,4-dioxane rises, remedial technology selection process must consider approaches to remove chlorinated solvents as well as 1,4-dioxane. Aerobic biodegradation of 1,4-dioxane is possible in the naturally changing redox conditions of plumes as they move downgradient from anaerobic source zones toward more aerobic environments.(30) Few studies have evaluated the versatility and abilities of 1,4-dioxane degrading microorganisms in divergent redox environments. Opposing redox conditions favored by chlorinated ethene- and 1,4-dioxane-degrading bacteria pose a challenge for concurrent bioremediation of both contaminants.

The objective of this study was to formulate a microbial community to simultaneously or sequentially degrade chlorinated ethenes and 1,4-dioxane under changing redox conditions. After various anaerobic incubation periods, the reactivation of the monooxygenase enzymes to aerobically biodegrade 1,4-dioxane and chlorinated solvents was also investigated.

2.2 Materials and Methods

2.2.1 Chemicals

1,4-Dioxane (99.8%, ACS grade), TCE (≥99.5%, ACS grade), cis-DCE (97%), sodium lactate (60% w/w), and titanium trichloride ($TiCl_3$) (≥99.9%), were obtained from Sigma-Aldrich. Saturated chlorinated stocks were prepared as previously described.(31)

2.2.2 Bacterial Cultures and Growth Conditions

The widely used and resilient mixed consortium, KB-1, containing *Dehalococcoides*, was grown in a defined medium (31), with 20 mg/L TCE (aqueous) as electron acceptor and 60 mg/L lactate as carbon source.(32) Sterile 160 mL serum bottles containing media were sparged for 3 minutes with filtered (0.2 μm) N_2 to achieve anaerobic conditions (Appendix Figure A-1) and sealed with 20 mm butyl rubber stoppers. $TiCl_3$ was also used as reductant. CB1190 seed cultures were prepared using a 1% (v/v) transfer from an actively growing pure culture under aerobic conditions in the lactate-free medium previously used for growing KB-1. Experimental bottles were inoculated with stock cultures in their late exponential or early stationary phase after TCE (KB-1) or 1,4-dioxane (CB1190) was degraded to below 1,000 μg/L.

2.2.3 Design of Batch Experiments

The microcosms were prepared in sterile 500 mL glass bottles and maintained with 1:5 liquid to headspace ratios with the following conditions: 1) KB-1 + CB1190 that transitioned from anaerobic to aerobic, 2) CB1190 only that transitioned from anaerobic to aerobic, and 3) CB1190 only that remained anaerobic. Experimental bottles were inoculated with 10% (v/v) CB1190 and 5% (v/v) KB-1. Once TCE was degraded to cis-DCE by KB-1, 60 mL of filtered, high purity oxygen was amended to transition anaerobic to aerobic conditions. All bottles were incubated upright at 30°C with 150 rpm shaking. TCE and 1,4-dioxane concentrations were

amended as liquid concentrations. At each time point, 200 µL of liquid sample were collected and filtered for 1,4-dioxane quantification.

2.2.4 Analytical Methods

Chlorinated ethenes were measured by direct headspace injections (10 or 100 µL depending on concentration) using gas chromatography-mass spectrometry (GC-MS; Agilent 6890 GC and 5973 MS). 1,4-Dioxane concentrations higher than 1,000 µg/L were measured using a GC equipped with a flame ionization detector in 2 µL aqueous samples, while 1,4-dioxane samples containing <1,000 µg/L were measured by GC-MS after samples were prepared by a frozen microextraction technique.(33) The detection limits for chlorinated ethenes and 1,4-dioxane were 5 µg/L and 2 µg/L, respectively.

2.2.5 Total Nucleic Acids Extraction, Quantitative Polymerase Chain Reaction, and cDNA Synthesis

Total nucleic acids were extracted from cell pellets using a phenol-chloroform extraction method.(33) The effect of anaerobic incubation on CB1190's gene expression in pure and mixed cultures was determined by amplification of 1,4-dioxane biomarker targets (*dxmB* and *aldH*) (13) CB1190 and KB-1's cellular growth over time was estimated using the *dxmB* and *tceA* gene copy numbers.(13, 34) Gene expression was quantified using the $2^{-\Delta\Delta CT}$ method, as described by Livak and Schmittgen.(35) Gene expression data were first normalized to the housekeeping gene, RNA polymerase σ subunit D (*rpoD*), followed by normalization to the values obtained at the end of the anaerobic incubation period and after 1,4-dioxane was degraded below 1,000 µg/L. Quantitative Polymerase Chain Reaction (qPCR) using the SYBR-green based detection reagents were utilized to quantify gene copy numbers of CB1190 and KB-1 as well as gene transcripts of CB1190.

2.3 Results and Discussion

2.3.1 Chlorinated Ethene Biodegradation by the Mixed Microbial Community

TCE was reductively dechlorinated under anaerobic conditions to cis-DCE only in the KB-1 + CB1190 anaerobic/aerobic bottles. After the transition to aerobic conditions, CB1190 cells within the mixed microbial community oxidatively biodegraded cis-DCE. KB-1 + CB1190 anaerobic/aerobic and CB1190 anaerobic/aerobic bottles remained anaerobic for 16 hours. This anaerobic incubation period corresponded to the time it took KB-1 to biodegrade TCE to cDCE. After oxygen was amended, the bottles with KB-1 + CB1190 degraded 1,300 µg/L of cDCE at a rate of 0.206±0.002 /day (Figure 2-1A and Appendix Figure A-1). Higher concentrations of TCE and 1,4-dioxane were also successfully tested with the mixed microbial community (Appendix Figures A-1 to A-5). Oxygen amendments resulted in cessation of KB-1's activity, as confirmed by no further increase in *tceA* copies/mL (Figure 2-1A, Appendix Figure A-6, Appendix Figure A-10). This was likely due to the oxidative stress on the enzymes that make up alternative respiratory chain in anaerobes, as well as the production of reactive species, such as superoxide radicals and hydrogen peroxide.(36) Additionally, VC remained below 2 µg/L in anaerobic as well as aerobic incubation periods. The CB1190 only anaerobic/aerobic bottles and CB1190 only anaerobic bottles did not show significant TCE biodegradation (Figure 2-1A).

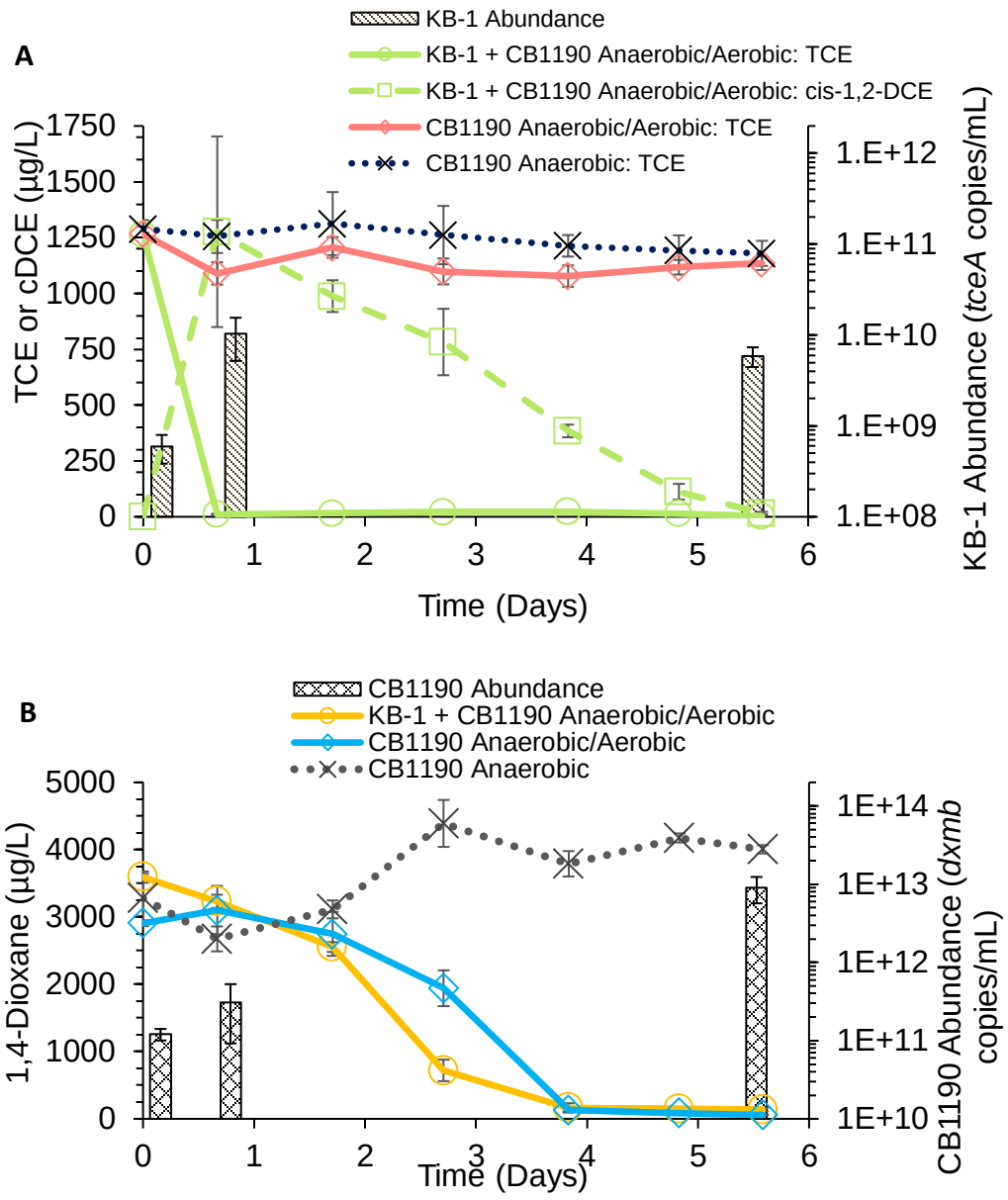

Figure 2-1 Biodegradation in pure CB1190 and KB-1 + CB1190
A). Chlorinated ethene (TCE & cDCE) concentrations. cDCE was degraded by CB1190 during aerobic phase 2-1B). 1,4-Dioxane concentrations. KB-1 + CB1190 anaerobic/aerobic and CB1190 anaerobic/aerobic degraded 1,4-dioxane. The CB1190 pure cultures did not degrade TCE under anaerobic or aerobic conditions, while KB-1 + CB1190 anaerobic/aerobic biodegraded TCE anaerobically and its transformation product, cDCE, aerobically. The *dxmB* and *tceA* genes were used to quantify cell numbers and the mixed culture cell abundance results are shown. KB-1 grew significantly during the anaerobic phase and CB1190 grew significantly during the aerobic phase. Vinyl chloride was not detected. Error bars indicate the standard deviation of triplicates, and oxygen was amended on day 1 thus ending the anaerobic phase.

Aerobic biodegradation of cDCE by CB1190 with and without a prior anaerobic incubation phase was first recorded in the present study (Figure 2-1A and Appendix Figures A-2 to A-3 and Appendix Figure A-8 to A-9). Biodegradation of cDCE by CB1190 can mitigate cDCE's inhibition of 1,4-dioxane biodegradation (37-39) as well as prevents VC production. This reduces the need to amend additional microorganisms and their primary substrates to oxidatively cometabolize cDCE.

2.3.2 1,4-Dioxane Biodegradation and Microbial Growth in the Mixed Community

After the transition to aerobic conditions, CB1190 in pure and mixed culture experienced a short lag phase before beginning to biodegrade 1,4-dioxane. KB-1 + CB1190 anaerobic/aerobic degraded 3,000 µg/L of 1,4-dioxane at a rate of 0.195±0.002 /day (Figure 2-1B, Appendix Figure A-5), and CB1190 only anaerobic/aerobic bottles at a rate of 0.199±0.001 /day (Figure 2-1B). CB1190-mediated 1,4-dioxane degradation rates were calculated using the end of the anaerobic phase and after 1,4-dioxane was degraded to below detection. All bottles had an average initial CB1190 cell density of 1.21±0.2 x 10^{11} *dxmB* copies/mL and the KB-1 + CB1190 bottles had an average initial KB-1 cell density of 5.9±2.1 x 10^{8} *tceA* copies/mL (Figure 2-1A and Appendix Figures A-9 and A-10). The KB-1 + CB1190 anaerobic/aerobic grew at 1.56±0.7 x 10^{12} *dxmB* copies/mL/day (Figure 2-1B). The CB1190 anaerobic/aerobic cultures grew at 5.22±0.02 x 10^{11} *dxmB* copies/mL/day but the CB1190 that was always anaerobic did not show significant growth (Appendix Figure A-7 and Appendix Figure A-11).

Previous studies have cultured aerobic microbes from anaerobic environemnts as well as combined aerobic and anaerobic bacteria to enhance the biodegradation of recalcitrant pollutants such as polychlorinated biphenyls, chlorobenzenes, dinitrotoluenes, and azo dyes.(40-43) Although these studies developed consortia containing anaerobes and aerobes, some were

conducted in spatially and functionally separate bottles using immobilized cells. In our study, all microbes were added together into the same medium with chlorinated ethenes and 1,4-dioxane. Another report of degradation of TCE and 1,4-dioxane under changing redox conditions utilized a microbially driven Fenton reaction using the facultative anaerobe, *Shewanella oneidensis*, to drive the production of HO• radicals.(44) By contrast, our study relies on the TCE-reductase enzymes in *Dehalococcoides* (45) to break down TCE by replacing a covalently-bonded chlorine with a hydrogen and the monooxygenase enzyme in CB1190 to cleave the carbon-oxygen bond in 1,4-dioxane (12), leading to benign end products for both compounds. These previous studies serve as a foundation for considering this approach for removing multiple contaminants with bacteria that favor diverse redox conditions. The present study is the first report of biodegradation of 1,4-dioxane and chlorinated ethenes by a mixed microbial consortium containing aerobic and anaerobic bacteria, and describes its potential implications for bioremediation strategies for sites contaminanted with pollutant mixtures.

2.3.3 Strain CB1190 Survivability and 1,4-Dioxane Biodegradation After Anaerobic Incubation

After 7, 14, 21, 28, 35, and 56 days of anaerobic incubation, strain CB1190 was able to biodegrade 1,4-dioxane to below the detection limit after oxygen addition. Strain CB1190 was initially inoculated into anaerobic media and amended with 1,4-dioxane for time periods ranging from 7 to 56 days. The aerobic bottles were continually amended with 1,4-dioxane and maintained in an aerobic environment as positive controls. The 56 days anaerobic bottles did not receive oxygen and served as anaerobic controls throughout the experiment. There was minimal lag phase for 1,4-dioxane biodegradation in each set of bottles that were amended with oxygen (Figure 2-2).

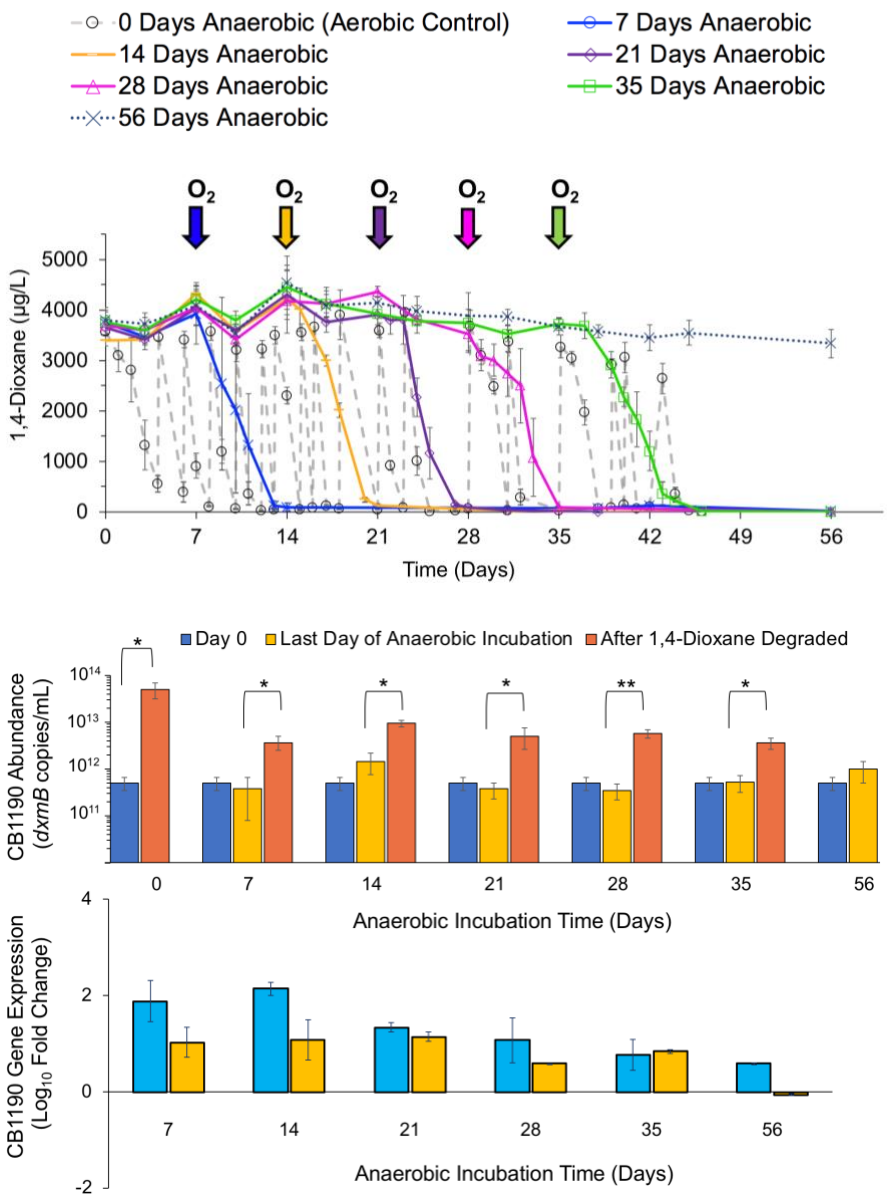

Figure 2-2 Dioxane biodegradation, gene abundance, and gene expression in Strain CB1190 after various anaerobic incubation periods

CB1190 was able to persist alone under anaerobic conditions and completely degrade 1,4-dioxane upon addition of O_2. Error bars indicate standard deviations of triplicates. 2A. 1,4-Dioxane biodegradation by CB1190. Every week only one set of triplicate bottles was amended with O_2 (indicated by arrows). 2B. CB1190 gene abundance on day 0, the last day of anaerobic incubation, and after 1,4-dioxane was degraded. * p-value < 0.05 and ** p-value< 0.01 2C. CB1190 gene expression All cDNA copy numbers were first normalized to *rpoD* housekeeping gene and then to the end of the anaerobic phase. The 56 days anaerobic bottles were sampled on day 42 and 56 for gene expression.

The bottles, which, were anaerobic for 35 days, had a slightly longer lag phase than bottles that were anaerobic for 7 days. The 1,4-dioxane biodegradation rate for each set was as follows: 0 Days Anaerobic (Aerobic Control): 0.211±0.009 /day 7 Days Anaerobic: 0.162±0.003 /day, 14 Days Anaerobic: 0.139±0.003 /day, 21 Days Anaerobic: 0.140±0.001 /day, 28 Days Anaerobic: 0.139±0.0001 /day, and 35 Days Anaerobic: 0.105±0.0002 /day. Bottles were amended with uniform cellular densities and had average initial biomass concentrations of $4.93 \pm 1.5 \times 10^{11}$ *dxmB* copies/mL. During the anaerobic phase, the % oxygen in the headspace averaged 2.5±0.7% (ORP -53±4.1 mV), which is considered a reducing environment.(46) After the anaerobic phase, the oxygen averaged 11.6±0.9% in the headspace (Appendix Figure A-12).

2.3.4 CB1190 Cell Growth and Gene Expression After Anaerobic Incubation

1,4-Dioxane biodegradation that occurred after the restoration of aerobic conditions produced a carbon and energy source for CB1190 growth. Significant CB1190 growth was observed in bottles that were kept anaerobic for 7, 14, 21, 28, and 35 days and then provided with oxygen amendments (Figure 2-2). The aerobic bottles were replenished with 1,4-dioxane to demonstrate CB1190 biodegradation rates in the presence of continual oxygen and carbon substrate availability. Additionally, CB1190's survivability in the presence of varying reductants, media, and lactate amounts were also verified (Appendix Figures A-13 to A-15). Upregulation of *dxmB* and *aldH* genes were observed in days 7 through 35 demonstrating that 1,4-dioxane biodegradation was initiated and continued as the intermediates were produced (Figure 2-2). The bottles that were maintained under anaerobic conditions were sampled at the beginning of day 42 and 56. The *dxmB* gene was upregulated in the anaerobic bottles, but the *aldH* gene transcripts were unchanged. This could be explained by the fact that the *dxmB* gene is induced by 1,4-dioxane and can be expressed even if oxygen levels are insufficient. The *aldH* gene, which is

induced by 1,4-dioxane biodegradation intermediates, was not upregulated likely because 1,4-dioxane had not been degraded. The anaerobic always bottles were subsequently kept for a total of 100 days and then provided oxygen and to our surprise within two weeks CB1190 was able to biodegrade the remaining 1,4-dioxane (Appendix Figure A-16).

CB1190's apparent dormancy under prolonged oxygen limited conditions could be explained by its ability to quickly adapt to stress and to utilize other substrates for fermentative growth . Similar aerobic bacteria, *Mycobacterium tuberculosis* and *Mycobacterium bovis*, were previously grown in microaerophilic and anaerobic conditions.(47) Those cells appeared to produce a thickened cell wall to withstand oxygen deficient conditions *in vivo*. Specifically, the heat shock protein played a role in stabilizing the cell structure in the long-term by creating a multi-layer, peptidoglycan protective casing.(47) CB1190 could be utilizing a hydrogenase enzyme to survive anaerobic incubation. Traditionally, hydrogenase enzymes have been associated with anaerobic metabolism because a majority are deactivated in the presence of oxygen. However, they are often present among aerobic bacteria and rarely studied among obligate aerobes.(48) CB1190 can fix CO_2 when provided hydrogen and maintain very slow cellular growth.(49) The hydrogenase enzyme in CB1190 was reported to utilize H_2 coupled with trace amounts of CO_2 or biocarbonate to remain active.(49) At low pE values, which are commonly found in anaerobic waters (50), the PREEQC model showed that the chemical components of the modified media could produce H_2 in micromolar to nanomolar concentrations. We postulate that CB1190 could be utilizing the low amounts of hydrogen to remain dormant but quickly revive when sufficient oxygen becomes available for aerobic metabolism. Reactivation of the *dxmB* and *aldH* in CB1190 were crucial in validating that CB1190 could endure oxygen restrictions in the subsurface. As our findings with CB1190

demonstrate, bacteria that harbor the ability to maintain cellular viability and metabolism when exposed to divergent redox conditions could provide a wider variety of solutions for chlorinated ethene and 1,4-dioxane bioremediation. The results of this study demonstrate that an intrinsic or bioaugmented mixed microbial community can withstand the changing redox conditions that may be experienced by a plume and biodegrade chlorinated ethenes as well as 1,4-dioxane.

2.4 References

(1) Anderson, R.H., J.K. Anderson, and P.A. Bower. Co-Occurrence of 1,4-Dioxane with Trichloroethylene in Chlorinated Solvent Groundwater Plumes at Us Air Force Installations: Fact or Fiction. Integr. Environ. Asses., 2012, 8, 731-737.

(2) Adamson, D.T., R.H. Anderson, S. Mahendra, and C.J. Newell. Evidence of 1,4-Dioxane Attenuation at Groundwater Sites Contaminated with Chlorinated Solvents and 1,4-Dioxane. Environ. Sci. Technol., 2015, 49, 6510-6518.

(3) Stickney, J.A., S.L. Sager, J.R. Clarkson, L.A. Smith, B.J. Locey, M.J. Bock, R. Hartung, and S.F. Olp. An Updated Evaluation of the Carcinogenic Potential of 1,4-Dioxane. Regul. Toxicol. Pharmacol., 2003, 38, 183-195.

(4) Toxicological Review of Trichloroethylene, U.S. EPA, 2011.

(5) Toxicological Review of cis-& trans-1,2-Dichloroethylene, U.S. EPA, 2009.

(6) Shukla, A.K., S.N. Upadhyay, and S.K. Dubey. Current Trends in Trichloroethylene Biodegradation: A Review. Crit. Rev. Biotechnol., 2014, 34, 101-114.

(7) Zhang, S., P.B. Gedalanga, and S. Mahendra. Advances in Bioremediation of 1,4-Dioxane-Contaminated Waters. J. Environ. Manage., 2017, 204, 765-774.

(8) Suthersan, S., M. Schnobrich, J. Martin, J.F. Horst, and E. Gates. Three Decades of Solvent Bioremediation: The Evolution from Innovation to Conventional Practice. Ground Water Monit. R., 2017, 37, 14-23.

(9) Vogel, T.M. and P.L. McCarty. Biotransformation of Tetrachloroethylene to Trichloroethylene, Dichloroethylene, Vinyl Chloride, and Carbon Dioxide under Methanogenic Conditions. Appl. and Environ. Microbiol., 1985, 49, 1080-1083.

(10) Suttinun, O., E. Luepromchai, and R. Müller. Cometabolism of Trichloroethylene: Concepts, Limitations and Available Strategies for Sustained Biodegradation. Reviews in Environ. Sci. Biotechnol., 2012, 12, 100-114.

(11) Frascari, D., G. Zanaroli, and A.S. Danko. In Situ Aerobic Cometabolism of Chlorinated Solvents: A Review. J. Hazard. Mater., 2015, 283, 382-399.

(12) Mahendra, S., C.J. Petzold, E.E. Baidoo, J.D. Keasling, and L. Alvarez-Cohen. Identification of the Intermediates of in vivo Oxidation of 1,4-Dioxane by Monooxygenase-Containing Bacteria. Environ. Sci. & Technol., 2007, 41, 7330-7336.

(13) Gedalanga, P.B., P. Pornwongthong, R. Mora, S.-Y.D. Chiang, B. Baldwin, D. Ogles, and S. Mahendra. Identification of Biomarker Genes to Predict Biodegradation of 1,4-Dioxane. Appl. Environ. Microbiol., 2014, 80, 3209-3218.

(14) Grostern, A., C.M. Sales, W. Zhuang, O. Erbilgin, and L. Alvarez-Cohen. Glyoxylate Metabolism is a Key Feature of the Metabolic Degradation of 1,4-Dioxane by *Pseudonocardia dioxanivorans* strain CB1190. Appl. Environ. Microbiol., 2012, 78, 3298-3308.

(15) He, Y., J. Mathieu, Y. Yang, P. Yu, L.B.S. Marcio, and P.J.J. Alvarez. 1,4-Dioxane Biodegradation by *Mycobacterium dioxanotrophicus* PH-06 is Associated with a Group-6 Soluble Di-Iron Monooxygenase. Environ. Sci. Technol. Lett., 2017, 4.

(16) Aoyagi, T., F. Morishita, Y. Sugiyama, D. Ichikawa, D. Mayumi, Y. Kikuchi, A. Ogata, K. Muraoka, H. Habe, and T. Hori. Identification of Active and Taxonomically Diverse 1,4-Dioxane Degraders in a Full-Scale Activated Sludge System by High-Sensitivity Stable Isotope Probing. ISME J., 2018, 12, 2376-2388.

(17) Mahendra, S. and L. Alvarez-Cohen. *Pseudonocardia dioxanivorans* sp Nov., a Novel Actinomycete That Grows on 1,4-Dioxane. Int. J. of Syst. and Evol. Micr., 2005, 55, 593-598.

(18) Parales, R.E., J.E. Adamus, N. White, and H.D. May. Dedegradation of 1,4-Dioxane by an Actinomycete in Pure Culture. Appl. Environ. Microbiol., 1994, 60, 4527-4530.

(19) Masuda, H., K. McClay, R.J. Steffan, and G.J. Zylstra. Biodegradation of Tetrahydrofuran and 1,4-Dioxane by Soluble Di-Iron Monooxygenase in *Pseudonocardia* sp. strain Env478. J. Mol. Microbiol. Biotechnol., 2012, 22, 312-316.

(20) Vainberg, S., K. McClay, H. Masuda, D. Root, C. Condee, G.J. Zylstra, and R.J. Steffan. Biodegradation of Ether Pollutants by *Pseudonocardia* sp Strain Env478. Appl. Environ. Microbiol., 2006, 72, 5218-5224.

(21) Mahendra, S. and L. Alvarez-Cohen. Kinetics of 1,4-Dioxane Biodegradation by Monooxygenase-Expressing Bacteria. Environ. Sci. & Technol., 2006, 40, 5435-5442.

(22) Ryan, M.P., J.T. Pembroke, and C.C. Adley. *Ralstonia pickettii* in Environmental Biotechnology: Potential and Applications. J. Appl. Microbiol., 2007, 103, 754-764.

(23) Fishman, A., Y. Tao, and T.K. Wood. Toluene 3-Monooxygenase of *Ralstonia pickettii* PKO1 Is a Para-Hydroxylating Enzyme. J. Bacteriol., 2004, 186, 3117-3123.

(24) Hand, S., B. Wang, and K.H. Chu. Biodegradation of 1,4-Dioxane: Effects of Enzyme Inducers and Trichloroethylene. Sci. Total Environ., 2015, 520, 154-159.

(25) Barajas-Rodriguez, F.J. and D.L. Freedman. Aerobic Biodegradation Kinetics for 1,4-Dioxane under Metabolic and Cometabolic Conditions. J. Hazard. Mater., 2018, 350, 180-188.

(26) Hood, E.D., D.W. Major, J.W. Quinn, W.S. Yoon, A. Gavaskar, and E.A. Edwards. Demonstration of Enhanced Bioremediation in a Tce Source Area at Launch Complex 34, Cape Canaveral Air Force Station. Ground Water Monit. R., 2008, 28, 98-107.

(27) Ellis, D.E., E.J. Lutz, J.M. Odom, R.J. Buchanan, C.L. Bartlett, M.D. Lee, M.R. Harkness, and K.A. Deweerd. Bioaugmentation for Accelerated in situ Anaerobic Bioremediation. Environ. Sci. Technol., 2000, 34, 2254-2260.

(28) Lendvay, J.M., F.E. Loffler, M. Dollhopf, M.R. Aiello, G. Daniels, B.Z. Fathepure, M. Gebhard, R. Heine, R. Helton, J. Shi, R. Krajmalnik-Brown, C.L. Major, M.J. Barcelona, E. Petrovskis, R. Hickey, J.M. Tiedje, and P. Adriaens. Bioreactive Barriers: A Comparison of Bioaugmentation and Biostimulation for Chlorinated Solvent Remediation. Environ. Sci. Technol., 2003, 37, 1422-1431.

(29) Major, D.W., M.L. McMaster, E.E. Cox, E.A. Edwards, S.M. Dworatzek, E.R. Hendrickson, M.G. Starr, J.A. Payne, and L.W. Buonamici. Field Demonstration of Successful Bioaugmentation to Achieve Dechlorination of Tetrachloroethene to Ethene. Environ. Sci. Technol., 2002, 36, 5106-5116.

(30) Christensen, T.H., P.L. Bjerg, S.A. Banwart, R. Jakobsen, G. Heron, and H.-J. Albrechtsen. Characterization of Redox Conditions in Groundwater Contaminant Plumes. J. Contam. Hydrol., 2000, 45, 165-241.

(31) Alvarez-Cohen, L. and P. McCarty. Effects of Toxicity, Aeration, and Reductant Supply on Trichloroethylene Transformation by a Mixed Methanotrophic Culture. Appl. Environ. Microbiol., 1991, 57, 228-235.

(32) He, J., V.F. Holmes, P.K.H. Lee, and L. Alvarez-Cohen. Influence of Vitamin B12 and Cocultures on the Growth of *Dehalococcoides* Isolates in Defined Medium. Appl. Environ. Microbiol., 2007, 73, 2847-2853.

(33) Li, M., P. Conlon, S. Fiorenza, R.J. Vitale, and P.J.J. Alvarez. Rapid Analysis of 1,4-Dioxane in Groundwater by Frozen Micro-Extraction with Gas Chromatography-Mass Spectrometry. Ground Water Monit. R., 2011, 31, 70-76.

(34) Waller, A.S., R. Krajmalnik-Brown, F.E. Loffler, and E.A. Edwards. Multiple Reductive-Dehalogenase-Homologous Genes Are Simultaneously Transcribed During Dechlorination by *Dehalococcoides*-Containing Cultures. Appl. Environ. Microbiol., 2005, 71, 8257-8264.

(35) Livak, K.J. and T.D. Schmittgen. Analysis of Relative Gene Expression Data Using Real-Time Quantitative Pcr and the 2(-Delta Delta C(T)) Method. Methods, 2001, 25, 402-408.

(36) Rocha, E.R. and J.C. Smith. Role of the Alkyl Hydroperoxide Reductase (Ahpcf) Gene in Oxidative Stress Defense of the Obligate Anaerobe Bacteroides Fragilis. J. Bacteriol., 1999, 181, 5701-5710.

(37) Mahendra, S., A. Grostern, and L. Alvarez-Cohen. The Impact of Chlorinated Solvent Co-Contaminants on the Biodegradation Kinetics of 1,4-Dioxane. Chemosphere, 2013, 91, 88-92.

(38) Zhang, S., P.B. Gedalanga, and S. Mahendra. Biodegradation Kinetics of 1,4-Dioxane in Chlorinated Solvent Mixtures. Environ. Sci. & Technol., 2016, 50, 9599-9607.

(39) Zhao, L., X. Lu, A. Polasko, N.W. Johnson, Y. Miao, Z. Yang, S. Mahendra, and B. Gu. Co-Contaminant Effects on 1,4-Dioxane Biodegradation in Packed Soil Column Flow-through Systems. Environ. Poll., 2018, 243, 573-581.

(40) Brown, D. and B. Hamburger. The Degradation of Dyestuffs: Part III - Investigations of Their Ultimate Degradability. Chemosphere, 1987, 16, 1539-1553.

(41) Fathepure, B.Z. and T.M. Vogel. Complete Degradation of Polychlorinated Hydrocarbons by a Two-Stage Biofilm Reactor. Appl. Environ. Microbiol., 1991, 57, 3418-3422.

(42) Beunink, J. and H.-J. Rehm. Synchronous Anaerobic and Aerobic Degradation of Ddt by an Immobilized Mixed Culture System. Appl. Microbiol. Biotechnol., 1988, 29, 72-80.

(43) Anid, P.J., B.P. Ravest-Webster, and T.M. Vogel. Effect of Hydrogen Peroxide on the Biodegradation of Pcbs in Anaerobically Dechlorinated River Sediments. Biodegradation, 1993, 4, 241-248.

(44) Sekar, R., M. Taillefert, and T.J. DiChristina. Simultaneous Transformation of Commingled Trichloroethylene, Tetrachloroethylene, and 1,4-Dioxane by a Microbially Driven Fenton Reaction in Batch Liquid Cultures. Appl. Environ. Microbiol., 2016, 82, 6335-6343.

(45) Magnuson, J.K., R.V. Stern, J.M. Gossett, S.H. Zinder, and D.R. Burris. Reductive Dechlorination of Tetrachloroethene to Ethene by a Two-Component Enzyme Pathway. Appl. Environ. Microbiol., 1998, 64, 1270-1275.

(46) Parsons, F., G.B. Lage, and R. Rice. Biotransformation of Chlorinated Organic Solvents in Static Microcosms. Environ. Toxicol. Chem., 1985, 4, 739-742.

(47) Cunningham, A.F. and C.L. Spreadbury. Mycobacterial Stationary Phase Induced by Low Oxygen Tension: Cell Wall Thickening and Localization of the 16-Kilodalton A-Crystallin Homolog. J. Bacteriol., 1998, 180, 801-808.

(48) Michael, B., G. Chris, H. Kiel, C. Desmond, and C.G. M. Three Different [NiFe] Hydrogenases Confer Metabolic Flexibility in the Obligate Aerobe *Mycobacterium smegmatis*. Environ. Microbiol., 2014, 16, 318-330.

(49) Grostern, A. and L. Alvarez-Cohen. Rubisco-Based CO2 Fixation and C1 Metabolism in the Actinobacterium *Pseudonocardia dioxanivorans* CB1190. Environ. Microbiol., 2013, 15, 3040-3053.

(50) De, A.K., Environmental Chemistry: Fifth Edition. 2003, Daryaganj, New Delhi: New Age International.

Chapter 3 *In Situ* Aerobic Biostimulation and Bioagumentation for 1,4-Dioxane and Chlorinated Volatile Organic Compounds

3.1 Introduction

1,4-Dioxane (DX) and chlorinated volatile organic compounds (CVOCs) are pervasive groundwater contaminants that often co-occur (1). This has largely been attributed to DX's use as a solvent stabilizer for 1,1,1-trichloroethane (TCA), historical use of TCA with trichloroethene (TCE), and improper disposal methods (2). Until recently, many remediation plans have only addressed CVOCs, but continued research and predicted regulatory changes have shown that there is a growing need to also remediate DX. While traditional physical and chemical (e.g. sorption, oxidation, filtration) methods are available for removing DX and CVOCs (3), bioremediation offers a promising solution for eliminating these contaminants due to its low cost, reduced energy/chemical inputs, and *in situ* transformation of the pollutants. (4) Anaerobic biological reduction is a common remediation tactic for CVOCs (5, 6). However, under some conditions, intermediate daughter products such as cis-1,2-dichloroethene (cDCE) and vinyl chloride (VC) (a known carcinogen) accumulate. (7) Aerobic cometabolic biodegradation of CVOCs can be challenging due to the additional amendments required to sustain microbial growth (8). Contrastingly, DX is known to be biodegraded aerobically, and no anaerobic biodegradation pathways have been identified yet. The opposing redox conditions favored by CVOC- and DX-degrading bacteria pose a difficult challenge for concurrent bioremediation.

Recently, bench-scale research has shown that combining anaerobic and aerobic microbes can be beneficial for sequential or simultaneous biodegradation of both of these contaminant classes (9). Dechlorinating microorganisms (e.g. KB-1) can reduce CVOCs when conditions are anaerobic whereas aerobic microbes (e.g. *Pseudonocardia dioxanivoran*s

CB1190) can oxidize DX and cDCE when oxygen becomes available. Particularly, this novel technology is relevant at sites where enhanced reductive dechlorination (ERD) has been deployed, but degradation has stalled at cDCE due to oxygen intrusion. Currently, there is a need to demonstrate field-scale readiness of this technology for complex geochemical and co-contaminated groundwater sites. Our goal was to conduct a pilot-scale test to evaluate *in situ* biostimulation and bioaugmentation with CB1190 post ERD for the removal of DX and CVOCs.

3.2 Materials and Methods

3.2.1 Pure Strain CB1190 Growth Conditions

Pure strain CB1190 was grown in the UCLA Modified Medium at circumneutral pH at 30°C with 150 rpm shaking.(9) A 1:5 liquid to headspace ratio in 2 L Erlenmeyer flasks with a vent cap was used to ensure adequate oxygen. Cells were allowed to degrade multiple rounds of 100 mg/L DX and subsequent subcultures were made using a 1% (v/v) transfer to fresh media. Periodically, the culture's purity was monitored by plating 100 µL of liquid onto R2A agar plates and placed in a stationary incubator at 30°C for 2-3 days. After the culture reached late-exponential or early-stationary-phase and DX was degraded to below the GC-FID detection limit, cultures were used to inoculate experimental bottles.

3.2.2 Design of Batch Experiments

Batch experiments were prepared using sterile 500 mL glass bottles and maintained a 1:5 liquid to headspace ratio. Bottles were made anaerobic (dissolved oxygen (DO) $\leq$ 0.5 mg/L) by flushing filtered N_2 gas through the bottles as described in Polasko et al. 2019.(9) Sacrificial bottles were also made under the same conditions to validate the DO via an Orion 083005 MD DO probe (Thermo Scientific). After anaerobic incubation, bottles were made aerobic by amending 60 mL of filtered high purity oxygen DO reached 5 mg/L. Bottles containing CB1190

cells were toggled between anaerobic and aerobic environments to simulate potential groundwater conditions. Three-, two-, and one-week anaerobic phases were tested followed by a one-week aerobic phase. The following conditions were prepared with two cycles each of: 1). One week anaerobic, one week aerobic 2). Two weeks anaerobic, one weeks aerobic 3). Three weeks anaerobic, one week aerobic 4). Aerobic always (positive control).

3.2.3 Site and Well Description

The field demonstration site was previously utilized for aluminum pipe manufacturing and contains both CVOCs (TCE, cDCE, 1,1-dichloroethene, VC, TCA) and DX. The groundwater flow beneath the site moves both down-dip to the north and laterally along the strike. The site is located in a groundwater discharge zone where water moves not only laterally along fractures and bedding planes but also upward from depth. The siltstone and shale layers within the subsurface appear to be acting as a semi-confining zone between the shallow, unconfined water bearing zone and the deeper water bearing zone. In 2019, ERD with *Dehalococcoides spp*. was implemented at the source zone to remove CVOCs, but intermediate products, namely cDCE and VC, accumulated. Two wells were selected for this study—monitoring well-31 (MW-31) and monitoring well-32 (MW-32). MW-31 is upgradient of MW-32 and received biostimulation (i.e., air sparging). Whereas MW-32 received biostimulation and bioaugmentation (i.e., air sparging and CB1190). Both wells were sampled every 2-4 weeks for a total of 34 weeks (8 months) and continual monitoring was performed for CVOCs, DX, microbial populations, DO, and pH. On July 1, 2020, 100 L of water containing nutrients (e.g. N & P) and CB1190, were injected into MW-32 along with an air sparging system. MW-31 did not receive biostimulation until week 8.

3.2.4 Analytical Methods

DX and CVOC concentrations in ranges 5-2,000 µg/L and 2-2,000 µg/L, respectively, were measured using a Agilent 6890 gas chromatograph equipped with an Agilent 5973 mass spectrometer. Additional analytical method details are provided by Zhang, et al., *Environ. Sci. Technol.*, 2016 (10). qPCR using the SYBR-green-based detection reagents were utilized to quantify gene copy numbers of total community abundance (total 16S rRNA), DX degradation (*dxmB, aldH*, CB1190-specific 16S rRNA), propane monooxygenase (*prmo*), and soluble methane monooxygenase (*smmo*).(11)

3.3 Results and Discussion

3.3.1 CB1190 Biodegrades 1,4-Dioxane After Anaerobic/Aerobic Cycles

Due to the fact that many contaminant plumes have anaerobic and aerobic zones that change in size and redox potential depending upon the seasonal and biogeochemical factors and subsurface depth, it was crucial to understand whether CB1190 could withstand anaerobic incubation, aerobic incubation, and cycles of these conditions. We have previously demonstrated that CB1190 can withstand anaerobic incubation for up to 100 days and degrade DX once oxygen is amended. However, it was unknown whether toggling anaerobic and aerobic environments would further inhibit CB1190's ability to degrade DX. To our surprise, CB1190 was able to biodegrade DX after two rounds of anaerobic incubation that had a duration of one, two, or three weeks (Figure 3-1). After the 1st round of anaerobic incubation, the DX biodegradation rates for the one-, two-, and three-week anaerobic incubation periods were: 372±13 µg/L/day; 370±12 µg/L/day; and 402±24 µg/L/day, respectively. CB1190 incubated under aerobic conditions throughout biodegraded DX the fastest with a rate of 483±17 µg/L/day. After the 2nd round of anaerobic incubation, the DX biodegradation rates for the one-, two-, and three-week anerobic incubation periods were: 400±29 µg/L/day; 423±18 µg/L/day; and 462±21

µg/L/day, respectively. There was no significant difference (p-value $\leq$ 0.05) between the biodegradation rates after the 1st or 2nd round of anaerobic incubation. This means that the second round of anaerobic incubation did not significantly inhibit CB1190's ability to reactivate the DX-monooxygenase to break down DX. After the 1st round of anaerobic incubation, there was no significant difference in biodegradation rates between the one, two, or three weeks of anaerobic incubation. This aligns with our previous research that anaerobic incubation periods less than 100 days will likely not cause significant delays in DX biodegradation after oxygen becomes present. The only significant difference was between the biodegradation rate of the aerobic always control and the experimental conditions. The rates were significantly lower for the one-, two-, and three-week anaerobic incubation periods compared to the aerobic always condition (p-value = 0.002, 0.002, and 0.02). CB1190's capacity to withstand anaerobic-aerobic cycles will be advantageous at sites where DX and other co-contaminants exist and DO concentrations may not be uniform throughout time and space.

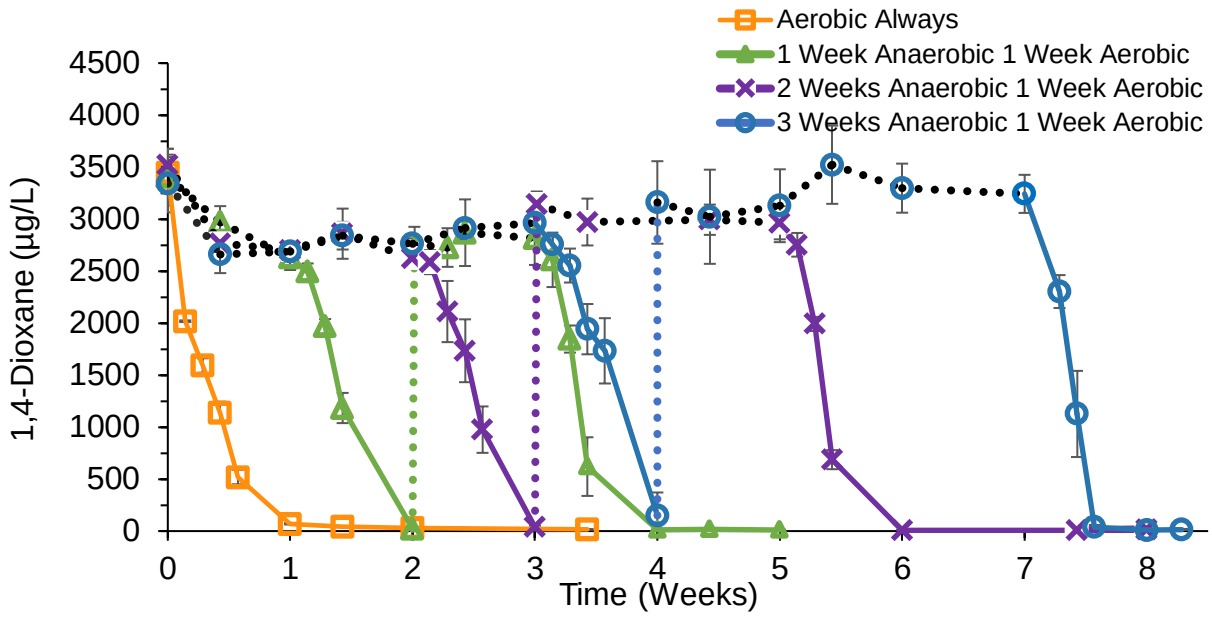

Figure 3-1 1,4-Dioxane Biodegradation After Anaerobic Cycling
Each set of bottles started under anaerobic conditions for one, two, or three weeks and then transitioned to aerobic conditions for one week. After that, the cycle was repeated. Following the first anaerobic-aerobic cycle, 1,4-dioxane was amended. The black dots indicate anaerobic incubation and the solid-colored lines indicate aerobic incubation for the corresponding experimental conditions. Error bars indicate the standard deviation of triplicates.

3.3.2 MW-31: Biostimulation (i.e. air sparging) Resulted in CVOC Removal but Limited 1,4-Dioxane Removal

W-31 is considered to be a source zone for CVOCs and DX (DX = 1,300 µg/L; TCE = 44 µg/L; cDCE = 1,200 µg/L; 1,1-DCE = 100 µg/L; VC = 170 µg/L). During the initial 8 weeks of the project, this well was under monitored natural attenuation (Figure 3-2). During this time period, a baseline for CVOCs, DX, DO, and pH were established. Air sparging was installed in MW-31 during week 8 and as a result the CVOCs measured decreased with the most significant being cDCE (cDCE = 79% decrease). This was to be expected as CVOCs have very high partial pressures and air stripping is a common remediation strategy. DX, contrastingly, did not decrease as drastically with only a 9% reduction during this initial period. Over the next 6 months (week 8-week 34), the compressor broke and was repaired twice which resulted in two additional periods of low oxygen levels (pink zones) and high oxygen levels (green zones). When the air

sparging was not in operation, the CVOCs increased, with cDCE eventually reaching historic concentrations. While the mechanical problems were unforeseen, it highlights the challenges of air sparging, which include its ability to remove volatile compounds while sparging is in operation and that being a non-destructive technology, which doesn't result in detoxification of contaminants. The native microbial population in MW-31 showed a total 16S gene abundance from $7.6x10^5$ to $2.1x10^8$ copies/mL (Figure 3-2). The highest total abundance for the community occurred during the air sparging periods, which potentially allowed certain aerobic and microaerophilic organisms to begin oxidizing these contaminant sources. DX degradation gene targets (*dxmB, aldH,* CB1190 16S) were also present, but at much lower concentrations than in MW-32. They ranged from $1.3x10^0$ to $1.0x10^4$ copies/mL. This background population may be considered an important factor for the slow, but significant DX removal over the total 8-month sampling period. Additionally, the *prmo* gene target did not significantly change with gene abundance ranging from $8.3x10^1$ to $4.5x10^2$ copies/mL. The *smmo* gene target decreased during the initial low oxygen period ($1.6x10^0$ copies/mL) and then slowly increased over time with a final concentration of $2.2x10^2$ copies/mL. This fluctuation is to be expected as higher O_2 levels can allow for increases in microbes equipped with "oxygenases".

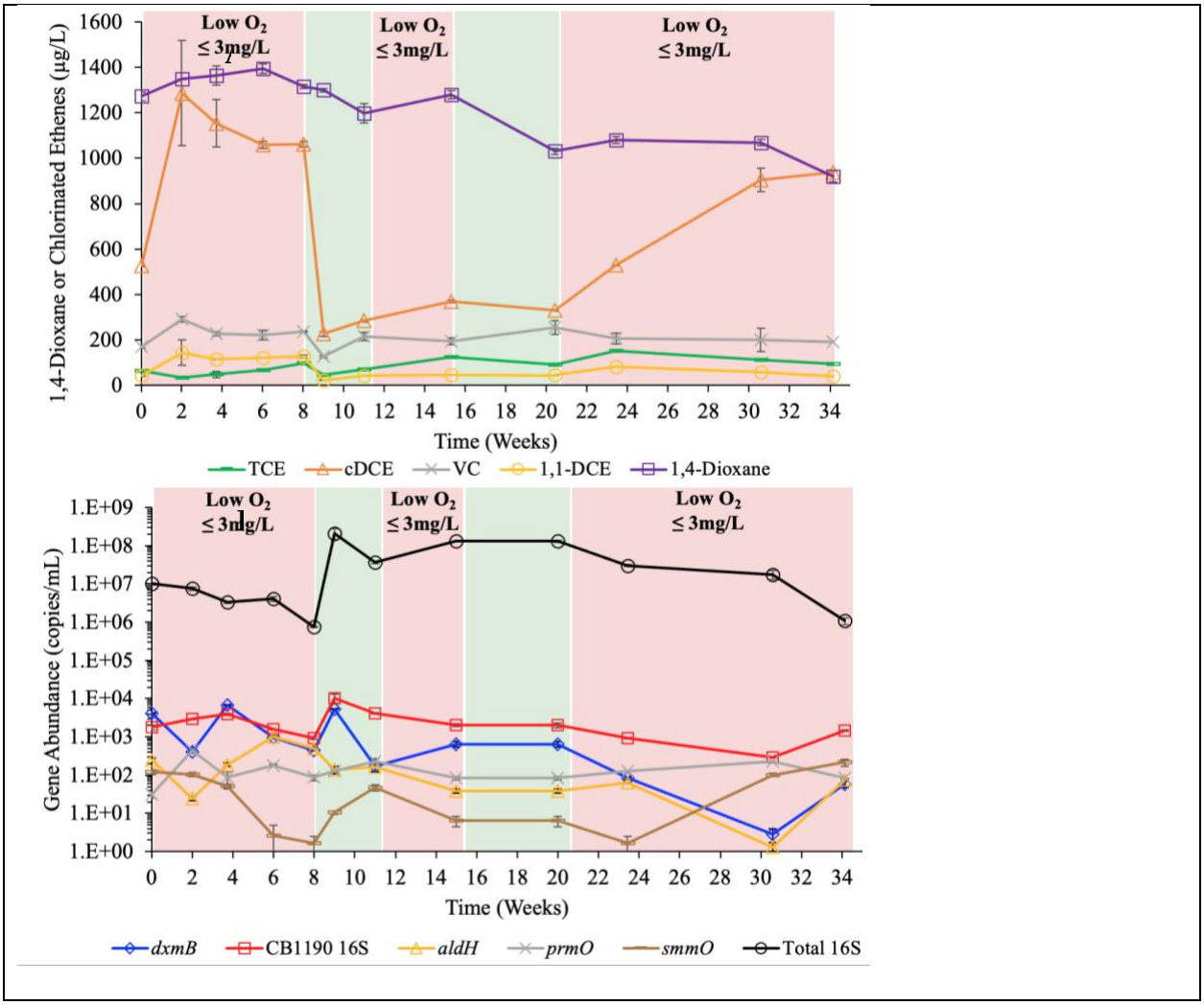

Figure 3-2 Chlorinated ethene, 1,4-dioxane, gene abundance, and oxgyen concentrations in Monitoring Well-31
Top). Chlorinated ethene and DX concentrations. Air sparging began on week 8. *Bottom)*. Gene abundances of the native ground water microbial population. The pink shaded areas indicate when dissolved oxygen was below or equal to 3 mg/L and the green shaded areas indicate when the oxygen was above 3 mg/L. Error bars indicate the standard deviation of analytical triplicates.

3.3.3 MW-32: CB1190 Bioaugmentation Resulted in CVOC and 1,4-Dioxane Removal When Oxygen ≥ 3 mg/L

The initial injection of nutrients and CB1190 culture resulted in a dilution of CVOCs and DX but these concentrations quickly equilibrated to historic concentrations (DX = 1,400 µg/L; TCE = 50 µg/L; cDCE = 970 µg/L; 1,1-DCE = 88 µg/L; VC = 127 µg/L) by the next sampling point (Figure 3-3). Over the 8-month period, degradation occurred most significantly during

aerobic conditions and was only interrupted by two periods of time when the average DO dropped below 3 mg/L. This was likely due to an air sparging pump malfunction. During these two low oxygen periods, CVOC and DX concentrations increased slightly due to the up-gradient source zone feeding into this area and the lack of electron acceptor for CB1190. The most notable changes in contaminants were observed during the initial 3 months where DX and cDCE were reduced by almost half (DX = 48% decrease; cDCE = 47% decrease) and the end of the project where DX, cDCE, VC, and 1,1-DCE were at historic lows. CB1190's biomass (as estimated by *dxmB*, *aldH*, and CB1190 16S), remained the highest during the first 3-month period, which ranged from $4.2x10^3$-$1.6x10^6$ copies/mL (Figure 3-3B). This is a large portion of the total 16S population and can be considered a significant factor in the removal of DX and CVOCs. Over the following 4 months, which contained two periods of low oxygen, CB1190's cell abundance slowly declined but still maintained DX and CVOC removal when DO was equal to or above 3 mg/L. The other gene targets monitored, *prmo* and *smmo*, slowly increased over time, which was likely due to the air sparging and nutrient amendments. By the end of the project, an estimated 130 mg of total DX was removed by CB1190.

In conclusion, the post-ERD treatment of recalcitrant groundwater contaminants such as CVOCs and DX can be further improved by combining aerobic biostimulation and bioaugmentation, particularly CB1190 + air sparging, for the removal of DX and cDCE *in situ*.

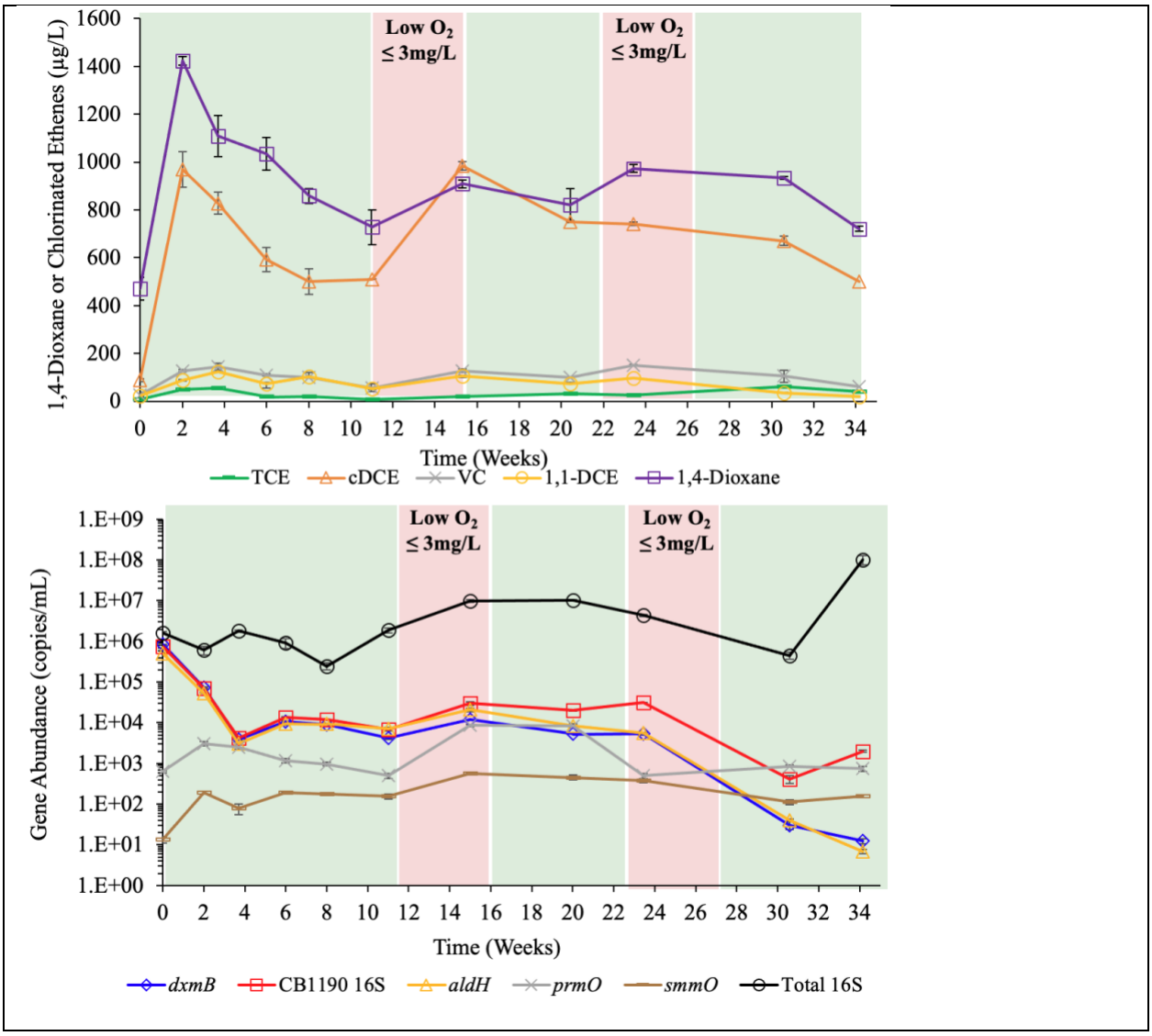

Figure 3-3 Chlorinated ethene, 1,4-dioxane, gene abundance, and oxygen concentrations in Monitoring Well-32

Top). Chlorinated ethene and DX concentrations post CB1190 bioaugmentation. *Bottom)*. CB1190 and native microbial gene abundances. The pink shaded areas indicate when dissolved oxygen was below or equal to 3 mg/L and the green shaded areas indicate when the oxygen was above 3 mg/L. Error bars indicate the standard deviation of analytical triplicates.

3.4 References

(1) Anderson, R.H., J.K. Anderson, and P.A. Bower. Co-Occurrence of 1,4-Dioxane with Trichloroethylene in Chlorinated Solvent Groundwater Plumes at Us Air Force Installations: Fact or Fiction. Integr. Environ. Asses., 2012, 8, 731-737.

(2) Mohr, T.K.G., W.H. DiGuiseppi, J.W. Hatton, and J.K. Anderson, Environmental Investigation and Remediation: 1,4-Dioxane and Other Solvent Stabilizers, Second Edition. 2020: CRC Press. 1-529.

(3) Godri Pollitt, K.J., J.-H. Kim, J. Peccia, M. Elimelech, Y. Zhang, G. Charkoftaki, B. Hodges, I. Zucker, H. Huang, N.C. Deziel, K. Murphy, M. Ishii, C.H. Johnson, A. Boissevain, E. O'Keefe, P.T. Anastas, D. Orlicky, D.C. Thompson, and V. Vasiliou. 1,4-Dioxane as an Emerging Water Contaminant: State of the Science and Evaluation of Research Needs. Sci. Total Environ., 2019, 690, 853-866.

(4) Zhang, S., P.B. Gedalanga, and S. Mahendra. Advances in Bioremediation of 1,4-Dioxane-Contaminated Waters. J. Environ. Manage., 2017, 204, 765-774.

(5) Steffan, R.J., K.L. Sperry, M.T. Walsh, S. Vainberg, and C.W. Condee. Field-Scale Evaluation of in Situ Bioaugmentation for Remediation of Chlorinated Solvents in Groundwater. Environ. Sci. Technol., 1999, 33, 2771-2781.

(6) Hood, E.D., D.W. Major, J.W. Quinn, W.S. Yoon, A. Gavaskar, and E.A. Edwards. Demonstration of Enhanced Bioremediation in a TCE Source Area at Launch Complex 34, Cape Canaveral Air Force Station. Ground Water Monit. R., 2008, 28, 98-107.

(7) Hinchee, R.E., A. Leeson, and L. Semprini, Bioremediation of Chlorinated Solvents. 1995, Colombus, OH: Battelle Press.

(8) Suttinun, O., E. Luepromchai, and R. Müller. Cometabolism of Trichloroethylene: Concepts, Limitations and Available Strategies for Sustained Biodegradation. Reviews in Environ. Sci. Biotechnol., 2013, 12, 99-114.

(9) Polasko, A.L., A. Zulli, P.B. Gedalanga, P. Pornwongthong, and S. Mahendra. A Mixed Microbial Community for the Biodegradation of Chlorinated Ethenes and 1,4-Dioxane. Environ. Sci. Technol. Lett., 2019, 6, 49-54.

(10) Zhang, S., P.B. Gedalanga, and S. Mahendra. Biodegradation Kinetics of 1,4-Dioxane in Chlorinated Solvent Mixtures. Environ. Sci. & Technol., 2016, 50, 9599-9607.

(11) Gedalanga, P.B., P. Pornwongthong, R. Mora, S.-Y.D. Chiang, B. Baldwin, D. Ogles, and S. Mahendra. Identification of Biomarker Genes to Predict Biodegradation of 1,4-Dioxane. Appl. Environ. Microbiol., 2014, 80, 3209-3218.

Chapter 4 Vinyl Chloride and 1,4-Dioxane Metabolism by *Pseudonocardia dioxanivorans* CB1190

4.1 Introduction

Vinyl chloride (VC) is a known carcinogen and priority pollutant that serves as a continual threat to groundwater quality (1-3). Despite the fact it is largely used in the production of poly vinyl chloride (4), its presence in groundwater is mainly due to biological reduction of the widespread groundwater pollutant, trichloroethylene (TCE) (5). Biological reductive dechlorination is often implemented as a remediation strategy for sites containing chlorinated ethenes because microorganisms equipped with reductive dehalogenases can respire these compounds to form the benign end-product, ethene (6-9). VC reduction is critical for achieving complete detoxification of chlorinated ethenes (5, 10). Although this process results in a non-toxic compound, the initiation and termination of this reaction can be disturbed by the presence of oxygen, insufficient electron donor or carbon source, substrate inhibition, or competition

among other microorganisms. These disturbances can lead to the accumulation of toxic intermediates such as cis-1,2-dichloroethene (cDCE) or VC (11-14). Currently, the Environmental Protection Agency has set a federally regulated maximum contaminant level (MCL) of 2 µg/L for VC, which is among the lowest for chlorinated ethenes (e.g. TCE MCL= 5 µg/L; cDCE MCL= 70 µg/L; 1,1-dichloroethene (1,1-DCE) MCL= 7 µg/L) (15). Microorganisms can transform VC and use it as an electron acceptor (respiration), electron donor (metabolism), or fortuitous, non-growth supporting (cometabolic) processes.

Cometabolic VC degradation has been observed under both anaerobic and aerobic environments. For example, anaerobic VC oxidation can be carried out via the non-growth linked process, oxidative acetogenesis (16). In this VC mineralization pathway, acetate is formed as a major intermediate and then readily degraded to CH_4 and CO_2 (16-18). Studies have indicated that this process is cometabolic due to the disappearance of VC and lack of ethene production, stable isotope fractionation analyses, and dependence on glucose as a growth substrate (16, 18-21). Anaerobic oxidative acetogenesis has been reported in environmental samples under Fe(III)-reducing, humic acid-reducing, Mn(IV)-reducing, SO_4^{2-}-reducing, and methanogenic conditions (22-27).

Aerobic cometabolic oxidation of VC can be carried out by hydrocarbon-oxidizing bacteria that are equipped with mono- and di-oxygenase enzymes. These enzymes transform VC into products such as phenols, alcohols, or epoxides that can be further broken down spontaneously (14, 28). Both anaerobic and aerobic cometabolism of VC have benefits which include a broad distribution of bacteria with functional redundancies and an ability to rely on diverse carbon sources to maintain cellular activity. However, these processes also have significant disadvantages including 1). competition for oxygenase active sites by the growth

substrate and chloroethene co-substrate, 2). product toxicity from reactive intermediates, and 3). increased energy requirements such as the presence of a consistent but periodic growth substrates (14, 28).

Metabolic VC degradation has been observed under aerobic conditions by a variety of genera such as *Brevundimonas* (29), *Mycobacterium* (30-34), *Pseudomonas* (35, 36), *Nocardioides* (32), *Ochrobactrum* (36), *Rhodoferax* (29), *Ralstonia* (37), and *Tissierella* (29). VC-assimilating bacteria often initiate degradation via a monooxygenase-mediated epoxidation, which ultimately results in the terminal end product, CO_2. This process is advantageous not only because of reduced carbon source inputs, but also because multiple strains have shown to exhibit low half-velocity constants with respect to VC and oxygen (32). This indicates that they can degrade VC to low concentrations under microaerophilic conditions (32).

Chlorinated solvents, such as TCE and VC, frequently co-occur with the solvent stabilizer, 1,4-dioxane (dioxane or DX) (38, 39). DX is a stable cyclic ether and probable human carcinogen that presently can only be biodegraded under aerobic conditions (40-42). When DX is found with TCE or one of its intermediate by-products such as VC, particular bioremediation challenges arise due to opposing redox conditions favored by chlorinated ethene-and-DX-degrading bacteria. The co-occurrence of VC and DX will continue to grow as sites where TCE is remediated via enhanced reductive dechlorination or anaerobic natural attenuation. After mining data contained in the state of California's GeoTracker 2020 database, we found that of the 636 groundwater sites that had either DX or VC, approximately 1 in every 8 sites contained both pollutants and 2 out of 3 contained only VC (43). While various microorganisms exist that can metabolize VC under aerobic and anaerobic conditions, it would be advantageous to identify

a microbe that can survive fluctuating redox conditions and metabolize VC along with co-occurring contaminants like DX.

The objectives of this study were to evaluate simultaneous VC and DX biodegradation by *Pseudonocardia dioxanivorans* CB1190 under aerobic conditions. To better understand the molecular transformations happening inside the cell, we utilized the high-throughput technology, metabolomics, to obseccrve metabolic changes that occurred during the degradation process. Tracing the fate of ^{13}C-labeled VC during the growth phase of CB1190 would reveal the intermediates of the biodegradation pathway and the key enzymatic steps therein. This study would broaden the number of pure strains that can assimilate VC aerobically while also uniquely mineralizing DX. The microbial capabilities discovered would contribute substantially to field applications where complex contaminant mixtures and biogeochemical parameters are present in groundwater.

4.2 Materials and Methods

4.2.1 Chemicals

DX (99.8%, ACS grade) and sodium formate (99.0%, ACS grade) were obtained from Sigma-Aldrich. VC gas was purchased from Synquest Laboratory (Alachua, FL) and ^{13}C labeled VC (98%, 2% hydroquinone) was purchased from Cambridge Isotope Laboratories (Tewksbury, MA). The extraction solvent was composed of acetonitrile (ACS grade, 99.5%) and methanol (ACS grade, 99.8%), both of which were obtained from Fisher Scientific. The R2A agar was obtained from Millipore Sigma.

4.2.2 CB1190 Growth Conditions

Strain CB1190 was grown in the aerobic, circumneutral UCLA Modified Medium containing 2.292 g/L TES, 1 g/L NaCl, 0.3 g/L NH_4Cl, 0.3 g/L KCl, 0.2 g/L KH_2PO_4, 0.5

$MgCl_2$-$6H_20$, 0.015 g/L $CaCl_2$-$2H_2O$, 1mL per liter of trace elements stock solution A (Appendix Table B-1), and 1 mL per liter selenium/tungsten stock solution B (Appendix Table B-2) and allowed to degrade multiple amendments of 100 mg/L DX. These CB1190 cells were grown up using a 1% (v/v) transfer from an actively growing pure culture and incubated at 30°C with 150 rpm shaking. Periodically, the culture's purity was monitored by plating 100 µL of liquid onto R2A agar plates and incubated at 30°C for 2-3 days. After the culture reached late-exponential or early-stationary-phase and DX was degraded below 800 µg/L, cultures were used to inoculate experimental bottles.

4.2.3 Design of Batch Experiments

Batch experiments were carried out using sterile 1,000 mL glass serum bottles aliquoted with 200 mL of homogenized liquid culture and sealed with rubber stoppers and aluminum crimps. This 1:5 headspace ratio allowed for sufficient oxygen transfer to the cells, thus maintaining an aerobic environment. Killed control bottles were prepared in the same manner as experimental bottles apart from the cells being autoclaved for 30 min at 121°C. Aqueous VC concentrations were calculated based on Henry's Law constants (44). After VC amendments, bottles were allowed to equilibrate upright for 30 min at 30°C with 150 rpm shaking. To accurately measure VC at time 0, bottles containing abiotic media and VC were prepared beforehand and measured at the start of the experiment. This provided adequate equilibration time for the VC in the live and killed control bottles. Periodically, replicate samples were collected to measure VC, DX, total nucleic acids, and metabolites.

In order to track VC degradation metabolites, CB1190 cells were exposed to VC with ^{13}C-labeled carbon atoms. ^{13}C-labeled VC was amended to bottles via a gas tight syringe and measured using the same analytical method as non-isotopic VC.

4.2.4 Analytical Methods

4.2.4.1 Vinyl Chloride

VC concentrations were measured over time by extracting 500 µL of headspace from the experimental bottles and injecting the sample into an Agilent 6890 gas chromatograph (GC) equipped with a flame-ionized detector (FID) (Hewlett-Packard, Atlanta, GA) with a Restek® Stabilwax-DB capillary column (30 m × 0.53 mm i.d. × 1 µm). The injector was set at 220°C in splitless mode and the detector at 250 °C. The oven temperature was maintained at 100°C for 1 minute, then increased at 25°C/min to 150°C, at which it was held constant for an additional 0.5 min. The limit of VC detection using the GC-FID was 25 µg/L.

4.2.4.2 1,4-Dioxane

DX concentrations in the range of 800-10,000 µg/L were measured as previously described (45). 2 µL aqueous samples that were filtered by sterile 0.2 µm syringe filters and injected into the aforementioned Agilent 6890 GC, equipped with a Restek® Stabilwax-DB capillary column and FID. The limit of detection for DX using the GC-FID was 800 µg/L. DX concentrations in the range of 5-2,000 µg/L were measured using an Agilent 6890 gas chromatograph with a 5973 mass spectrometer detector and a Supelco SPB-1 Sulfur column (30 m × 0.32 mm i.d. × 4 µm) (GC-MS). The collected aqueous samples were prepared and processed using a previously described (46). 5 µL of processed sample was injected into the GC-MS equipped with a pulsed splitless injection. The limit of detection for DX using the GC-MS was 5 µg/L.

4.2.4.3 Metabolite Extraction, Measurement, and Quantification

For extraction of metabolites, 5-10 mL of liquid culture was removed using a sterile syringe and quickly vacuum-filtered onto a nylon membrane filter (0.45 µm, Millipore). Immediately following filtration, the membrane was submerged in a petri dish containing 500 µL extraction

solvent (40% acetonitrile:40% methanol:10% water) that had been pre-cooled to -20°C. The petri dish was then incubated at -20°C for 20 min. The cell extract was carefully pipetted into an Eppendorf tube and centrifuged at 13,000 x g for 10 min at 4°C. Following centrifugation, the supernatant was collected and prepared for liquid chromatography (LC) coupled to a high-resolution mass spectrometer (MS) via electrospray ionization (47). LC separation was achieved by a XBridge BEH Amide XP column (130Å, 2.5 μm, 2.1 mm x 150 mm; Waters) on a Vanquish Duo UHPLC system. A Q Exactive Plus Orbitrap mass spectrometer was operated in positive and negative modes scanning m/z 60-900 with a resolution (at m/z 200) of 140,000 (Full Width at Half Maxima). The LC-MS results were analyzed via the Metabolomic Analysis and Visualization Engine (MAVEN); the peaks were identified using authenticated standards and integrated for relative metabolite quantitation (48). Isotope labeled fractions were corrected for their natural abundance of ^{13}C as well as the impurities in the labeled substrates.

4.2.4.4 Total Nucleic Acids Extraction, Quantitative Polymerase Chain Reaction and cDNA Synthesis

A previously described phenol-chloroform extraction (46) was utilized to isolate total nucleic acids from samples that had been periodically collected from the experimental and killed control bottles. Upon total nucleic acid extraction, a quantitative polymerase chain reaction was performed to enumerate the cell abundance, as well as the level of expression for specific gene targets. SYBR-Green-based detection targets were utilized to quantify gene abundance and gene transcripts. The specific biomarker targets used to determine cell abundance and gene expression were 16S, *rpoD*, CB-*etn*ABCD, CB-*dioxy*ABCDE, *aldH*, and *dxmB* (46, 49, 50) and the primer sequences are listed in Table S3. We calculated the abundance of these targets and first normalized them to the copy numbers of the housekeeping gene RNA polymerase σ subunit D

(*rpoD*), and then subsequently, to those values obtained at time 0. The $2^{-\Delta\Delta CT}$ method was utilized to quantify gene transcripts (51).

4.3 Results and Discussion

4.3.1 Dioxane Biodegradation by CB1190 in the Presence of Vinyl Chloride

VC caused a dose dependent inhibition of DX biodegradation by CB1190 (Figure 4-1A-C, Appendix Figure B-1). An initial concentration of 100 µg/LVC decreased the 1,000 µg/L, 4,000 µg/L, and 10,000 µg/L DX biodegradation rates by 78±0.4% (24.4±1 µg-DX/L/h), 61±9% (84.1±8.6 µg-DX/L/h), and 92±0.9% (53.6±8.3 µg-DX/L/h), respectively, when compared to the DX biodegradation rates in VC free controls. The highest initial VC concentration (4,000 µg/L VC) decreased the 1,000 µg/L, 4,000 µg/L, and 10,000 µg/L DX biodegradation rates by 80±3% (22.3±5 µg-DX/L/h), 74±11% (52.6±9 µg-DX/L/h), 94±1.3% (44.3±12 µg-DX/L/h), respectively when compared to the DX biodegradation rates with 0 µg/L VC. This dose response relationship between VC and DX biodegradation could be the result of the membrane bound protein's susceptibility to inhibitor binding, membrane disruptions, or structural changes (52, 53).

DX mass removal generally decreased with increasing VC concentrations from 100 µg/L to 4,000 µg/L (Table 4-1). However, CB1190 with an initial DX concentration of 1,000 µg/L removed the same amount of DX mass in the presence of 100 µg/L VC or 0 µg/L VC. This could indicate that when VC is below an inhibitory threshold, which in this case was 100 µg/L VC, DX biodegradation may not be negatively impacted. Similarly, lower concentrations of certain CVOCs (e.g. 1,1,1-trichloroethane (1,1,1-TCA)) and metals (e.g. Ni, Zn, Cr (IV)) have been reported to also be non-inhibitory to CB1190's DX biodegradation rates (53-56). Increasing *dxmB* gene expression was dependent upon the initial concentration of DX and DX mass

remaining, despite increasing VC concentrations (Table 4-1, Appendix Figure B-2). This could indicate that VC does not directly repress the transcription of *dxmB* genes. Higher VC concentrations resulted in less DX removal and consequently more DX remaining to induce the *dxmB* gene target.

To date, 1,1-DCE was reported to be the most inhibitory chlorinated ethene towards DX biodegradation, but this study demonstrates that similar concentrations of VC are even more inhibitory. For example, DX biodegradation rates were 10 times higher in the presence of 5,000 µg/L TCE or cDCE (53) than 4,000 µg/L VC. Additionally, CB1190's DX biodegradation rate was approximately twice as high in the presence of 5,000 µg/L 1,1-DCE, one of the strongest CVOC inhibitors, compared to 4,000 µg/L VC (53). Similarly, in the presence of 2,000 µg/L 1,1-DCE or TCE, the tetrahydrofuran monooxygenase DX biodegradation rate decreased by an average of 75% and 70%, respectively (55). Convergently, 1,1-DCE has been shown to inhibit bacteria that biodegrade DX after growth on primary substrates such as propane (55, 57, 58). It is likely that VC would also be a stronger DX biodegradation inhibitor than 1,1-DCE to these microorganisms. Because many bacteria that cometabolize CVOCs also cometabolize DX, measurement and modeling of VC inhibition kinetics on DX cometabolism biodegradation would be complex but necessary to predict *in situ* degradation rates and clean up times. Unexpectantly, ethenes with a lower degree of chlorination such as VC have a stronger inhibition towards DX biodegradation (VC > 1,1-DCE > cDCE > TCE > 1,1,1-TCA).

Table 4-1 DX mass removal by CB1190 in the presence of VC and the corresponding *dxmB* gene expression.

VC (µg/L)	DX (µg/L) µg total mass	DX Mass Removed (µg)	DX Mass Remaining (µg)	*dxmB* Gene Expression (log_{10} Fold Change)
0	(0) 0 µg	--	--	--
100		--	--	-0.57 ± 0.17
1,500		--	--	-0.72 ± 0.29
4,000		--	--	**0.12 ± 0.23**
0	(1,000) 200 µg	225 ± 10	0	--
100		225 ± 10	0	**0.01 ± 0.27**
1,500		74 ± 9.4	151±1	-0.67 ± 0.26
4,000		47 ± 11	177±3	-0.85 ± 0.30
0	(4,000) 800 µg	700 ± 13	0	--
100		431 ± 25	267±23	-0.25 ± 0.47
1,500		267 ± 2.9	433±11	**0.89 ± 0.27**
4,000		171 ± 11	529±18	**0.75 ± 0.37**
0	(10,000) 2,000 µg	1,821 ± 37	0	--
100		739 ± 50	1,082±14	**0.95 ± 0.09**
1,500		286 ± 36	1,535±11	**0.60 ± 0.33**
4,000		200 ± 57	1,622±21	**0.76 ± 0.26**

Note:
dxmB gene expression values were normalized to the *rpoD* housekeeping gene and hour 20.
Relative positive *dxmB* gene expression values are bolded.
Mass removal and remaining was calculated using the VC concentrations at hour 0 and hour 40.

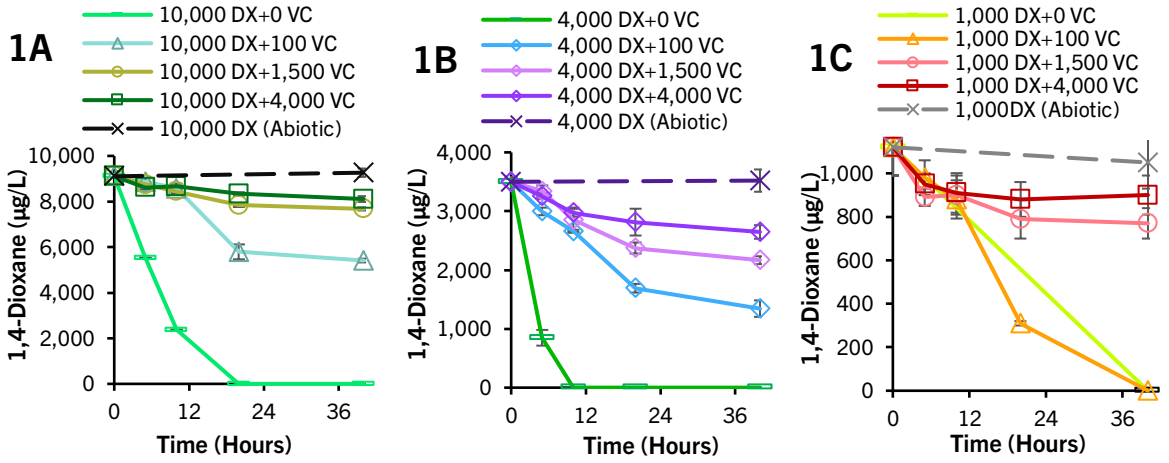

Figure 4-1 Inhibition on DX biodegradation by VC.
1A). 10,000 µg/L DX + VC 1B). 4,000 µg/L DX + VC 1C). 1,000 µg/L DX

4.3.2 Vinyl Chloride Biodegradation by CB1190 without and with Dioxane

After prior growth on DX, CB1190 was able to aerobically biodegrade VC. The degradation rates of VC by CB1190 cells at initial concentrations of 40 µg/L, 280 µg/L, or 780 µg/L VC

were calculated utilizing the first 12 hours of data and were as follows: 1.6 ± 0.05 µg VC/L/h, 6.4 ± 0.38 µg VC/L/h, 5.5 ± 0.71 µg VC/L/h, respectively (Figure 4-2A). The 40 µg/L VC bottles were reamended with VC on day two because CB1190 had successfully degraded VC to below detection limit. Increase in cell abundance was limited, which could be expected due to low growth yield and similar trends seen during the aerobic metabolic oxidation of cDCE (17) (Appendix Figure B-3). During VC biodegradation, CB1190 upregulated alkene monooxygenase (akMO) genes, namely CB-*etnABCD*, and down regulated the *dxmB* and dioxygenase genes (Appendix Figures B-4 to B-5). Comparably, previous research has shown that other VC-metabolizing genera utilize the akMO to catalyze epoxidation of VC to chlorooxirane and that these genes are inducible by VC (59-61). While the enzymes responsible for VC biodegradation in CB1190 are likely part of the soluble di-iron monooxygenase family, VC is likely not degraded by the DX-monooxygenase or dioxygenases.

CB1190 was able to simultaneously biodegrade VC and DX, regardless of the concentration. To determine the impact of DX on VC biodegradation, CB1190 was exposed to 2,000 µg/L DX and 40 µg/L, 280 µg/L or 780 µg/L VC (Figure 4-2B, Figure 4-2C). The VC degradation rates for 40 µg/L VC + DX, 280 µg/L VC + DX, and 780 µg/L VC + DX were 1.8 ± 0.06 µg VC/L/h, 4.7 ± 0.35 µg VC/L/h, and 4.0 ± 1.4 µg VC/L/h, respectively. While presence of DX decreased 280 µg/L VC's biodegradation rate (p-value < 0.05), the inverse was true for 40 µg/L VC, meaning CB1190's VC biodegradation rate at 40 µg/L was significantly higher in the presence of DX than DX free controls (p-value < 0.05). There was no significant difference in the VC biodegradation rates with or without DX at the highest VC concentration (780 µg/L VC). CB1190's gene abundance in the presence of VC and DX followed a similar trend to the VC only conditions (Appendix Figure B-6). When CB1190 cells were grown on dextrose or toluene

instead of DX, to prevent *dxmB* induction (46), the cells were still able to biodegrade VC (Appendix Figures B-7 to B-8). Interestingly, the converse was true for DX degradation meaning, when CB1190 cells were grown on toluene or glucose, DX degradation was stalled or inhibited (46). While CB1190 is largely known as a DX-metabolizing microorganism, it also has the unique ability to concurrently biodegrade inhibitory co-contaminants such as cDCE (62) and VC.

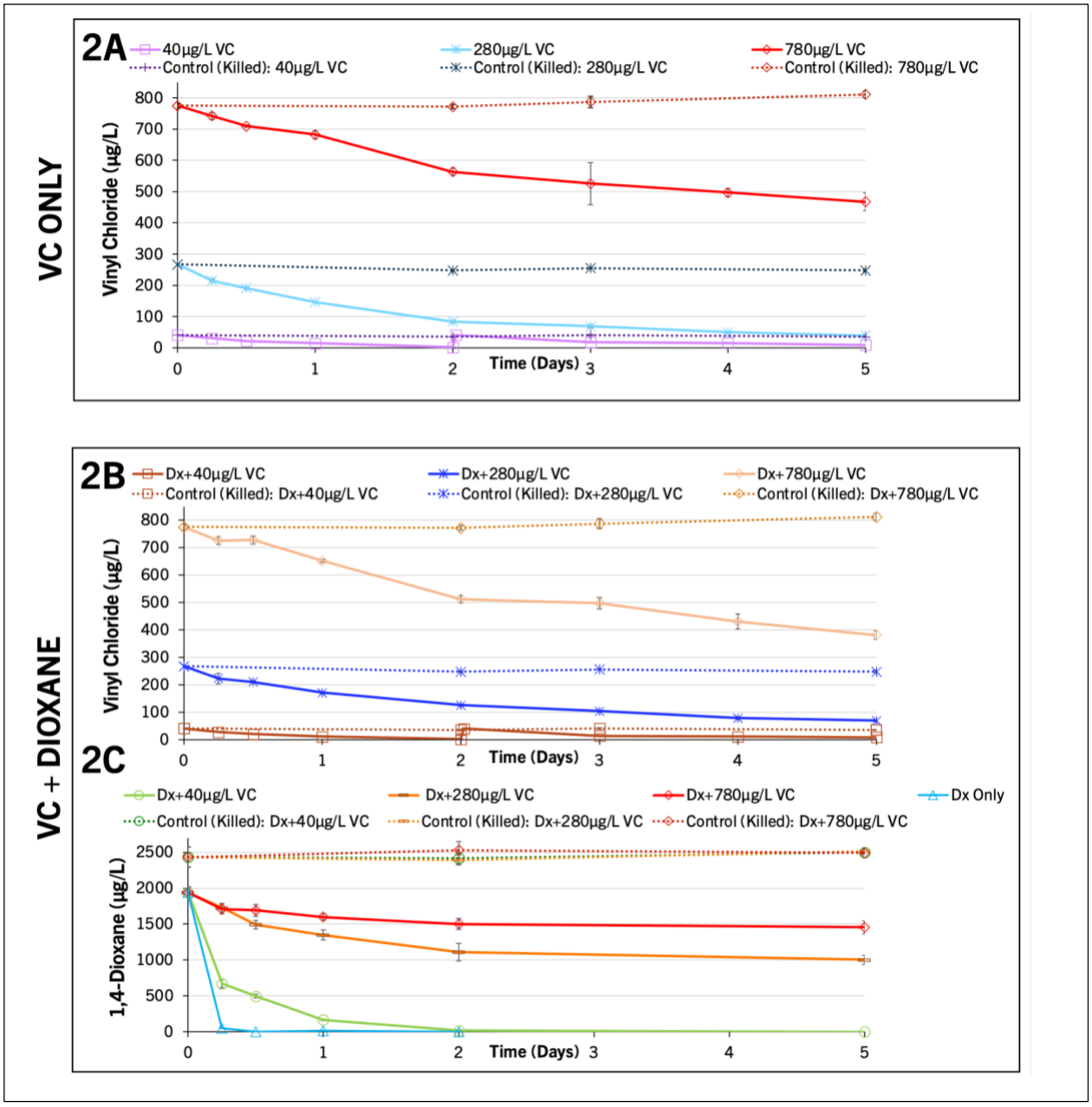

Figure 4-2 Biodegradation of VC by CB1190 with and without DX. **2A).** VC biodegradation at 40 µg/L, 280 µg/L, and 780 µg/L VC. **2B).** VC biodegradation in the presence of 2,000 µg/L DX **2C).** DX biodegradation occurring simultaneously with VC biodegradation. Error bars represent standard deviation of triplicates

4.3.3 Vinyl Chloride Assimilation by CB1190

VC incorporation into CB1190 cells was confirmed via introducing ^{13}C-labeled VC to the culture media and then observing the appearance of ^{13}C in the intracellular metabolites. As the concentration of isotopically labeled VC decreased in the media, M+1 labeling fraction by ^{13}C

increased for metabolites engaged in lipid and protein synthesis (e.g., aspartate, succinate, alpha ketoglutarate, serine, acetyl-CoA), nucleotide biosynthesis (e.g., hexose-6-phosphate and pentose-5-phosphate), and energy production (e.g., ATP) increased (Figure 4-3). These amino acids, keto acids, and sugar phosphate molecules are associated with metabolic pathways (e.g. TCA and glyoxylate cycle) in CB1190 as well as other microorganisms (63, 64). The isotopic labeling of these metabolites provides proof of incorporation of VC into the intracellular metabolism of CB1190. Moreover, the relative metabolite concentration fold change over time demonstrated that as VC was degraded, there was an increase in acetyl-CoA, which initiates the central carbon metabolism (Figure 4-3, Appendix Figure B-9). The isotopic labeled metabolites as well as relative metabolite changes provides direct evidence to the incorporation of VC into the intracellular metabolism. This indicates that CB1190 can use VC for its growth.

CB1190's conversion of VC to CO_2 is implied by the incorporation of labeled metabolites into pathways that result in organic carbon mineralization and ATP production. This also aligns with previous literature which demonstrated that aerobic metabolic oxidation of VC results in mineralization (14, 23, 28). For example, microcosms containing sediment and ^{14}C-VC showed near complete mineralization of 57 µM VC in just 2 days (24).

Collectively, these results confirm that CB1190 utilizes VC, a strong DX degradation inhibitor, as a sole source of carbon and energy. The identification of microorganisms capable of aerobically metabolizing DX, cDCE, and VC will increase our capacity to remove pollutant mixtures in varying redox zones across contaminated sites or wastewater streams.

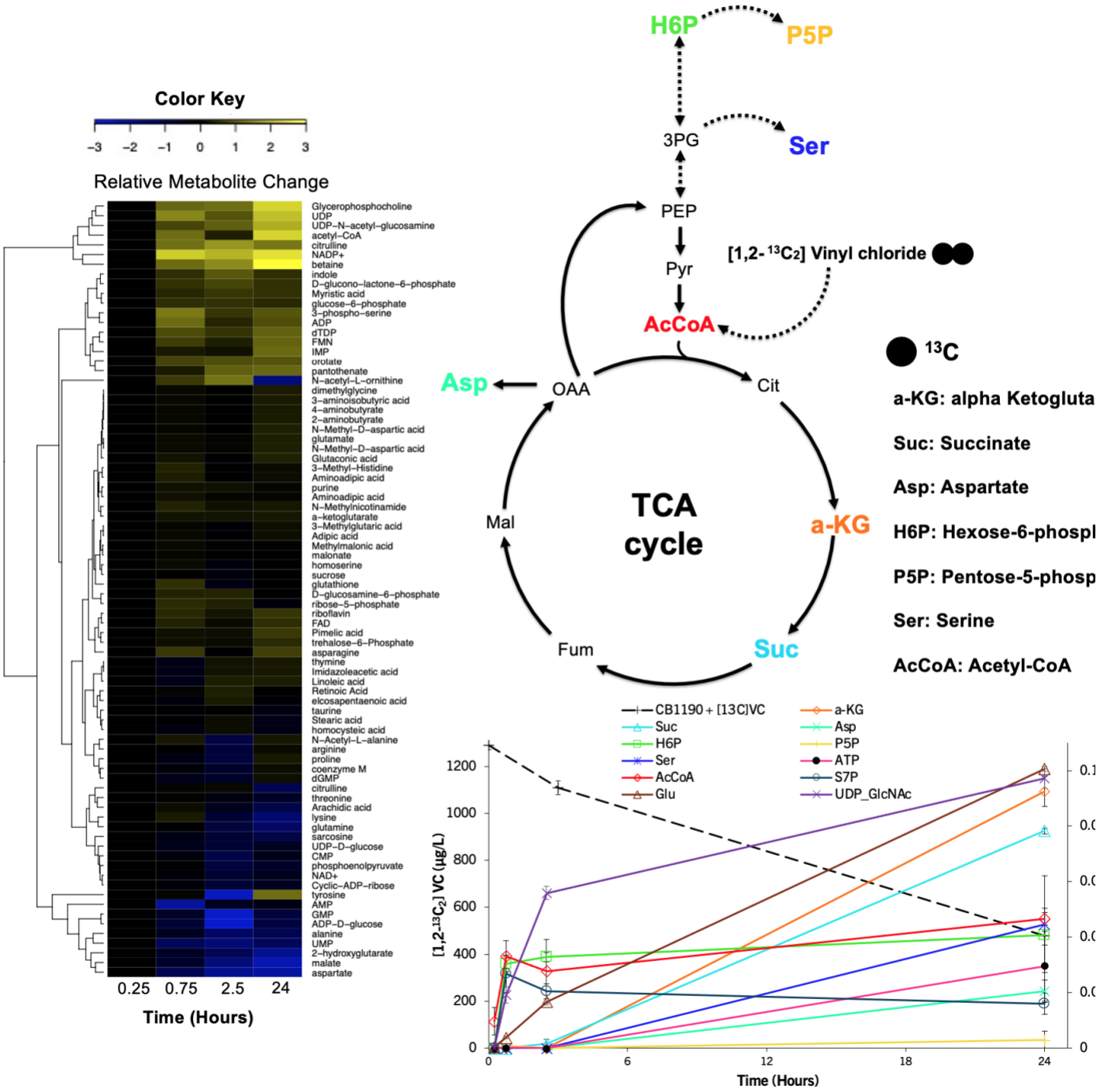

Figure 4-3 Assimilation of VC by CB1190.
The heatmap represents the intracellular change in metabolites present in CB1190. The samples were normalized to 0.25 hours, which was when the first sample was taken. The fraction of 1,2-$^{13}C_2$ VC (M+1) labeled in CB1190 are shown over time with the biodegradation curve of 1,2-$^{13}C_2$ VC. Labeled compounds that were detected are presented in TCA cycle. Error bars represent standard deviation of triplicates. Additional metabolite abbreviations correspond to the following S7P = Sedoheptulose-7-phosphate; Glu = Glutamate; Gln = Glutamine; UDP_GlcNAc = UDP-N-acetyl-glucosamine.

4.4 References

(1) *Toxicological Review of Vinyl Chloride*, U.S. EPA, 2000.

(2) Feron, V.J., C.F.M. Hendriksen, A.J. Speek, H.P. Til, and B.J. Spit. Lifespan Oral Toxicity Study of Vinyl Chloride in Rats. Food Cosm. Toxicol., 1981, 19, 317-333.

(3) Addendum to the Toxicological Profile for Vinyl Chloride. *Agency for Toxic Substances and Disease Registry*, 2016.

(4) Toxicological Profile for Vinyl Chloride. *Agency for Toxic Substances and Disease Registry*, 2006.

(5) Vogel, T.M. and P.L. McCarty. Biotransformation of Tetrachloroethylene to Trichloroethylene, Dichloroethylene, Vinyl Chloride, and Carbon Dioxide under Methanogenic Conditions. Appl. Environ. Microbiol., 1985, 49, 1080-1083.

(6) Major, D.W., M.L. McMaster, E.E. Cox, E.A. Edwards, S.M. Dworatzek, E.R. Hendrickson, M.G. Starr, J.A. Payne, and L.W. Buonamici. Field Demonstration of Successful Bioaugmentation to Achieve Dechlorination of Tetrachloroethene to Ethene. Environ. Sci. Technol., 2002, 36, 5106-5116.

(7) Quinn, J., C. Geiger, C. Clausen, K. Brooks, C. Coon, S. O'Hara, T. Krug, D. Major, W.-S. Yoon, A. Gavaskar, and T. Holdsworth. Field Demonstration of DNAPL Dehalogenation Using Emulsified Zero-Valent Iron. Environ. Sci. Technol., 2005, 39, 1309-1318.

(8) Scheutz, C., N.d. Durant, P. Dennis, M.H. Hansen, T. Jørgensen, R. Jakobsen, E.e. Cox, and P.L. Bjerg. Concurrent Ethene Generation and Growth of *Dehalococcoides* Containing Vinyl

Chloride Reductive Dehalogenase Genes During an Enhanced Reductive Dechlorination Field Demonstration. Environ. Sci. Technol., 2008, 42, 9302-9309.

(9) Okutsu, N., W. Tamura, M. Mizumoto, T. Ueno, H. Ishida, and T. Iizumi. Field Demonstration of Bioaugmentation in Trichloroethene-Contaminated Groundwater. Water Prac. Technol., 2012, 7.

(10) He, J., K.M. Ritalahti, K.-L. Yang, S.S. Koenigsberg, and F.E. Löffler. Detoxification of Vinyl Chloride to Ethene Coupled to Growth of an Anaerobic Bacterium. Nature, 2003, 424, 62-65.

(11) Abe, Y., R. Aravena, J. Zopfi, B. Parker, and D. Hunkeler. Evaluating the Fate of Chlorinated Ethenes in Streambed Sediments by Combining Stable Isotope, Geochemical and Microbial Methods. J. Contam. Hydrol., 2009, 107, 10-21.

(12) Middeldorp, P.J.M., M.L.G.C. Luijten, B.A.v.d. Pas, M.H.A.v. Eekert, S.W.M. Kengen, G. Schraa, and A.J.M. Stams. Anaerobic Microbial Reductive Dehalogenation of Chlorinated Ethenes. Bioremediation J., 1999, 3, 151-169.

(13) Wei K., Grostern A., Chan W.W.M., Richardson R.E., and Edwards E.A., *Electron Acceptor Interactions between Organohalide-Respiring Bacteria: Cross-Feeding, Competition, and Inhibition*, in *Organohalide-Respiring Bacteria*. 2016, Springer: Berlin, Heidelberg.

(14) Mattes, T.E., A.K. Alexander, and N.V. Coleman. Aerobic Biodegradation of the Chloroethenes: Pathways, Enzymes, Ecology, and Evolution. FEMS Microbiol. Rev., 2010, 34, 445-475.

(15) National Primary Water Regulations. *U.S. Environmental Protection Agency*, 2020.

(16) Bradley, P.M. and F.H. Chapelle. Acetogenic Microbial Degradation of Vinyl Chloride. *Environ. Sci. Technol., 2*000b, 34, 2761-2763.

(17) Bradley, P.M. and F.H. Chapelle. Aerobic Microbial Mineralization of Dichloroethene as Sole Carbon Sour*ce. Environ. Sci. Technol.*, 2000a, 34, 221-223.

(18) P.M., B. History and Ecology of Chloroethene Biodegradation: A Review. Biorem. J., 2003, 7, 81-109.

(19) Smits, T.H.M., A. Assal, D. Hunkeler, and C. Holliger. Anaerobic Degradation of Vinyl Chloride in Aquifer Microcosms. J. Environ. Qual., 2011, 40, 915-922.

(20) Hata, J., N. Miyata, E. Kim, K. Takamizawa, and K. Iwahori. Anaerobic Degradation of cis-1,2-Dichloroethylene and Vinyl Chloride by *Clostridium* sp. Strain DC1 Isolated from Landfill Leachate Sediment. *J. Biosci. Bioeng., 2*004, 97, 196-201.

(21) Kim, E., I. Nomura, Y. Hasegawa, and K. Takamizawa. Characterization of a Newly Isolated cis-1,2-Dichloroethylene and Aliphatic Compound-Degrading Bacterium, *Clostridium* sp. strain KYT-1. Biotechnol. Bioproc. , 2006, 11, 553-556.

(22) Bradley, P.M. and F.H. Chapelle. Anaerobic Mineralization of Vinyl Chloride in Fe(III)-Reducing Aquifer Sediments. Environ. Sci. Technol. 1996, 30, 2084-2086.

(23) Bradley, P.M. and F.H. Chapelle. Microbial Mineralization of VC and DCE under Different Terminal Electron Accepting Conditions. Anaerobe, 1998a, 4, 81-87.

(24) Bradley, P.M. and F.H. Chapelle. Effect of Contaminant Concentration on Aerobic Microbial Mineralization of DCE and VC in Stream-Bed Sediments. Environ. Sci. Technol., 1998b, 32, 553-557.

(25) Bradley, P.M. and F.H. Chapelle. Role for Acetotrophic Methanogens in Methanogenic Biodegradation of Vinyl Chloride. Environ. Sci. Technol., 1999a, 33, 3473-3476.

(26) Bradley, P.M. and F.H. Chapelle. Acetogenic Microbial Degradation of Vinyl Chloride. *Environ. Sci. Technol.,* 2000, 34, 2761-2763.

(27) Bradley, P.M., S. Richmond, and F.H. Chapelle. Chloroethene Biodegradation in Sediments at 4c. Appl. Environ. Microb., 2005, 71, 6414-6417.

(28) Dolinová, I., M. Štrojsová, M. Černík, J. Němeček, J. Macháčková, and A. Ševců. Microbial Degradation of Chloroethenes: A Review. Environ. Sci. Pollut. Res., 2017, 24, 13262-13283.

(29) Paes, F., X. Liu, T.E. Mattes, and A.M. Cupples. Elucidating Carbon Uptake from Vinyl Chloride Using Stable Isotope Probing and Illumina Sequencing. Appl. Microbiol. Biotechnol., 2015, 99, 7735-7743.

(30) Hartmans, S., J.A.M. de Bont, J. Tramper, and K.C.A.M. Luyben. Bacterial Degradation of Vinyl Chloride. Biotechnol. Lett., 1985, 7, 383-388.

(31) Hartmans, S. and J.A. De Bont. Aerobic Vinyl Chloride Metabolism in *Mycobacterium aurum* L1. Appl. Environ. Microbiol., 1992, 58, 1220-1226.

(32) Coleman, N.V., T.E. Mattes, J.M. Gossett, and J.C. Spain. Phylogenetic and Kinetic Diversity of Aerobic Vinyl Chloride-Assimilating Bacteria from Contaminated Sites. Appl. Environ. Microbiol., 2002b, 68, 6162-6171.

(33) Fathepure, B.Z., V.K. Elango, H. Singh, and M.A. Bruner. Bioaugmentation Potential of a Vinyl Chloride-Assimilating *Mycobacterium* Sp., Isolated from a Chloroethene-Contaminated Aquifer. FEMS Microbiol. Lett., 2005, 248, 227-234.

(34) Taylor, A.E., M.E. Dolan, P.J. Bottomley, and L. Semprini. Utilization of Fluoroethene as a Surrogate for Aerobic Vinyl Chloride Transformation. Environ. Sci. Technol., 2007, 41, 6378-6383.

(35) Verce, M.F., R.L. Ulrich, and D.L. Freedman. Characterization of an Isolate That Uses Vinyl Chloride as a Growth Substrate under Aerobic Conditions. Appl. Environ. Microbiol., 2000, 66, 3535-3542.

(36) Danko, A.S., M. Luo, C.E. Bagwell, R.L. Brigmon, and D.L. Freedman. Involvement of Linear Plasmids in Aerobic Biodegradation of Vinyl Chloride. Appl. Environ. Microbiol., 2004, 70, 6092-6097.

(37) Elango, V.K., A.S. Liggenstoffer, and B.Z. Fathepure. Biodegradation of Vinyl Chloride and cis-Dichloroethene by a *Ralstonia* sp. strain TRW-1. Appl. Microbiol. Biotechnol., 2006, 72, 1270-1275.

(38) Adamson, D.T., R.H. Anderson, S. Mahendra, and C.J. Newell. Evidence of 1,4-Dioxane Attenuation at Groundwater Sites Contaminated with Chlorinated Solvents and 1,4-Dioxan*e*. Environ. Sci. Technol., 2015, 49, 6510-6518.

(39) Anderson, R.H., J.K. Anderson, and P.A. Bower. Co-Occurrence of 1,4-Dioxane with Trichloroethylene in Chlorinated Solvent Groundwater Plumes at Us Air Force Installations: Fact or Fiction. Integr. Environ. Asses., *2*012, 8, 731-737.

(40) Mohr, T.K.G., W.H. DiGuiseppi, J.W. Hatton, and J.K. Anderson, *Environmental Investigation and Remediation: 1,4-Dioxane and Other Solvent Stabilizers, Second Edition*. 2020: CRC Press. 1-529.

(41) *Technical Fact Sheet-1,4-Dioxane: Scope of the Risk Evaluation for 1,4-Dioxane.*, U.S. EPA, 2017.

(42) Zhang, S., P.B. Gedalanga, and S. Mahendra. Advances in Bioremediation of 1,4-Dioxane-Contaminated Waters. J. Environ. Manage., *20*17, 204, 765-774.

(43) Tsai, K., A. Polasko, and S. Mahendra, *From* "Wet Lab" to Matlab: Invesitaging Potential Groundwater Sites Where Bioremediation Can Be an Effective Strategy, in *Annual Biomedical Research Conference for Minority Students*. 2020: Virtual.

(44) Gossett, J.M. Measurement of Henry's Law Constants for C_1 and C_2 Chlorinated Hydrocarbons. Environ. Sci. Technol., 1987, 21, 202-208.

(45) Myers, M.A., N.W. Johnson, E.Z. Marin, P. Pornwongthong, Y. Liu, P.B. Gedalanga, and S. Mahendra. Abiotic and Bioaugmented Granular Activated Carbon for the Treatment of 1,4-Dioxane-Contaminated Wa*ter*. Environ. Pollut., 2018, 240, 916-924.

(46) Gedalanga, P.B., P. Pornwongthong, R. Mora, S.-Y.D. Chiang, B. Baldwin, D. Ogles, and S. Mahendra. Identification of Biomarker Genes to Predict Biodegradation of 1,4-Dioxane. Appl. Environ. Microbiol., 2014, 80, 3209-3218.

(47) Wang, L., X. Xing, L. Chen, L. Yang, X. Su, H. Rabitz, W. Lu, and J.D. Rabinowitz. Peak Annotation and Verification Engine for Untargeted LC–MS Metabolomics. Anal. Chem., 2019, 91, 1838-1846.

(48) Clasquin, M.F., E. Melamud, and J.D. Rabinowitz. LC-MS Data Processing with Maven: A Metabolomic Analysis and Visualization Engine. Curr. Protoc. Bioinformatics, 2012, Chapter 14, Unit14.11.

(49) Amann, R.I., W. Ludwig, and K.H. Schleifer. Phylogenetic Identification and in Situ Detection of Individual Microbial Cells without Cultivation. Microbiol. Rev., 1995, 59, 143-169.

(50) Sales, C.M., A. Grostern, J.V. Parales, R.E. Parales, and L. Alvarez-Cohen. Oxidation of the Cyclic Ethers 1,4-Dioxane and Tetrahydrofuran by a Monooxygenase in Two *Pseudonocardia* Species. Appl. and Environ. Microbiol., 2013, 79, 7702-7708.

(51) Livak, K.J. and T.D. Schmittgen. Analysis of Relative Gene Expression Data Using Real-Time Quantitative PCR and the 2(-Delta Delta C(T)) Method. Methods, 2001, 25, 402-408.

(52) Ely, R.L., K.J. Williamson, M.R. Hyman, and D.J. Arp. Cometabolism of Chlorinated Solvents by Nitrifying Bacteria: Kinetics, Substrate Interactions, Toxicity Effects, and Bacterial Response. Biotechnol. Bioeng., 1997, 54, 520-534.

(53) Zhang, S., P.B. Gedalanga, and S. Mahendra. Biodegradation Kinetics of 1,4-Dioxane in Chlorinated Solvent Mixtures. *Environ. Sci. & Technol., 2016,* 50, 9599-9607.

(54) Johnson, N.W., P.B. Gedalanga, L. Zhao, B. Gu, and S. Mahendra. Cometabolic Biotransformation of 1,4-Dioxane in Mixtures with Hexavalent Chromium Using Attached and Planktonic Bacter*ia. Sci. Total Environ., 20*20, 706, 135734.

(55) Li, F., D. Deng, and M. Li. Distinct Catalytic Behaviors between Two 1,4-Dioxane-Degrading Monooxygenases: Kinetics, Inhibition, and Substrate Range. Environ. Sci. Technol., 2020, 54, 1898-1908.

(56) Pornwongthong, P., A. Mulchandani, P.B. Gedalanga, and S. Mahendra. Transition Metals and Organic Ligands Influence Biodegradation of 1,4-Dioxane. Appl. Biochem. Biotechnol., 2014, 173, 291-306.

(57) Deng, D., F. Li, C. Wu, and M. Li. Synchronic Biotransformation of 1,4-Dioxane and 1,1-Dichloroethylene by a Gram-Negative Propanotroph *Azoarcus* sp. DD4. Environ. Sci. Technol. Lett., 2018, 5, 526-532.

(58) Mahendra, S., *In Situ Biodegradation of 1,4-Dioxane: Effects of Metals and Chlorinated Solvent Co-Contaminants*. 2020, Strategic Environmental Research and Development Program (SERDP): ER-2300.

(59) Coleman, N.V. and J.C. Spain. Epoxyalkane: Coenzyme M Transferase in the Ethene and Vinyl Chloride Biodegradation Pathways of *Mycobacterium* strain JS60. J. Bacteriol., 2003a, 185, 5536-5545.

(60) Mattes, T.E., N.V. Coleman, J.C. Spain, and J.M. Gossett. Physiological and Molecular Genetic Analyses of Vinyl Chloride and Ethene Biodegradation in *Nocardioides* sp. strain JS614. Arch. Microbiol., 2005, 183, 95-106.

(61) Chuang, A.S. and T.E. Mattes. Identification of Polypeptides Expressed in Response to Vinyl Chloride, Ethene, and Epoxyethane in *Nocardioides* sp. strain JS614 by Using Peptide Mass Fingerprinting. Appl. Environ. Microbiol., 2007, 73, 4368-4372.

(62) Polasko, A.L., A. Zulli, P.B. Gedalanga, P. Pornwongthong, and S. Mahendra. A Mixed Microbial Community for the Biodegradation of Chlorinated Ethenes and 1,4-Dioxane. Environ. Sci. Technol. Lett., 2019, 6, 49-54.

(63) Grostern, A., C.M. Sales, W. Zhuang, O. Erbilgin, and L. Alvarez-Cohen. Glyoxylate Metabolism Is a Key Feature of the Metabolic Degradation of 1,4-Dioxane by *Pseudonocardia Dioxanivorans* strain CB1190. Appl. Environ. Microbiol., 2012, 78, 3298-3308.

(64) Mahendra, S., C.J. Petzold, E.E. Baidoo, J.D. Keasling, and L. Alvarez-Cohen. Identification of the Intermediates of *in vivo* Oxidation of 1,4-Dioxane by Monooxygenase-Containing Bacteria. Environ. Sci. & Technol., 2007, 41, 7330-7336.

Chapter 5 Assessment of Microbial Adhesion to Modified Substrates and Multipronged Approach for the Accurate Quantification of Biofilms on Surfaces

5.1 Introduction

According to a national survey performed in 2007, about 1.7 million hospital-acquired infections (HAIs) are reported annually, accounting for more than 99,000 deaths and ~$30 billion in direct medical costs.(1) Despite the reduction of HAIs in recent years through improved antiseptic techniques, surgical procedures, and diagnosis, HAIs declines are slowing down indicating the need for new preventive methods.(2) It is estimated that 60-70% of HAIs are associated with the use of implantable medical devices. These infections occur due to the colonization of bacteria on the device surfaces and most, if not all, devices are affected.(3)

It is estimated that half of all HAIs are attributed to the growth of biofilms.(4) Biofilms form when replicating bacterial cells secrete extracellular polymeric substances that contain an insoluble mixture of proteins and polysaccharides.(5) This three-dimensional gelatinous matrix protects the pathogenic cells from the host defense mechanisms and reduces the diffusion rate of drugs through the matrix, rendering the cells within the biofilm significantly more resistant to antibiotics than in their planktonic state.(6) Furthermore, biofilms are linked to recurring infections, and already-formed biofilms are extremely difficult to resolve.(7) As medical device surfaces are a nidus for biofilm growth, significant research has focused on the prevention of biofilm growth to reduce HAIs.(8-10)

The biofilm formation cascade is initiated by planktonic bacterial cell adhesion to a surface. Without initial attachment, the biofilm formation is prevented or reduced. Early research on biofilm growth demonstrated that weak van der Waals forces and hydrophobic interactions enable the first colonizers to reversibly adhere to surfaces.(11, 12) Using self-assembled

monolayers, Whitesides et al. surveyed several functional groups to determine surface functionalities that promote or hinder the non-specific adsorption of proteins.(13, 14) The functional groups that exhibited the lowest adhesion were electrostatically neutral hydrophilic moieties that contained hydrogen bond donating groups.(13) From these design rules, many material coatings have been developed and shown to reduce adhesion of proteins and microorganisms. However, these coatings are substrate dependent, require pretreatment steps, and/or require extreme reaction conditions that do not enable the surfaces to be permanently modified.(15-20) For these reasons, commercial use of antifouling coatings in medical devices are uncommon. Current commercial coatings rely on the elution of antibiotics from a polymer matrix that are costly and only partially effective.(10)

Here, we describe a permanent antifouling coating that resists protein and bacterial adhesion utilizing a simple, scalable photo-activated treatment. Our criteria for the coating were as follows: (i) the coating must be able to permanently bind to clinically relevant plastics and rubbers; (ii) the coating must be applied rapidly under ambient conditions; and (iii) the coating must be non-toxic. The zwitterionic polymer polysulfobetaine (PSB) was selected as the antifouling component of the coating to benefit from its biocompatibility, ultralow-fouling properties, and oxidative stability. By adsorbing water electrostatically, PSB coatings form a thin hydration barrier that prevents organic materials from adhering to surfaces.(21) Commonly used approaches to attach PSB coatings to surfaces, such as radical-initiated graft polymerizations of PSB-methacrylate necessitate the use of oxygen-free conditions,(22) preconditioning steps,(23) or long reaction times (24) that do not meet scalability requirements. To circumvent the use of air-free graft polymerizations, we employ perfluorophenylazide (PFPA) chemistry as a molecular anchor to link the PSB coatings onto the surfaces of polymeric materials under

ambient conditions. When triggered with UV-light, PFPA moieties generate a highly reactive nitrene that forms covalent bonds with materials containing amines, C=C double bonds, and C-H bonds.(25, 26) With this method, PSB is rapidly coated onto a broad range of substrates using UV light under ambient conditions with no preconditioning steps. Thus, many different medical devices may be quickly and conveniently coated on a manufacturing level.

We demonstrate the effect of the coating on PDMS as an exemplary, extremely difficult to permanently modify, model for a common rubber used in medical devices. Commonly known as silicone, PDMS is widely used for its biocompatibility, good chemical stability, ease of fabrication using injection molding or extrusion, and low cost. Many implantable device makers have moved away from classical medical elastomers and plastics such as latex and polyvinyl chloride due to allergens (27) or plasticizers (28) in these materials that leach out and lead to irritation. PDMS-based devices do not require plasticizers and have been shown to lead to fewer complications than latex and polyurethane-based devices.(29)

Despite its ideal properties, the non-polar nature of PDMS facilitates the adhesion of organic materials. Bacteria, platelets, proteins, and other biomolecules bind strongly to the hydrophobic surfaces of PDMS elastomers, leading to the colonization and proliferation of biofilms.(21) When common hydrophilic surface treatments are performed on PDMS, such as plasma oxidation,(30) UV-ozone,(31) or corona discharge,(32) the effects are short-term due to strong hydrophobic recovery. The highly mobile chains of PDMS (glass transition temperature ~ -120 °C) can reorient themselves to “hide” the surface modified elastomers, when exposed to air, within hours.(33) Other methods seeking long-lasting hydrophilic PDMS surfaces typically require preconditioning steps with silane (34-36) chemistry or radical polymerization.(34, 37) These steps must be performed in closed containers, and/or under the protection of inert gas. Due

to the high solubility of oxygen relative to nitrogen in PDMS,(38) additional steps and time are required to remove the oxygen from PDMS so that the radical reaction can proceed efficiently. These strict reaction conditions have significantly increased the treatment costs and limited the surface modification of PDMS to lab scale demonstrations. With our method, for the first time, PDMS substrates can be permanently and rapidly modified under ambient conditions, without pretreatment. We then demonstrate the coating's exceptional antibiofouling efficacy by challenging it against protein, mammalian cells, bacteria, and fungus. To support its use in implantable devices, the cytotoxicity of the coating has also been investigated.

Chronic infections are associated with microbial growth in the form of adhered colonies surrounded by large exopolysaccharide matrices, which are used to establish hazardous biofilms.(39) Biofilms are less susceptible to host defenses such as macrophage phagocytosis and can become resistant to antibiotics resulting in reduced treatability.(40) Medical tubing is a target for biofilm formation and is often the cause of severe infections, especially because it serves as a hiding place for microbes where the immune system is less effective.(41, 42) For example, urinary catheter tubing is associated with over 75% of urinary tract infections, which are the most common health care-associated infections (HCAIs).(43)

There is currently no 'gold standard' available to evaluate the presence of microbial biofilms from medical tubing to assist in the diagnosis and prevention of clinical infections.(8) Current standard methods target: 1) Viable cells via plate counting or flow cytometry, 2) Total biomass via optical density, 3) Extracellular polymeric substances via resazurin dye, crystal violet dye, or live/dead staining, or 4) Cellular activity via ATP quantification (44-47). Reliable detection by these assays is limited by factors such as small-colony variants, non-culturable microbes, and false positives resulting from the inability to distinguish live from dead cells. Despite these tests'

broad availability, they are rarely performed together. Furthermore, the above limitations prevent an accurate quantification of the biofilms (44-47). Therefore, it is necessary to develop culture independent methods for biofilm quantification.

Due to the widespread occurrence of biofilms and their negative effects on patient outcomes (48), catheters were used as model surfaces to test our approach of quantifying biofilms. The goals of this study were to: (1) optimize the extraction protocol of biofilms from catheter segments; (2) formulate a protocol for biofilm quantification that provides data on both the cellular constituents and the extracellular matrix; and (3) develop a multipronged approach that is reproducible, sensitive, culture independent, and suitable for clinical settings.

5.2 Materials and Methods

5.2.1 Chemicals

Polydimethylsiloxane (PDMS) base and the curing agent (SYLGARD™ 184 Elastomer Kit, Dow Corning, MI, USA) were used to make the PDMS substrates and channels. The polysulfobetaine polymer containing perfluorphenylazide moieties was provided by Hydrophilix, Inc., CA, USA. Nylon 6/6, polystyrene, polyvinyl chloride, and polyethylene slabs were all purchased from McMaster-Carr, CA, USA. Milli-Q water (electrical resistivity ~18.2 MΩ cm at 25 °C) was provided by Millipore Corporation. Microbial species were purchased from ATCC. Luria-Bertani (LB), nutrient broth, trypticase soy broth (TSB), and yeast mold (YM) broth were obtained from Fisher Scientific. SYTO 9 live/dead Baclight Bacterial Viability Kit L13152 was from Molecular Probes. Dextran (dextran from *Leuconostoc* spp. Mr ~40,000. 31389, Fluka) was obtained from MilliporeSigma (Burlington, MA). Acetic acid (99.7%, ACS grade) and Luria Bertani (LB) broth (BD Difco) were obtained from Sigma-Aldrich (St. Louis, MO).

5.2.2 Substrates and Surface Modifications

PDMS substrates were prepared by mixing a 10:1 ratio of elastomer:curing agent (Syglard 184), followed by curing at 80 °C for 1 h. The PDMS sheets were cut with a laser cutter into 3 mm diameter disks. A PSB coating solution (30 µL) with a concentration of ~2, 5, or 10 mg mL^{-1} was placed and spread out on the surface of each disk, followed by crosslinking on the discs by exposure to 254 nm UV light for 10 min under sterile conditions, rinsing with Milli-Q water, and drying with air. Petri dishes (dimeter ~55 mm) were filled with a 10:1 elastomer to curing agent (Sylgard 184) and allowed to cure at room temperature for at least 48 h to form a 3 mm thick PDMS film on the bottom of the dishes. Modified plates were coated with a solution containing PSB and irradiated with 254 nm UV light as explained previously.

5.2.3 Pure Strain Growth Conditions and Petri Dish Inoculations

Bacterial species, Escherichia coli, Staphylococcus epidermidis, Staphylococcus aureus Rosenbach, Staphylococcus aureus (MRSA), Pseudomonas aeruginosa PAO1, and Candida albicans were used in this work. All strains were incubated at 30 °C at 150 rpm until a mid-exponential phase was acquired to harvest the cells by centrifugation at 3800 x g for 8 min. E. coli was grown on a Luria-Bertani (LB) broth, S. epidermidis, P. aeruginosa, and S. aureus Rosenbach were grown on nutrient broth; S. aureus (MRSA) was grown on a trypticase soy broth (TSB); and C. albicans was grown on a yeast mold (YM) broth. These initial cultures were then adjusted to an optical density of 1 at 600 nm and had an initial total cell number ranging from 1×10^7 cells per mL to 1×10^8 cells per mL.

Each modified and unmodified PDMS-lined dish was inoculated with 4 mL of bacterial or fungal suspensions, which were purchased from ATCC, and incubated for 24-72 h (shaken at 25 rpm) at 35 °C. The bacterial or fungal suspensions were then removed and stored for further

microscopy. The Petri dishes were gently rinsed with sterile, deionized water using a Pasteur pipette, and covered in 4 mL of a dye solution (SYTO 9 live/dead Baclight Bacterial Viability Kit L13152) for 15 min. The SYTO 9 solution was prepared by dissolving the contents of component A of the kit in 30 mL of sterile, deionized water. After the staining was complete, the Petri dishes were gently rinsed with deionized water and imaged using a 4X CCD camera (Axiocam MRm System) attached to a Zeiss Axioskop 2 microscope with a 10X objective, 40X objective, a fluorescent lamp, and a blue excitation filter. During observation, the images were taken at an excitation range of 450-490 nm. The numbers of attached microorganisms in all fluorescent images were determined using ImageJ software.

5.2.4 Microfluidic Coating and Bacterial Adhesion

PDMS microfluidic channels were fabricated using conventional soft lithography, and fluorescent fibrinogen (Fibrinogen Alexa flour 546) was utilized for static and flow experiments to evaluate the repelling effect of coating against protein adsorption in microfluidic channels. Simple straight PDMS channels (150 μm tall and 600 μm wide) were replicated from a mold of SU-8 photoresist (MicroChem, Corp.) on a 4-inch wafer. The mold was fabricated by standard photolithography, involving the spin-coating of a photoresist layer on the wafer, illuminating UV through a mask with the designed pattern of the channel, and developing the pattern with the SU-8 developer. The PDMS precursor (Sylgard 184) and crosslinker were mixed in a 10:1 ratio, poured onto the mold, degassed in a desiccator, and incubated in an oven at 60 ºC overnight. The crosslinked PDMS was cut and peeled out of the mold, punched with 2 holes for inlet and outlet, and covalently bonded onto a glass slide after plasma treatment. The static experiment was conducted by incubating fibrinogen inside the sealed PDMS channel for 1 h. The channel was rinsed with DI water and then imaged using a fluorescent microscope. The dynamic bacterial

adhesion experiments were conducted by flowing a fluorescent *E. coli* (ATCC® 25922GFP) solution (10^8 cells/mL) through the uncoated and PSB-coated microfluidic PDMS channels for 24 h.

5.2.5 Pure Strain Clinical Isolates and Catheter Conditions

In vitro experiments were carried out using common microbial pathogens encountered in catheter-associated urinary tract infection patients. Clinical isolates of *Staphylococcus aureus*, methicillin resistant-*Staphylococcus aureus* (*MRSA*), *Pseudomonas aeruginosa*, and *Candida albicans* were previously isolated from urine preserved in boric acid by UCLA Department of Pathology and Laboratory Medicine. Ten catheter samples, which had resided in male patients from 2-30 days, were obtained in collaboration with Cedars-Sinai Urology Towers. Once removed, the catheters were placed on ice and transported to UCLA for further analysis (additional detail in Appendix C).

5.2.6 Design of *In Vitro* Experiments and Detachment of Adhered Biofilms

5.2.6.1 Catheter Preparation and Incubation

In vitro experiments were performed by cutting the catheter tubing into 1-inch segments (16 Fr diameter, 5.3 mm, Type: Foley) and placing each segment into a sterile, 20 mL glass scintillation vial (Appendix Figure C-1). Silicone catheters and silicone catheters modified with a hydrophilic coating (additional detail in SI) were selected due to their widespread clinical use (49) and reduced biofilm formation susceptibility (50, 51). After each 1-inch coated or uncoated catheter segment was placed into a scintillation vial, it was submerged in 10 mL of bacterial or fungal isolate broth with an OD of 0.1 and allowed to incubate at 37°C with 120 rpm shaking. After the initial 24 hours, 9 mL of culture were removed and replenished with 9 mL of LB broth to ensure sufficient nutrient content. The samples were then allowed to incubate for an additional

24 hours. After the total 48-hour incubation period, the catheters were removed and dried by rolling the full segment's perimeter on sterile absorbent paper and gently tapping each edge of the tube to remove any excess liquid, loosely bound cells, and liquid adhered to the inner lumens. Each catheter segment was then transferred into 5 mL of sterile deionized (DI) water in 15 mL Falcon tubes.

5.2.6.2 Biofilm Extraction

The extraction of tightly bound cells and EPS components was carried out as previously described by Mandakhalikar *et al.* (52). Falcon tubes containing sterile DI water and the dried catheter segments were vortexed continuously at full speed (10 speed) for 1 minute. The samples were then subjected to 50 seconds of probe sonication (QSonica, Newtown, CT) at 20 kHz and 12 volts amplitude. Finally, samples were vortexed for another minute (10 speed). After the vortex-sonication-vortex sequence was completed, the catheter pieces were removed from the tube and the remaining suspension was used to carry out subsequent analyses. Optimization parameters of this method included the use of 16 Fr diameters instead of 3-14 Fr diameters, 1 inch vs 1 cm segments, and probe sonication duration.

5.2.7 Analytical Methods

5.2.7.1 Total Nucleic Acids Extraction and Quantitative Polymerase Chain Reaction

Extraction of nucleic acids was carried out using a phenol-chloroform extraction method as previously described (53). For cell density measurements, 500 µL liquid samples were collected after incubation, with cells harvested via centrifugation (21,000 x *g*, 10 min at 4°C) and the supernatant was discarded. Additional details are presented in the SI. The number cells were determined by amplification of the 16S rRNA or 18S rRNA taxonomic genes. Primer sequences are listed in Appendix Table C-1. Quantitative Polymerase Chain Reaction (qPCR) with SYBR-

green-based detection reagents were utilized to quantify gene copy numbers in each isolate. Each plate consisted of a calibration curve with a no template control. Melt curve analyses were performed after each run to ensure single product amplification.

5.2.7.2 Modified Lowry Assay for Protein Quantification

Tightly bound protein measurements were accomplished with the Pierce Modified Lowry Protein assay (Fisher Scientific, Pittsburgh, PA), using bovine serum albumin as the standard (1 mg/L - 1,500 mg/L). 40 µL of sample or standard was combined with 200 µL of Modified Lowry Reagent and incubated for 10 minutes. Subsequently, 20 µL of 1X Folin-Ciocalteau Reagent was amended and the plate was re-incubated for 30 minutes. Absorbance was measured at 750 nm using VICTOR 3 V plate reader (PerkinElmer, Waltham, MA) at 1 second intervals in a 96-well clear bottom, opaque-walled plate.

5.2.7.3 Adenosine Triphosphate Assay (ATP) for Cell Viability

The adenosine triphosphate (ATP) concentration was measured using the BacTiter-Glo™ Microbial Cell Viability assay (Promega, Madison, WI). A calibration curve was prepared from lyophilized luciferase (Sigma-Aldrich) ranging from 0.0057 mg/L to 5.7 mg/L. 100 µL of cell sample and 100 µL of BacTiter-Glo reagent were pipetted into a 96-well opaque flat bottom and opaque-walled plate. Samples were incubated at room temperature for 5 minutes and analyzed for luminescence using the spectrophotometer plate reader mentioned above. Background luminescence was determined by following the same procedure as experimental samples but with sterile deionized water and BacTiter-Glo reagent. In order to account for variations in clinical isolate samples, bound ATP was normalized to the amount of ATP in the corresponding supernatant as shown below in Equation 1.

$$\frac{Bound\ ATP_{catheter\ segment} - Background\ ATP_{deionized\ water}}{Supernatant\ ATP_{catheter\ segement} - Background\ ATP_{deionized\ water}}$$

5.2.7.4 Periodic-Schiff Assay for Carbohydrate Quantification

The polysaccharide fraction, as calibrated by dextran, was extracted from samples using a modified carbohydrate extraction method as described previously (54, 55). For this assay, 25 µL sample or standard were pipetted into a 96-well plate with 120 µL of freshly prepared solution containing 0.06% periodic acid in 7% acetic acid with gentle pipette mixing. Then a cover was secured to the multiwell plate, paraffined and incubated for 30 minutes at 37°C with 60 rpm shaking. After incubation, 100 µL of room temperature Schiff reagent was pipetted into each well, mixed via tapping the well plate, and incubated again at 37°C for 20 hours to allow for color development. Absorbance was read in a 96-well clear bottom, opaque-walled plate at 550 nm using the spectrophotometer plate reader mentioned above. Dextran, a homopolymer of glucose, had a standard solution range from 210 mg/L to 50,000 mg/L.

5.2.7.5 Statistical Analyses

Statistical differences between the coated and uncoated catheters were determined by a two-tailed, two-sample *t*-test that assumes equal variance. All experiments were performed in triplicate with analytical duplicates or triplicates. The results are presented as the mean $\pm$ the standard deviations (SD). The values were deemed statistically significant at p-values < 0.05.

5.3 Results and Discussion

5.3.1 Assessment of Microbial Adhesion to Perfluorphenylazide Moieties-Polysulfobetaine-coated Polydimethylsiloxane Substrates

To demonstrate the adhesion resistance of pathogenic cells, bacterial and fungal cells were incubated directly on bare and PSB coated PDMS substrates, stained with Syto 9 fluorescent nucleic acid dye, and analyzed with fluorescent microscopy. Figure 5-1A displays images of the substrates using fluorescent microscopy (inset) and quantitative analysis results from microbial adhesion after 24-48 h of incubation on PSB-modified and unmodified surfaces. The PSB-modified surfaces significantly decreased the bacterial and fungal adhesion as well as the biofilm formation compared with the unmodified surfaces across all tested microorganisms. The coating reduced the biofouling by inhibiting the attractive interactions of microorganisms with anchoring proteins responsible for bioadhesion,(56) impairing bacterial adhesion and/or biofilm forming cascades. Similar results were obtained when a fluorescent *E. coli* solution was flowed through the uncoated and coated microfluidic channels for 24 h, as can be seen in Figure 5-1B. In the bare PDMS channel, *E. coli* adhesion to the channel walls was observed after 3 h and continued to increase and form a thick film after 24 h. In contrast, the bacterial adhesion to the PSB-coated channels was scarce even after 24 hours of flow. Figure 5-1C presents the dynamics of increase in intensity based on the quantification of fluorescent images in Figure 5-1B. While the bacterial flow rendered the uncoated channels green, yielding more than 160% increase in intensity in only 24 hours, the coated channels remained protected against the bacterial adhesion and did not show a significant increase in the fluorescent intensity.

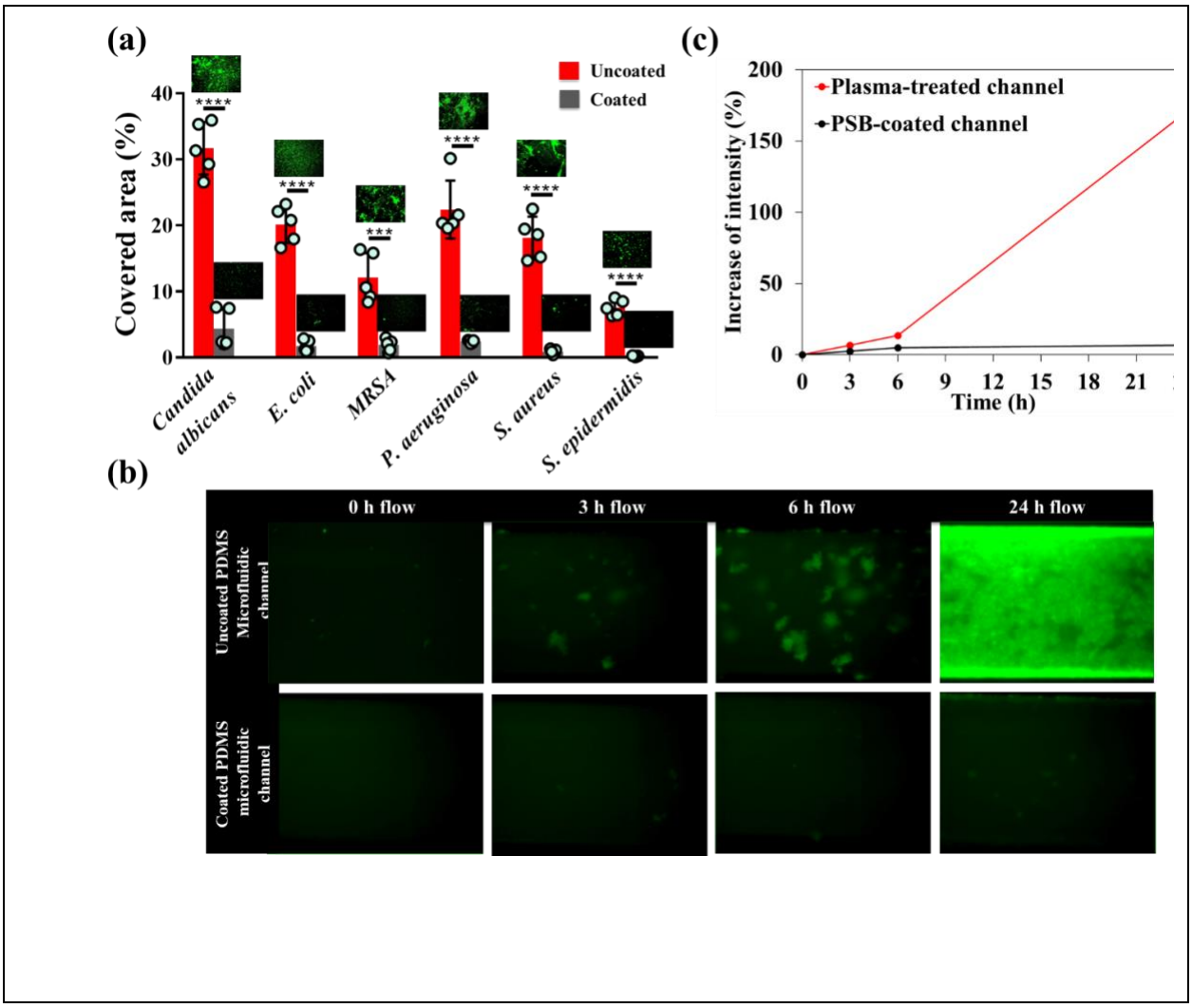

Figure 5-1 Assessment of microbial (bacterial and fungal) adhesion to PFPA-PSB-coated PDMS substrates

A). Percentage of fungal and bacterial cell coverage on bare and PSB-coated PDMS substrates obtained from fluorescent microscopy images (insets). B). Adsorption of fluorescent E. coli (ATCC® 25922GFP) to PDMS microfluidic channels under flow within 24 h shows that the uncoated channels permitted full coverage, whereas the PSB-coated channels did not support bacterial adhesion. The scale bars represent 100 µm. C). Increase of intensity over time based on the quantification of fluorescent images in panel B). shows that while uncoated channels underwent more than 160% increase in intensity in 24 h as a result of bacterial deposition, the coated channels remained protected against the bacterial adhesion.

5.3.2 Quantification of Adhered Biofilms Resulting from Clinical Isolates to Catheter Segments *In Vitro*

The enumeration of DNA in extracellular polymeric matrices attached to catheters is a critical parameter that facilitates microbial growth, adhesion, and overall biofilm integrity.

Extracellular DNA (eDNA) typically originates from cell lysis and/or active or passive extrusion mechanisms (57, 58). eDNA has been shown to be a universal adhesive substance and aids in biofilm formation (59, 60), which is why this parameter is of great importance when trying to quantify biofilm presence and growth. qPCR is a rapid and targeted quantification method that can accurately detect various nucleic acid biomarkers (61).

qPCR and universal gene targets effectively identify and enumerate nucleic acids, yet this technique remains largely absent from methods striving to quantify adhered biofilms on medical surfaces. By targeting highly conserved and reliable sites within the genome via the 16S or 18S primers, gene abundance inside the biofilm was quantified on catheter segments. Cycle threshold (C_T), which is proportional to the -log of the nucleic acid concentration, is reported because of its use in clinical settings to diagnose patient infections (62-64). Results demonstrated that within the adhered biofilm, bacterial or fungal DNA was successfully detected across all undiluted catheter segment samples, but that the ability to accurately quantify the DNA decreased when samples were diluted 10-fold and 100-fold to represent clinically-ambiguous copy numbers (Figure 5-2A, Figure 5-3A, Appendix Figure C-2, Appendix Table C-3). *MRSA* and *P. aeruginosa* clinical isolates showed the greatest overall surface attachment to uncoated catheters both with an average C_T value of 15.1 (Appendix Figure C-3). Studies have shown that several species including *S. aureus* and *P. aeruginosa*, can utilize eDNA to promote or modulate the development of biofilms (59, 65). Microbial cells have also been shown to prefer hydrophobic surfaces when developing a biofilm (66). Our results showed that bound DNA was significantly greater on the uncoated silicone segments compared to coated hydrophilic segments across all clinical isolates tested. This could be attributed to the fact that eDNA enhances adhesion to hydrophobic surfaces due to the amphiphilic nature of DNA (67). Correspondingly, *P.*

aeruginosa showed the most significant difference between coated and uncoated catheters (*p*-value < 0.01).

Quantifying proteins in the biofilm of pathogenic microorganisms is an important metric because it provides indicators of components contributing to adhesion, as well as to an infection's virulence (68-74). Protein components of biofilm include secreted extracellular proteins, protein subunits of pili or flagella, proteins of outer membrane vesicles, and cell surface adhesins (68).

The modified Lowry method was selected because it has been shown to be the optimal protein quantification method for natural biofilms when compared to others such as the Bicinchoninic acid (BCA) or Bradford Coomassie protein assays. For example, the Lowry assay has a lower detection limit than both the BCA and Coomassie assays. Additionally, the Coomassie assay has been shown to underestimate the concentration of glycoproteins, and the BCA assay shows interference with saccharides (10 mM-100 mM) (75, 76). Furthermore, all reagents used in the Lowry assay are stable at room temperature, granting it a relatively low susceptibility to experimental error or reagent degradation.

Total protein content measured by the modified Lowry assay showed greater protein association to uncoated catheter segments compared to coated segments (Figure 5-2B and Figure 5-3B). The greatest amount of protein on unmodified catheters corresponded to *S. aureus* with values of 176 ± 19.6 mg/L, while the least amount of protein was measured for *MRSA* (98 ± 6.8 mg /L) on coated catheters. Differences between amounts of protein measured among strains may indicate differences in their ability to colonize surfaces, but also result from the fact that the composition of extracellular matrix varies between species, as well as among strains of the same species (e.g., *MRSA* vs. *S. aureus*) (77). The greatest difference between uncoated/coated

catheters occurred with *P. aeruginosa* (p-value < 0.01). *P. aeruginosa* proteomics have shown that the EPS of this species contains mostly outer membrane proteins, but also includes cytoplasmic, secreted, and periplasmic proteins, which are directly linked to adhesion and biofilm stability (68).

ATP plays an essential role in cellular respiration, metabolism, and energy storage (78). The ATP concentration within a biofilm matrix can provide insight into the performance of the biofilm and overall cellular virility (79). Viable microbial load within the biofilm was quantified via the BacTiter-Glo cell viability assay (80). Previous studies have shown that there is a linear relationship between intracellular ATP and the number of viable cells (81, 82), which is why this assay was selected to characterize and quantify biofilm production. This luminescence-based assay enables the detection of ATP in catheter-associated biofilms.

ATP concentrations were successfully quantified across all samples and showed that greater ATP was associated with the uncoated catheters than the coated catheters (Figure 5-2C and Figure 5-3C). Coated catheter segments had significantly less ATP than uncoated segments across all clinical isolates. *P. aeruginosa* showed the greatest difference between the coated (6.88 $\pm$ 2.44 mg/L) and uncoated (2.87 $\pm$ 1.22 mg/L) catheters. This could be linked to the fact that the phosphate kinase gene (PPK), which encodes for the inorganic phosphate in ATP in *P. aeruginosa*, is responsible for thick and differentiated biofilm formation (83). Contrastingly, *C. albicans* had the lowest overall concentrations of ATP on the catheters, but still showed significantly more ATP on uncoated catheter segments (1.77 $\pm$ 0.45 mg/L) than coated catheter segments (0.81 $\pm$ 0.13 mg/L). These results are consistent with Haghighi *et al.*, (84) in which the ATP assay was used to measure the ability of TiO_2-coated catheters to resist *C. albicans* adhesion.

Quantifying total carbohydrates is essential in evaluating the presence of biofilm because EPS is the most abundant component of the extracellular matrix of many biofilm-forming pathogens (77). Additionally, polysaccharides are integral constituents in determining biofilm structure and integrity (85). For instance, one of the prevalent carbohydrates in *P. aeruginosa* facilitates cell-to-cell adhesion within the biofilm by crosslinking eDNA within the extracellular matrix (77). Carbohydrate quantification is thus considered a crucial component in the evaluation of biofilms due to their significance for biofilm stability.

Detection and analysis of complex carbohydrates is typically performed via colorimetric assays, including phenol-sulfuric acid (86), Monsigny resorcinol (87), resazurin (88) and crystal violet (89). The Periodic Acid-Schiff reagent (PAS) is widely used to visualize tissues by staining glycogen and other polysaccharides (54, 90, 91). In contrast to other methods, the PAS assay does not face interference from proteins or sugars, has the ability to capture neutral and charged carbohydrates, and is not specific to any kind of glycosidic linkage (54, 55). This is important when concerned with quantifying carbohydrates in real biofilms because there are many carbohydrates present in EPS, even within the EPS of a single species (77). For instance, studies on the extracellular matrix of *P. aeruginosa* have shown that different strains secrete as much as three types of matrix exopolysaccharides (77, 92-95). Ensuring the universality of the assay is critical for its widespread clinical applicability. Kilcoyne *et al.*, (54) developed a method to use the PAS assay in a microtiter plate format for the *in vitro* quantification of dissolved carbohydrates (54), introducing the possibility to use it as a high-throughput method. However, this method had yet to be explored as a strategy for quantifying biofilms extracted from indwelling medical tubing.

Results from the PAS assay showed that the concentration of bound carbohydrates was significantly greater in uncoated catheter segments compared to coated ones (Figure 5-2D and Figure 5-3D). *P. aeruginosa* had the greatest amount of bound carbohydrate on coated catheters (3,411 ± 505 mg equivalent dextran/L), while *MRSA* had the lowest concentration (411 ± 126 mg equivalent dextran/L) on coated catheters. *S. aureus* showed the greatest difference between uncoated/coated segments (p-value < 0.001). The linearity of the response of a number of polysaccharides to the assay indicates (54) that it can be reliably used for different strains regardless of the dominant carbohydrate in their EPS. Thus, in contrast to other methods, the selected assay is not only useful for a large range of microorganisms but can also be confidently used with microbial communities, such as those present in clinical settings. Additionally, the PAS assay requires low sample volume and generates small amounts of non-hazardous waste, so it has the potential to be used as a high-throughput assay for biofilm quantification in clinical settings.

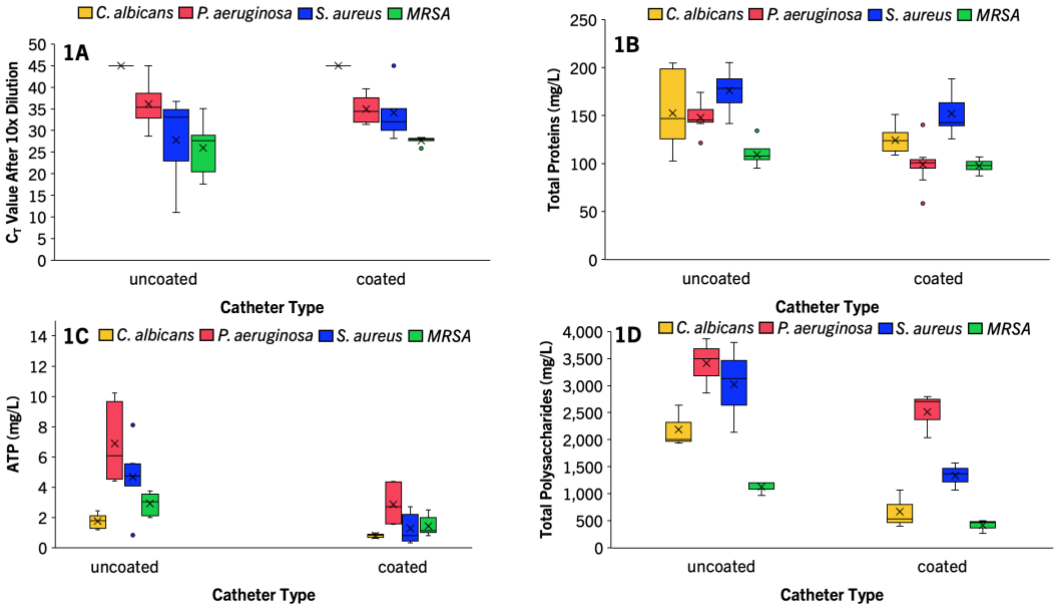

Figure 5-2 Gene abundance, total protein, ATP, and total polysaccharide concentrations from adhered biofilms on coated and uncoated catheter segments A). Gene abundance represented by CT values. B). Total protein concentration as estimated via a bovine serum albumin standard. C). ATP concentration. D). Carbohydrate concentration as µg equivalents of dextran. Each value represents average and quartiles of experimental triplicates, each measured thrice (n = 9).

5.3.3 Quantification of Adhered Biofilms from Catheters Previously Residing in Patients

Figure 2 shows that all four assays were successful at detecting and quantifying biofilm extracted from catheters that were previously implanted in patients. ATP and gene abundance were evaluated for the same set of patient samples because both have a presence in clinical contexts. Gene abundance has been used to diagnose *S. aureus*, *C. albicans*, and *P. aeruginosa* infections via C_T value (62-64) and ATP has been used to estimate antimicrobial effects (80, 96). Based upon existing infection guidelines, patients 6 and 8 could be diagnosed relatively easily with only qPCR since the distance from the infection positive threshold was consistent for most of the replicates (Figure 5-3A, Appendix Table C-3). Correspondingly, the average ATP concentrations in patient 8 was high (likely infection) (0.66 mg/L) and low in the case of patient 6 (0.20 mg/L). However, for patients 2, 4, and 7 the distribution of points for gene abundance

was considered inconclusive in the diagnosis of an infection since the replicate analyses straddle the threshold (Figure 5-3A). In these instances, additional data would be needed. For example, the ATP measurements indicate that patient 2 had a high average amount of ATP (1.9 mg/L), while patients 4 and 7 had average ATP concentrations that were similar to a patient with a no infection qPCR result, (0.75 mg/L and 0.29 mg/L). Polysaccharides and total proteins were measured for patients 21-25 because these two methods are currently not widely used in clinical settings to diagnose infections and have no established threshold for presence or absence of infection. Figure 5-3B and Figure 5-3D show similar trends in the variation and distribution for proteins and polysaccharides in different patients, indicating the value of these multiple lines of evidence in accurate identification of infections caused by biofilms.

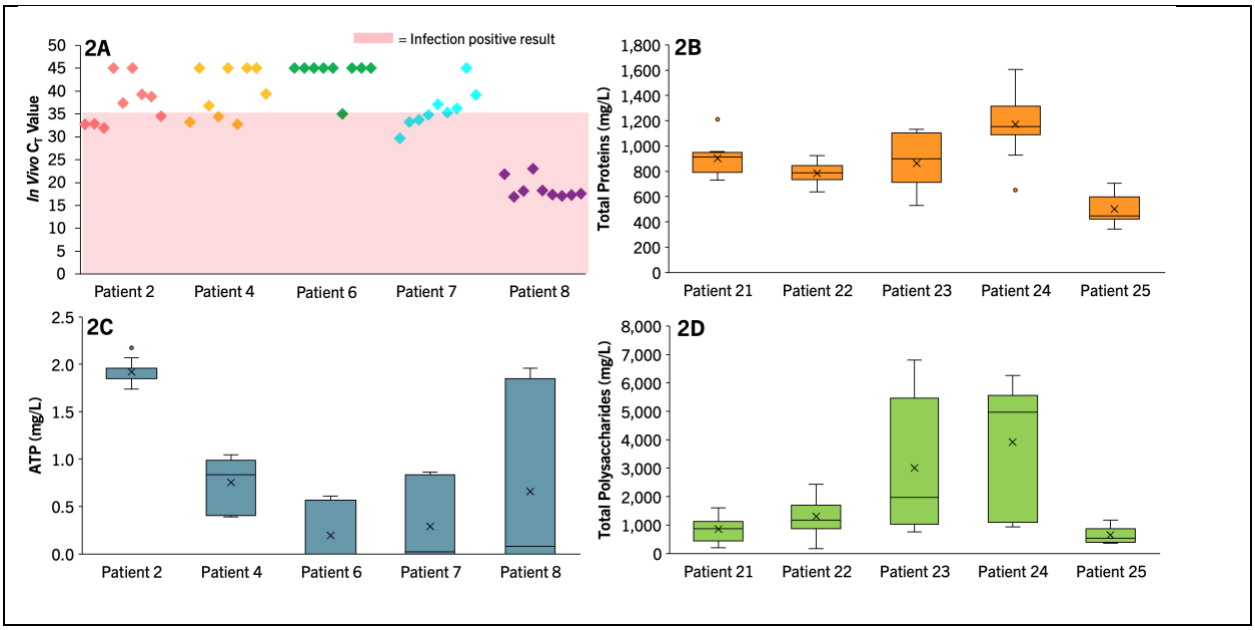

Figure 5-3 Quantification of gene abundance, total protein, ATP, and total polysaccharide concentrations adhered to uncoated catheters

In summary, this study emphasizes a multiple lines of evidence approach for characterizing and quantifying catheter-associated biofilms *in vitro* (Appendix Table C-2 and Appendix Table

C-3). When implemented in a clinical setting, these assays collectively aid the accurate enumeration of infections and inform costs and patient care decisions. Furthermore, these assays could be beneficial in the design and testing for materials to limit attachment of potentially pathogenic biofilms.

5.4 References

(1) Klevens, R.M., J.R. Edwards, C.L. Richards, Jr., T.C. Horan, R.P. Gaynes, D.A. Pollock, and D.M. Cardo. Estimating Health Care-Associated Infections and Deaths in U.S. Hospitals, 2002. Public health reports (Washington, D.C. : 1974), 2007, 122, 160-166.

(2) Data Summary of Hais in the Us: Assessing Progress 2006-2016, C.f.D.C.a. Prevention, 2017.

(3) Bryers, J.D. Medical Biofilms. Biotechnol. Bioeng., 2008, 100, 1-18.

(4) Herman-Bausier, P. and Y.F. Dufrêne. Force Matters in Hospital-Acquired Infections. Science, 2018, 359, 1464-1465.

(5) Flemming, H.C., J. Wingender, U. Szewzyk, P. Steinberg, S.A. Rice, and S. Kjelleberg. Biofilms: An Emergent Form of Bacterial Life. Nat. Rev. Microbiol., 2016, 14, 563-575.

(6) Lebeaux, D., J.M. Ghigo, and C. Beloin. Biofilm-Related Infections: Bridging the Gap between Clinical Management and Fundamental Aspects of Recalcitrance toward Antibiotics. Microbiol. Mol. Biol. Rev., 2014, 78, 510-543.

(7) Römling, U. and C. Balsalobre. Biofilm Infections, Their Resilience to Therapy and Innovative Treatment Strategies. J Intern Med, 2012, 272, 541-561.

(8) Percival, S.L., L. Suleman, C. Vuotto, and G. Donelli. Healthcare-Associated Infections, Medical Devices and Biofilms: Risk, Tolerance and Control. J. Med. Microbiol., 2015, 64, 323-334.

(9) Rodrigues, L.R. Inhibition of Bacterial Adhesion on Medical Devices. Adv. Exp. Med. Biol., 2011, 715, 351-367.

(10) Zhang, Z. and V.E. Wagner, Antimicrobial Coatings and Modifications on Medical Devices. 2017, Cambridge, MA, USA: Springer.

(11) Briandet, R., J. Herry, and M. Bellon-Fontaine. Determination of the Van Der Waals, Electron Donor and Electron Acceptor Surface Tension Components of Static Gram-Positive Microbial Biofilms. Colloids Surf. B. Biointerfaces, 2001, 21, 299-310.

(12) Takahashi, H., T. Suda, Y. Tanaka, and B. Kimura. Cellular Hydrophobicity of Listeria Monocytogenes Involves Initial Attachment and Biofilm Formation on the Surface of Polyvinyl Chloride. Lett. Appl. Microbiol., 2010, 50, 618-625.

(13) Ostuni, E., R.G. Chapman, R.E. Holmlin, S. Takayama, and G.M. Whitesides. A Survey of Structure-Property Relationships of Surfaces That Resist the Adsorption of Proteins. Langmuir, 2001, 17, 5605-5620.

(14) Holmlin, R.E., X. Chen, R.G. Chapman, S. Takayama, and G.M. Whitesides. Zwitterionic Sams That Resist Nonspecific Adsorption of Protein from Aqueous Buffer. Langmuir, 2001, 17, 2841-2850.

(15) Li, G., G. Cheng, H. Xue, S. Chen, F. Zhang, and S. Jiang. Ultra Low Fouling Zwitterionic Polymers with a Biomimetic Adhesive Group. Biomaterials, 2008, 29, 4592-4597.

(16) Schlenoff, J.B. Zwitteration: Coating Surfaces with Zwitterionic Functionality to Reduce Nonspecific Adsorption. Langmuir, 2014, 30, 9625-9636.

(17) Jiang, S. and Z. Cao. Ultralow-Fouling, Functionalizable, and Hydrolyzable Zwitterionic Materials and Their Derivatives for Biological Applications. Adv Mater, 2010, 22, 920-932.

(18) Smith, R.S., Z. Zhang, M. Bouchard, J. Li, H.S. Lapp, G.R. Brotske, D.L. Lucchino, D. Weaver, L.A. Roth, A. Coury, J. Biggerstaff, S. Sukavaneshvar, R. Langer, and C. Loose. Vascular Catheters with a Nonleaching Poly-Sulfobetaine Surface Modification Reduce Thrombus Formation and Microbial Attachment. Sci. Transl. Med., 2012, 4, 153ra132-153ra132.

(19) Mi, L. and S. Jiang. Integrated Antimicrobial and Nonfouling Zwitterionic Polymers. Angew Chem Int Ed Engl, 2014, 53, 1746-1754.

(20) Cheng, G., Z. Zhang, S. Chen, J.D. Bryers, and S. Jiang. Inhibition of Bacterial Adhesion and Biofilm Formation on Zwitterionic Surfaces. Biomaterials, 2007, 28, 4192-4199.

(21) Zhang, H. and M. Chiao. Anti-Fouling Coatings of Poly(Dimethylsiloxane) Devices for Biological and Biomedical Applications. J Med Biol Eng, 2015, 35, 143-155.

(22) Yang, R. and K.K. Gleason. Ultrathin Antifouling Coatings with Stable Surface Zwitterionic Functionality by Initiated Chemical Vapor Deposition (ICVD). Langmuir, 2012, 28, 12266-12274.

(23) Leigh, B.L., E. Cheng, L. Xu, A. Derk, M.R. Hansen, and C.A. Guymon. Antifouling Photograftable Zwitterionic Coatings on PDMS Substrates. Langmuir, 2019, 35, 1100-1110.

(24) Zhou, R., P.-F. Ren, H.-C. Yang, and Z.-K. Xu. Fabrication of Antifouling Membrane Surface by Poly(Sulfobetaine Methacrylate)/Polydopamine Co-Deposition. J. Membr. Sci., 2014, 466, 18-25.

(25) Liu, L.-H. and M. Yan. Perfluorophenyl Azides: New Applications in Surface Functionalization and Nanomaterial Synthesis. Acc. Chem. Res., 2010, 43, 1434-1443.

(26) Poe, R., K. Schnapp, M.J.T. Young, J. Grayzar, and M.S. Platz. J. Am. Chem. Soc., 1992, 114, 5055.

(27) Brehler, R. and B. Kütting. Natural Rubber Latex Allergy: A Problem of Interdisciplinary Concern in Medicine. Arch Intern Med, 2001, 161, 1057-1064.

(28) Erythropel, H.C., M. Maric, J.A. Nicell, R.L. Leask, and V. Yargeau. Leaching of the Plasticizer Di(2-Ethylhexyl)Phthalate (Dehp) from Plastic Containers and the Question of Human Exposure. Appl. Microbiol. Biotechnol., 2014, 98, 9967-9981.

(29) Wildgruber, M., C. Lueg, S. Borgmeyer, I. Karimov, U. Braun, M. Kiechle, R. Meier, M. Koehler, J. Ettl, and H. Berger. Polyurethane Versus Silicone Catheters for Central Venous Port Devices Implanted at the Forearm. Eur. J. Cancer, 2016, 59, 113-124.

(30) Bodas, D. and C. Khan-Malek. Hydrophilization and Hydrophobic Recovery of Pdms by Oxygen Plasma and Chemical Treatment—an Sem Investigation. Sensors Actuators B: Chem., 2007, 123, 368-373.

(31) Oláh, A., H. Hillborg, and G.J. Vancso. Hydrophobic Recovery of UV/Ozone Treated Poly(Dimethylsiloxane): Adhesion Studies by Contact Mechanics and Mechanism of Surface Modification. Appl. Surf. Sci., 2005, 239, 410-423.

(32) Hillborg, H. and U.W. Gedde. Hydrophobicity Recovery of Polydimethylsiloxane after Exposure to Corona Discharges. Polymer, 1998, 39, 1991-1998.

(33) Bausch, G.G., J.L. Stasser, J.S. Tonge, and M.J. Owen. Behavior of Plasma-Treated Elastomeric Polydimethylsiloxane Coatings in Aqueous Environment. Plasmas and Polymers, 1998, 3, 23-34.

(34) Zhou, J., A.V. Ellis, and N.H. Voelcker. Recent Developments in PDMS Surface Modification for Microfluidic Devices. Electrophoresis, 2010, 31, 2-16.

(35) Beal, J.H.L., A. Bubendorfer, T. Kemmitt, I. Hoek, and W. Mike Arnold. A Rapid, Inexpensive Surface Treatment for Enhanced Functionality of Polydimethylsiloxane Microfluidic Channels. Biomicrofluidics, 2012, 6, 36503.

(36) Karakoy, M., E. Gultepe, S. Pandey, M.A. Khashab, and D.H. Gracias. Silane Surface Modification for Improved Bioadhesion of Esophageal Stents. Appl. Surf. Sci., 2014, 311, 684-689.

(37) Zhang, Z., J. Wang, Q. Tu, N. Nie, J. Sha, W. Liu, R. Liu, Y. Zhang, and J. Wang. Surface Modification of Pdms by Surface-Initiated Atom Transfer Radical Polymerization of Water-Soluble Dendronized Peg Methacrylate. Colloids Surf. B. Biointerfaces, 2011, 88, 85-92.

(38) Merkel, T.C., V.I. Bondar, K. Nagai, B.D. Freeman, and I. Pinnau. Gas Sorption, Diffusion, and Permeation in Poly(Dimethylsiloxane). J. Polym. Sci. Part B: Polymer Physics, 2000, 38, 415-434.

(39) Cucarella, C., M.A. Tormo, C. Ubeda, M.P. Trotonda, M. Monzón, C. Peris, B. Amorena, I. Lasa, and J.R. Penadés. Role of Biofilm-Associated Protein Bap in the Pathogenesis of Bovine *Staphylococcus aureus*. Infect. Immun., 2004, 72, 2177-2185.

(40) Bjarnsholt, T. The Role of Bacterial Biofilms in Chronic Infections. APMIS Suppl, 2013, 1-51.

(41) Trevisani, L., S. Sartori, M.R. Rossi, R. Bovolenta, M. Scoponi, S. Gullini, and V. Abbasciano. Degradation of Polyurethane Gastrostomy Devices: What Is the Role of Fungal Colonization? Dig. Dis. Sci., 2005, 50, 463-469.

(42) Stickler, D.J. Clinical Complications of Urinary Catheters Caused by Crystalline Biofilms: Something Needs to Be Done. J. Intern. Med, 2014, 276, 120-129.

(43) CDC, Catheter-Associated Urinary Tract Infections, Centers for Disease Control & Prevention, National Center for Emerging and Zoonotic Infectious Diseases, Division of Healthcare Quality Promotion (DHQP), Editor. 2015.

(44) Stepanović, S., D. Vuković, I. Dakić, B. Savić, and M. Švabić-Vlahović. A Modified Microtiter-Plate Test for Quantification of Staphylococcal Biofilm Formation. J. Microbiol. Methods, 2000, 40, 175-179.

(45) Stepanović, S., D. Vuković, V. Hola, G. Di Bonaventura, S. Djukić, I. Cirković, and F. Ruzicka. Quantification of Biofilm in Microtiter Plates: Overview of Testing Conditions and Practical Recommendations for Assessment of Biofilm Production by *Staphylococci*. APMIS, 2007, 115, 891-899.

(46) Doll, K., K.L. Jongsthaphongpun, N.S. Stumpp, A. Winkel, and M. Stiesch. Quantifying Implant-Associated Biofilms: Comparison of Microscopic, Microbiologic and Biochemical Methods. J. Microbiol. Methods, 2016, 130, 61-68.

(47) Singh, A.K., P. Prakash, A. Achra, G.P. Singh, A. Das, and R.K. Singh. Standardization and Classification of in Vitro Biofilm Formation by Clinical Isolates of *Staphylococcus* Aureus. J Glob Infect Dis, 2017, 9, 93-101.

(48) Gomila, A., J. Carratalà, N. Eliakim-Raz, E. Shaw, C. Tebé, M. Wolkewitz, I. Wiegand, S. Grier, C. Vank, N. Cuperus, L. Van den Heuvel, C. Vuong, A. MacGowan, L. Leibovici, I. Addy, M. Pujol, R.S.G. on behalf of, and S. Study. Clinical Outcomes of Hospitalised Patients with Catheter-Associated Urinary Tract Infection in Countries with a High Rate of Multidrug-Resistance: The Combacte-Magnet Rescuing Study. Antimicrob. Resist. In., 2019, 8, 198.

(49) Feneley, R.C.L., I.B. Hopley, and P.N.T. Wells. Urinary Catheters: History, Current Status, Adverse Events and Research Agenda. J. Med. Eng. Technol., 2015, 39, 459-470.

(50) Lin, M.-F., Y.-Y. Lin, and C.-Y. Lan. A Method to Assess Influence of Different Medical Tubing on Biofilm Formation by *Acinetobacter baumannii*. J. Microbiol. Methods, 2019, 160, 84-86.

(51) Yan, Z., M. Huang, C. Melander, and B.V. Kjellerup. Dispersal and Inhibition of Biofilms Associated with Infections. J. Appl. Microbiol., 2020, 128, 1279-1288.

(52) Mandakhalikar, K.D., J.N. Rahmat, E. Chiong, K.G. Neoh, L. Shen, and P.A. Tambyah. Extraction and Quantification of Biofilm Bacteria: Method Optimized for Urinary Catheters. Sci. Rep., 2018, 8, 8069.

(53) Gedalanga, P.B., P. Pornwongthong, R. Mora, S.-Y.D. Chiang, B. Baldwin, D. Ogles, and S. Mahendra. Identification of Biomarker Genes to Predict Biodegradation of 1,4-Dioxane. Appl. Environ. Microbiol., 2014, 80, 3209-3218.

(54) Kilcoyne, M., J.Q. Gerlach, M.P. Farrell, V.P. Bhavanandan, and L. Joshi. Periodic Acid-Schiff's Reagent Assay for Carbohydrates in a Microtiter Plate Format. Anal. Biochem., 2011, 416, 18-26.

(55) Randrianjatovo-Gbalou, I., E. Girbal-Neuhauser, and C.E. Marcato-Romain. Quantification of Biofilm Exopolysaccharides Using an in Situ Assay with Periodic Acid-Schiff Reagent. Anal. Biochem., 2016, 500, 12-14.

(56) Habash, M. and G. Reid. Microbial Biofilms: Their Development and Significance for Medical Device-Related Infections. J. Clin. Pharmacol., 1999, 39, 887-898.

(57) Nagler, M., H. Insam, G. Pietramellara, and J. Ascher-Jenull. Extracellular DNA in Natural Environments: Features, Relevance and Applications. Appl. Microbiol. Biotechnol., 2018, 102, 6343-6356.

(58) Pietramellara, G., J. Ascher, F. Borgogni, M.T. Ceccherini, G. Guerri, and P. Nannipieri. Extracellular DNA in Soil and Sediment: Fate and Ecological Relevance. Biol. Fertil. Soils, 2009, 45, 219-235.

(59) Okshevsky, M. and R.L. Meyer. The Role of Extracellular DNA in the Establishment, Maintenance and Perpetuation of Bacterial Biofilms. Crit. Rev. Microbiol., 2015, 41, 341-352.

(60) Okshevsky, M., V.R. Regina, and R.L. Meyer. Extracellular DNA as a Target for Biofilm Control. Curr. Opin. Biotechnol., 2015, 33, 73-80.

(61) Kralik, P. and M. Ricchi. A Basic Guide to Real Time Pcr in Microbial Diagnostics: Definitions, Parameters, and Everything. Front. Microbiol., 2017, 8.

(62) Wellinghausen, N., D. Siegel, J. Winter, and S. Gebert. Rapid Diagnosis of Candidaemia by Real-Time PCR Detection of *Candida* DNA in Blood Samples. J. Med. Microbiol., 2009, 58, 1106-1111.

(63) Héry-Arnaud, G., E. Nowak, J. Caillon, V. David, A. Dirou, K. Revert, M.R. Munck, I. Frachon, A. Haloun, D. Horeau-Langlard, J. Le Bihan, I. Danner-Boucher, S. Ramel, M.P. Pelletier, S. Rosec, S. Gouriou, E. Poulhazan, C. Payan, C. Férec, G. Rault, G. Le Gal, and R. Le Berre. Evaluation of Quantitative Pcr for Early Diagnosis of *Pseudomonas aeruginosa* Infection in Cystic Fibrosis: A Prospective Cohort Study. Clin. Microbiol. Infect., 2017, 23, 203-207.

(64) Stenehjem, E., D. Rimland, E.K. Crispell, C. Stafford, R. Gaynes, and S.W. Satola. Cepheid Xpert *MRSA* Cycle Threshold in Discordant Colonization Results and as a Quantitative Measure of Nasal Colonization Burden. J. Clin. Microbiol., 2012, 50, 2079-2081.

(65) Allesen-Holm, M., K.B. Barken, L. Yang, M. Klausen, J.S. Webb, S. Kjelleberg, S. Molin, M. Givskov, and T. Tolker-Nielsen. A Characterization of DNA Release in *Pseudomonas aeruginosa* Cultures and Biofilms. Mol. Microbiol., 2006, 59, 1114-1128.

(66) Doyle, R.J. Contribution of the Hydrophobic Effect to Microbial Infection. Microb. Infect., 2000, 2, 391-400.

(67) Das, T., P.K. Sharma, B.P. Krom, H.C. van der Mei, and H.J. Busscher. Role of Edna on the Adhesion Forces between *Streptococcus* Mutans and Substratum Surfaces: Influence of Ionic Strength and Substratum Hydrophobicity. Langmuir, 2011b, 27, 10113-10118.

(68) Fong, J.N.C. and F.H. Yildiz. Biofilm Matrix Proteins. Microbiol Spectr, 2015, 3.

(69) Wong, E., G. Vaaje-Kolstad, A. Ghosh, R. Hurtado-Guerrero, P.V. Konarev, A.F.M. Ibrahim, D.I. Svergun, V.G.H. Eijsink, N.S. Chatterjee, and D.M.F. van Aalten. The Vibrio Cholerae Colonization Factor GbpA Possesses a Modular Structure That Governs Binding to Different Host Surfaces. PLoS Pathog., 2012, 8, e1002373.

(70) Stauder, M., A. Huq, E. Pezzati, C.J. Grim, P. Ramoino, L. Pane, R.R. Colwell, C. Pruzzo, and L. Vezzulli. Role of GbpA Protein, an Important Virulence-Related Colonization Factor, for Vibrio Cholerae's Survival in the Aquatic Environment. Environmental Microbiology Reports, 2012, 4, 439-445.

(71) Bhowmick, R., A. Ghosal, B. Das, H. Koley, D.R. Saha, S. Ganguly, R.K. Nandy, R.K. Bhadra, and N.S. Chatterjee. Intestinal Adherence of Vibrio Cholerae Involves a Coordinated Interaction between Colonization Factor Gbpa and Mucin. Infect. Immun., 2008, 76, 4968-4977.

(72) Cramton, S.E., C. Gerke, N.F. Schnell, W.W. Nichols, and F. Gotz. The Intercellular Adhesion (Ica) Locus is Present in *Staphylococcus aureus* and Is Required for Biofilm Formation. Infect. Immun., 1999, 67, 5427-5433.

(73) Gad, G.F., M.A. El-Feky, M.S. El-Rehewy, M.A. Hassan, H. Abolella, and R.M. El-Baky. Detection of Icaa, Icad Genes and Biofilm Production by *Staphylococcus aureus* and *Staphylococcus epidermidis* Isolated from Urinary Tract Catheterized Patients. J Infect Dev Ctries, 2009, 3, 342-351.

(74) Patel, J.D., E. Colton, M. Ebert, and J.M. Anderson. Gene Expression During *S. epidermidis* Biofilm Formation on Biomaterials. J. Biomed. Mater. Res. A, 2012, 100, 2863-2869.

(75) Richards, C., N. O'Connor, D. Jose, A. Barrett, and F. Regan. Selection and Optimization of Protein and Carbohydrate Assays for the Characterization of Marine Biofouling. Anal. Methods, 2020, 12, 2228-2236.

(76) Fountoulakis, M., J.-F. Juranville, and M. Manneberg. Comparison of the Coomassie Brilliant Blue, Bicinchoninic Acid and Lowry Quantitation Assays, Using Non-Glycosylated and Glycosylated Proteins. J. Biochem. Biophys. Methods, 1992, 24, 265-274.

(77) Floyd, K.A., A.R. Eberly, and M. Hadjifrangiskou, 3 - Adhesion of Bacteria to Surfaces and Biofilm Formation on Medical Devices, in Biofilms and Implantable Medical Devices, Y. Deng and W. Lv, Editors. 2017, Woodhead Publishing. p. 47-95.

(78) Mempin, R., H. Tran, C. Chen, H. Gong, K. Kim Ho, and S. Lu. Release of Extracellular ATP by Bacteria During Growth. BMC Microbiol., 2013, 13, 301.

(79) Heffernan, B., C.D. Murphy, and E. Casey. Comparison of Planktonic and Biofilm Cultures of *Pseudomonas fluorescens* DSM 8341 Cells Grown on Fluoroacetate. Appl. Environ. Microbiol., 2009, 75, 2899-2907.

(80) Sánchez, M.-C., A. Llama-Palacios, M.-J. Marín, E. Figuero, R. León, V. Blanc, D. Herrera, and M. Sanz. Validation of Atp Bioluminescence as a Tool to Assess Antimicrobial Effects of Mouthrinses in an in Vitro Subgingival-Biofilm Model. Med. Oral. Patol. Oral. Cir. Bucal., 2013, 18, e86-e92.

(81) Kapoor, R. and J.S. Yadav. Development of a Rapid Atp Bioluminescence Assay for Biocidal Susceptibility Testing of Rapidly Growing *Mycobacteria*. J. Clin. Microbiol., 2010, 48, 3725-3728.

(82) Herten, M., T. Bisdas, D. Knaack, K. Becker, N. Osada, G.B. Torsello, and E.A. Idelevich. Rapid in Vitro Quantification of *S. aureus* Biofilms on Vascular Graft Surfaces. Front. Microbiol., 2017, 8.

(83) Rashid, M.H. and A. Kornberg. Inorganic Polyphosphate Is Needed for Swimming, Swarming, and Twitching Motilities of Pseudomonas Aeruginosa. PNAS, 2000, 97, 4885-4890.

(84) Haghighi, F., R. Mohammadi Sh, P. Mohammadi, M. Eskandari, and S. Hosseinkhani. The Evaluation of *Candida albicans* Biofilms Formation on Silicone Catheter, PVC and Glass Coated with Titanium Dioxide Nanoparticles by XTT Method and Atpase Assay. Bratisl Lek Listy, 2012, 113, 707-711.

(85) Colvin, K.M., N. Alnabelseya, P. Baker, J.C. Whitney, P.L. Howell, and M.R. Parsek. Pela Deacetylase Activity Is Required for Pel Polysaccharide Synthesis in *Pseudomonas aeruginosa*. J. Bacteriol., 2013, 195, 2329-2339.

(86) Masuko, T., A. Minami, N. Iwasaki, T. Majima, S.-I. Nishimura, and Y.C. Lee. Carbohydrate Analysis by a Phenol–Sulfuric Acid Method in Microplate Format. Anal. Biochem., 2005, 339, 69-72.

(87) Monsigny, M., C. Petit, and A.-C. Roche. Colorimetric Determination of Neutral Sugars by a Resorcinol Sulfuric Acid Micromethod. Anal. Biochem., 1988, 175, 525-530.

(88) Peeters, E., H.J. Nelis, and T. Coenye. Comparison of Multiple Methods for Quantification of Microbial Biofilms Grown in Microtiter Plates. J. Microbiol. Methods, 2008, 72, 157-165.

(89) O'Toole, G.A. Microtiter Dish Biofilm Formation Assay. J. Vis. Exp., 2011, 2437.

(90) Speranza, A., G.L. Calzoni, and E. Pacini. Occurrence of Mono- or Disaccharides and Polysaccharide Reserves in Mature Pollen Grains. Sex. Plant Reprod., 1997, 10, 110-115.

(91) Bock, K.D., W. Derave, M. Ramaekers, E.A. Richter, and P. Hespel. Fiber Type-Specific Muscle Glycogen Sparing Due to Carbohydrate Intake before and During Exercise. J. Appl. Physiol., 2007, 102, 183-188.

(92) Hatch, R.A. and N.L. Schiller. Alginate Lyase Promotes Diffusion of Aminoglycosides through the Extracellular Polysaccharide of Mucoid *Pseudomonas aeruginosa*. Antimicrob. Agents Chemother., 1998, 42, 974-977.

(93) Jackson, K.D., M. Starkey, S. Kremer, M.R. Parsek, and D.J. Wozniak. Identification of Psl, a Locus Encoding a Potential Exopolysaccharide That Is Essential for *Pseudomonas aeruginosa* PAO1 Biofilm Formation. J. Bacteriol., 2004, 186, 4466-4475.

(94) Yang, L., K.B. Barken, M.E. Skindersoe, A.B. Christensen, M. Givskov, and T. Tolker-Nielsen. Effects of Iron on DNA Release and Biofilm Development by *Pseudomonas aeruginosa*. Microbiology, 2007, 153, 1318-1328.

(95) Zhao, K., B.S. Tseng, B. Beckerman, F. Jin, M.L. Gibiansky, J.J. Harrison, E. Luijten, M.R. Parsek, and G.C.L. Wong. Psl Trails Guide Exploration and Microcolony Formation in *Pseudomonas aeruginosa* Biofilms. Nature, 2013, 497, 388-391.

(96) Schwarz, F., A. Sculean, G. Romanos, M. Herten, N. Horn, W. Scherbaum, and J. Becker. Influence of Different Treatment Approaches on the Removal of Early Plaque Biofilms and the Viability of Saos2 Osteoblasts Grown on Titanium Implants. Clin. Oral Investig., 2005, 9, 111-117.

Chapter 6 Conclusions and Perspectives

6.1 Summary and Significance of Research

This research systematically approached the use and management of microorganisms through two research avenues. The first technique involved formulating and optimizing pure and mixed cultures to remove contaminants from groundwater and the second technique utilized surface chemistry and a multipronged assay approach to reduce microbial adhesion and quantify their population abundance.

A mixed microbial community composed of an anaerobic microbial consortium (KB-1®) and aerobic pure strain *Pseudonocardia dioxanivorans* CB1190 (CB1190) was assembled to evaluate the biodegradation of chlorinated ethenes and 1,4-dioxane under changing redox conditions. Conventional technologies have focused on removing each compound separately--anaerobes for trichloroethylene (TCE) and aerobes for 1,4-dioxane. However, this single consortium was able to reduce TCE in anaerobic environments and oxidize 1,4-dioxane after oxygen amendments. The mixed microbial community mitigated CVOC inhibition on 1,4-dioxane aerobic biodegradation as well as introduced CB1190's ability to biodegrade cDCE under aerobic conditions. Additionally, results showed that CB1190 was able to survive 100 days of anaerobic incubation and still grow in optimized medium when conditions turned aerobic. The monooxygenase enzyme present in CB1190 was reactivated after little to no lag and was able to catalyze 1,4-dioxane degradation. As a plume disperses throughout the saturated zone, the redox conditions frequently change from anaerobic (source zone) to aerobic (downgradient). The engineered microbial community survived these changes and biodegraded both CVOCs and 1,4-dioxane. This approach could reduce the cost, energy, and substrates required for *in situ* bioremediation for CVOCs and 1,4-dioxane.

Subsequently, an *in situ* biostimulation and bioaugmentation with CB1190 system was operated to promote the removal of chlorinated ethenes and 1,4-dioxane present in groundwater. Two monitoring wells (MW) were selected at this field demonstration site and sampled every two to four weeks over a total eight-month period. MW-31 received biostimulation in the form of air sparging and as a result there was significant removal of chlorinated ethenes with cDCE experiencing the largest decline (79% decrease). While air sparging was in operation, the chlorinated ethenes remained below 300 µg/L. However, when the air sparging pump experienced a malfunction, the chlorinated ethenes rapidly increased due to an upgradient source feeding into the area. 1,4-Dioxane decreased in concentration by 35% with the greatest reduction periods occurring when dissolved oxygen levels were above 3 mg/L. MW-32 received both air sparging as well as bioaugmentation with CB1190 + nutrients. This resulted in a 50% decrease in the 1,4-dioxane concentration as well as the cDCE concentration. Similar to MW-31, the greatest periods of contaminant removal in MW-32 occurred when the dissolved oxygen concentration were equal to or above 3 mg/L. By the end of the project, CB1190's gene abundance significantly decreased likely because of competition from the native bacterial population and nutrient limitations; however, an estimated 130 mg of total DX was removed by CB1190. In conclusion, the treatment of recalcitrant groundwater contaminants such as CVOCs and 1,4-dioxane can be further improved by combining biostimulation and bioaugmentation, particularly CB1190 + air sparging, for the removal of 1,4-dioxane and cDCE *in situ*.

The ability of CB1190 to metabolize the known carcinogen and groundwater pollutant, VC, with or without the co-contaminant, 1,4-dioxane, was examined in controlled experiments. While VC did pose inhibitory effects, CB1190 was able to biodegrade VC and utilize it as a growth substrate. CB1190 also demonstrated simultaneously degradation of VC and 1,4-dioxane.

Increasing concentrations of VC decreased 1,4-dioxane biodegradation rates, whereas increasing 1,4-dioxane did not have a strong effect on VC biodegradation. The *dxmB* and *aldH* gene targets were down regulated during VC biodegradation and were likely not induced by VC. After introducing ^{13}C-labeled VC to the culture media and then extracting the intracellular metabolites, molecules associated with the metabolic pathways such as tricarboxylic acid (TCA) cycle and gluconeogenesis increased. CB1190's ability to aerobically degrade VC as well as 1,4-dioxane would be beneficial at sites where enhanced reductive dechlorination stalled at VC due to oxygen intrusion or strain specific limitations.

An assessment of a novel hydrophilic coating's ability to resist microbial adhesion was carried out. Additionally, a multipronged method for quantifying cellular and extracellular polymeric matrix components attached to catheter surfaces was proposed in this research. Six microbial isolates comprised of one fungal strain and five bacterial strains were individually grown in petri dishes with hydrophilic-coated and uncoated silicone and results illustrated that the % area covered by the microorganisms was consistently less in the coated dishes than uncoated. Additionally, results showed that when a fluorescent *E. coli* solution was flowed through a silicone and hydrophilic-coated silicone microfluidic channel for 24 hours, the uncoated channel walls had significantly more biofilm than the coated channel. The microbial film detection approach was tested using four clinical isolates (*Pseudomonas aeruginosa*, *Staphylococcus aureus*, methicillin resistant-*Staphylococcus aureus*, *Candida albicans*) and two catheter types that were placed *in vitro* and *in vivo*. Results demonstrated that the shortcomings of standard approaches can be overcome through the conjunct analysis of total protein (modified Lowry), total biomass (quantitative polymerase chain reaction), cellular activity (ATP luminescence), and extracellular polymeric substances (Periodic Acid-Schiff). All four assays

were successful at detecting and quantifying biofilm extracted from catheters grown in microbial suspensions as well as catheters that were previously implanted in patients When implemented in a clinical setting, these assays collectively provide an accurate enumeration of infections and inform patient care decisions.

6.2 Future Research Directions

6.2.1 Application of novel omics approaches to characterize microbial communities capable of degrading contaminant mixtures

The study of genomes, proteomes, and metabolomes of microorganisms has been revolutionized by "omics" approaches. Genomics and transcriptomics are frequently being utilized to understand the cellular potential and function of contaminant degrading microorganisms. While this information does aid practitioners' ability optimize site remediation strategies, an even more direct measurement of the microbial system and activity is needed. Metabolomics, which is the study of metabolic profiles, intermediates and signaling molecules, can provide that direct line of evidence for contaminant biodegradation and is the reason why I believe future research within environmental engineering and specifically the bioremediation field should move to include widespread metabolomics studies. For example, while revealing CB1190's ability to metabolize VC will aid site clean-up where VC and 1,4-dioxane are present, future research is needed on the metabolites formed during the degradation of other CVOCs, such as TCE, cDCE, and 1,1-DCE, and 1,4-dioxane. This information would provide evidence of whether CB1190 metabolizes or co- metabolizes these pollutants and which products can serve as degradation indicators. To achieve this goal, stable isotope labeling of these compounds (e.g. TCE [U-$^{2}H_{1}$ or U-$^{13}C_{2}$], cDCE [U-$^{2}H_{2}$ or U-$^{13}C_{2}$], 1,1-DCE [U-$^{2}H_{2}$ or U-$^{13}C_{2}$], 1,4-dioxane [U-$^{2}H_{8}$ or U-$^{13}C_{4}$]) could be utilized to track metabolite fluxes, absolute metabolite concentrations, and incorporation of isotope signatures in amino acids and cellular components. Increased efforts

to combine isolating, enriching, and adaptively evolving microorganisms with high-throughput technologies like omics could open the door to using biodegradation for emerging and recalcitrant contaminants and aid the design and implementation of these complex systems.

6.2.2 Multipronged assay approaches for biofilm enumeration and clinical guidelines

Biofilms facilitate many of the key processes that are responsible for life on Earth such as nutrient cycling, atmospheric oxygen, gut health, pest control, contaminant removal, and the production of energy, food, and medicine. Contrastingly, they are also responsible for some of the most devastating losses of life from infections and disease to ecological degradation. Detection and enumeration of adhered cells is important for both environmental and public health. The research presented in this dissertation offer a multipronged approach for systematically quantifying components of biofilms adhered to medical tubing, which are notoriously known as a source for infections and biofilms. While this method has been shown to be effective for catheter surfaces *in vitro* and limitedly for catheters that resided in patients, I believe that future research is needed in testing these methods with larger number of samples collected from diverse patients as well as standardizing diagnoses and care based on this approach. Because biofilms have far greater mechanisms for survival compared to planktonic cultures, earlier detection of biofilms could result in fewer health complications and better patient outcomes. These assays would also be valuable in the testing of novel functional materials designed to mitigate biodeterioration in wide-ranging applications from shipping industry to dental health.

Appendix A:Supporting Information for A Mixed Microbial Community for the Biodegradation of Chlorinated Ethenes and 1,4-Dioxane

A-1 Methods and Materials

A-2 Culture Maintenance and Growth Conditions

The modified medium described by Cole et al.(1) contained: 2.3 g/L of TES buffer, 10 mL/L of 100x salt stock solution (100x stock solution: 100 g/L NaCl, 30 g/L NH_4Cl, 30 g/L KCl, 20 g/L KH_2PO_4, 50 g/L $MgCl_2$-$6H_2O$, 1.5 g/L $CaCl_2$-$2H_2O$), 1 mL/L of the Trace Element Solution A (Trace Element Solution A: 10 g/L HCl (25% w/w), 0.006 g/L H_3BO_3, 0.5 NaOH, 0.1 g/L $MnCl_2$-$4H_2O$, 1.5 g/L $FeCl_2$-$4H_2O$, 0.19 g/L $CoCl_2$-$6H_2O$, 0.07 g/L $ZnCl_2$, 0.002 g/L $CuCl_2$-$2H_2O$, 0.024 g/L $NiCl_2$-$6H_2O$, 0.036 g/L $NaMoO_4$-$6H_2O$), and 1 mL/L of Trace Element Solution B (Trace Element Solution B: 0.006 g/L Na_2SeO_4-$5H_2O$ and 0.008 g/L Na_2WO_4-$5H_2O$).(2) After the above ingredients were added, the medium's pH was adjusted to 7.2-7.3 and then autoclaved for 30 minutes at 121°C. The pH of the medium was measured periodically throughout the experiment. $TiCl_3$, the main reductant used, was prepared in an anaerobic glove box using 0.38 g of $TiCl_3$ powder in 100mL of sterile DI water. Varying amounts were added in order to reduce any trace amounts of oxygen in anaerobic cultures.

A-3 Total Nucleic Acids Extraction and qPCR

For cell density measurements, 500 µL liquid samples were collected during incubation, with cells harvested via centrifugation (21,000 x *g*, 10 min at 4°C) and the supernatant was discarded. Cells were lysed by adding 250 µL of lysis buffer (50 mM sodium acetate, 10 mM EDTA [pH 5.1]), 100 µL 10% sodium dodecyl sulfate, 1.0 mL pH 8.0 buffer-equilibrated phenol, and 1 g of 100 µm-diameter zirconia−silica beads (Biospec Products, Bartlesville, OK), followed by heating at 65°C for 2 min, bead beating for 2 min with a Mini-Beadbeater 16 (Biospec Products, Bartlesville, OK), incubating for 8 min at 65°C, and bead beating again for 2

min. The lysate was collected by centrifugation at 13000 *g* for 5 min, followed by phenol−chloroform−isoamyl alcohol purification (1 volume) and chloroform−isoamyl alcohol purification (1 volume). Precipitation of total nucleic acids was performed by the addition of 3 M sodium acetate (0.1 volume) and isopropanol (1 volume) followed by incubation at −20°C overnight. Nucleic acid pellets were collected by centrifugation at 4°C for 30 min at 20000 *g*. The precipitate was washed with 70% ethanol and resuspended in 100 μL DNase- and RNase-free water. The purity of DNA and RNA were determined by a Nanodrop 2000C spectrophotometer (Thermo Scientific, Wilmington, DE). For gene expression analyses, RNA was isolated from total nucleic acid extracts using a RapidOUT DNase Kit (Thermo Scientific, Waltham, MA). The cDNA was synthesized from purified total RNA using a Maxima First Strand cDNA Synthesis Kit (Thermo Scientific, Waltham, MA). All samples were stored at −80°C until further amplification and analyses. CB1190 primer sequences were used as described in Zhang et al. 2016 (3) and KB-1 primers were used as described in Waller et al. 2005.(4) All reactions were run on a StepOnePlus thermocycler (Life Technologies, Carlsbad, CA) using a total volume of 20 μL containing 1× Luminaris Color HiGreen−HiROX qPCR Master Mix (Thermo Scientific, Waltham, MA), 0.3 μM primers, and 2.5 μL of DNA (1−10 ng/μL) template. The cycling parameters to amplify the gene fragment included sample holds at 50°C for 2 min and 95°C for 10 min, followed by 40 cycles of 95°C for 15 s and 60°C for 45 s. All reactions were accompanied by a melt curve analysis to confirm the specificity of qPCR products. Melt-curve analyses that were within the ranges of 78.1−80.5°C (*rpoD*) and 81.5−83.6°C (*dxmB, aldH,* and 16S rRNA) were considered specific to each target gene.(3, 5, 6) The gene expression fold change was calculated using the following equation:

$$\Delta\Delta C_{q,\ \text{Target gene}} = (C_{q,\ \text{Target gene}} - C_{q,\ \text{Housekeeping gene}})_{\text{Treatment}} - (C_{q,\ \text{Target gene}} - C_{q,\ \text{Housekeeping gene}})_{\text{Control}}$$

A-4 Preparation of Chlorinated Solvent Stock Solutions

Chlorinated solvents were measured in samples collected from headspace of the bottles. They were converted to aqueous concentrations by using Henry's Law constants for each compound.(7, 8)

A-5 Oxygen Headspace, Dissolved Oxygen and Oxidation Reduction Potential Procedures

Headspace oxygen concentrations were measured using an O_2/CO_2 model 902D analyzer (Quantek Instruments, Grafton, MA). During experiments, 3 mL of headspace were sampled from each bottle and then immediately injected into the analyzer resulting in a % O_2 value. The headspace analyzer was chosen due to its relatively low sample volume requirement.

The oxidation-reduction potential (ORP) was measured using an Orion Triode Refillable ORP Probe (Thermo Fisher Scientific, Waltham, MA). Triplicate bottles containing 100 mL of modified media were sparged with two metal needles at 40 PSI for varying amounts of time up to three minutes and then measured on the ORP probe. The bottles were measured after equilibration for 1 hour at 30°C.

Dissolved oxygen and pH were measured using an Orion Versa Star (Thermo Fisher Scientific, Waltham, MA), and were measured in both anaerobic and aerobic conditions. The dissolved oxygen probe was calibrated using air saturated water (high oxygen concentrations) and a 50 g/L sodium sulfite solution for the zero point (low oxygen concentrations). Triplicate bottles containing 100 mL of modified media were sparged with two metal needles at 40 PSI for varying amounts of time up until three minutes. The bottles were measured after equilibration for 1 hour at 30°C. Appendix Figure A-1 shows a calibration curve between the amount of time sparged and dissolved oxygen (mg/L).

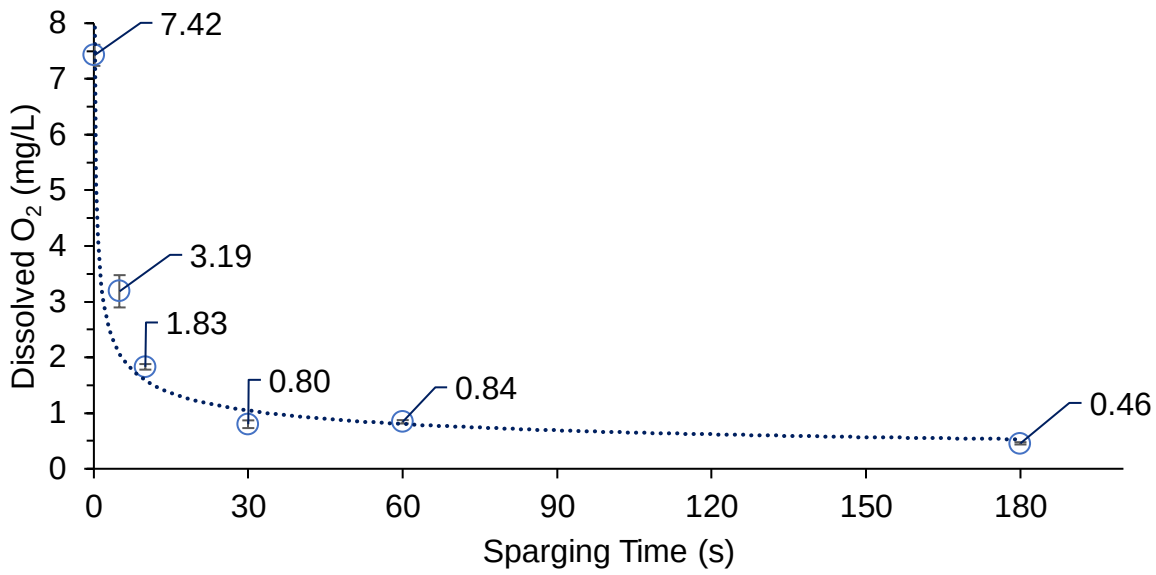

Appendix Figure A-1 Dissolved Oxygen
Dissolved Oxygen was measured in modified media after varying amounts of sparging time with N_2 gas. Bottles and media equilibrated to 30°C and measured using an Orion Versa Star DO probe.

A-6 Statistical Analysis

All experiments were performed in triplicate and are presented as the mean ± standard deviation. 1,4-Dioxane and chlorinated ethene inter and intragroup differences were estimated using a paired two sample for means t-Test. Intragroup biomass differences were estimated using a one-way paired t-Test. Values were considered statistically significant when the *p* values were < 0.05.

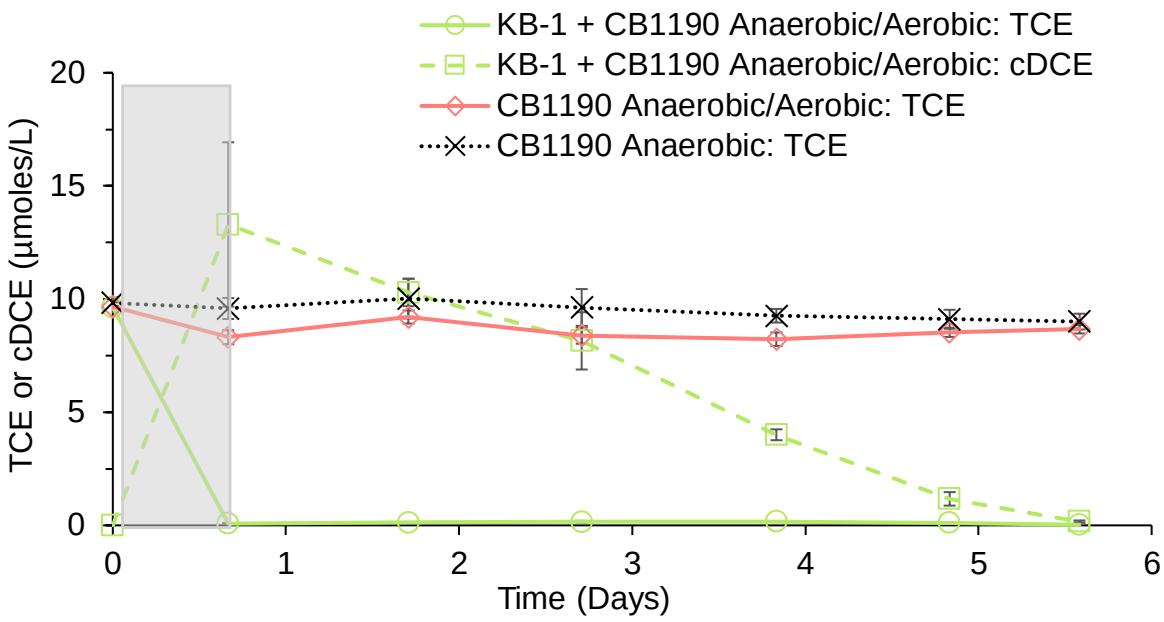

Appendix Figure A-2 Chlorinated ethene biodegradation (µmoles/L) in pure CB1190 and mixed cultures

The CB1190 anaerobic/aerobic pure culture did not degrade TCE under anaerobic or aerobic conditions, while KB-1 + CB1190 anaerobic/aerobic biodegraded TCE anaerobically and its transformation product, cDCE, aerobically. cDCE was degraded by CB1190 at a rate of 0.206±0.002 /day. Error bars indicate the standard deviation of triplicates, and the shaded grey area indicates the anaerobic phase.

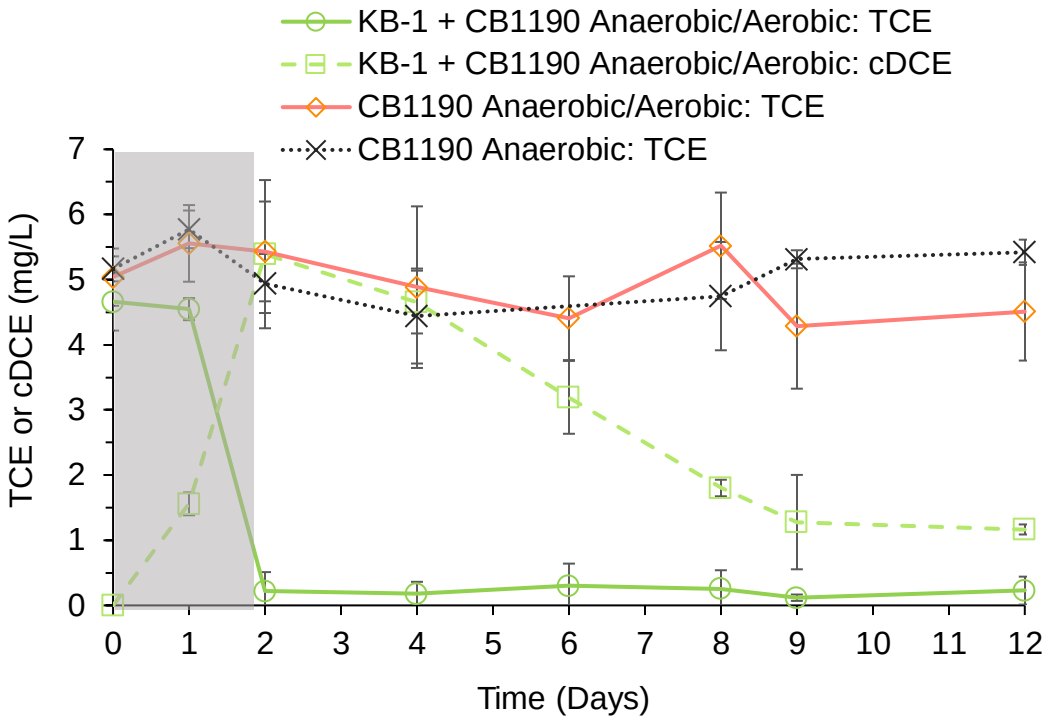

Appendix Figure A-3 Chlorinated ethene biodegradation (mg/L) in pure CB1190 and mixed cultures

The CB1190 anaerobic/aerobic pure culture did not degrade TCE under anaerobic or aerobic conditions, while KB-1 + CB1190 anaerobic/aerobic biodegraded TCE anaerobically and its transformation product, cDCE, aerobically. cDCE was degraded by CB1190 at a rate of 0.078±0.004 /day. Error bars indicate the standard deviation of triplicates, and the shaded grey area indicates the anaerobic phase.

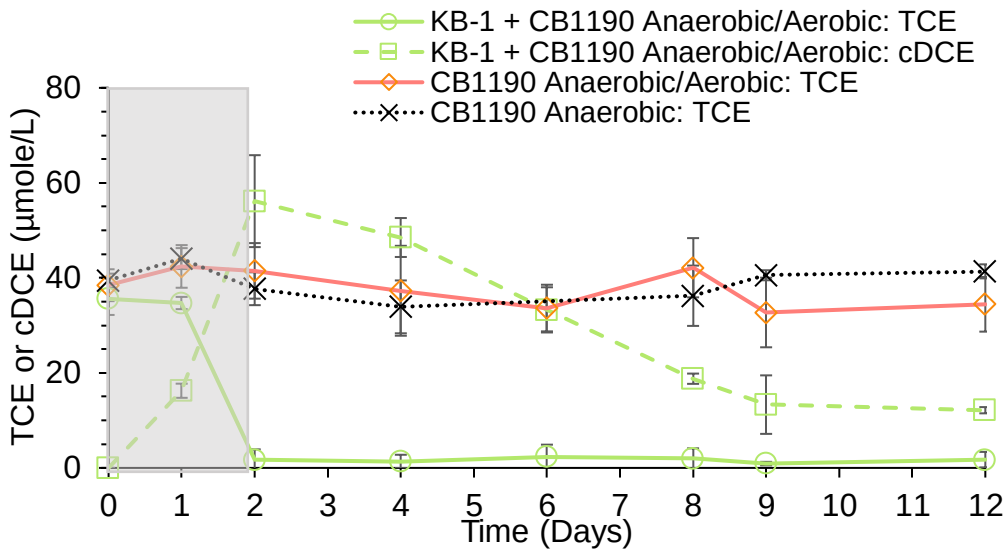

Appendix Figure A-4 Chlorinated ethene biodegradation (µmoles/L) in pure CB1190 and mixed cultures

The CB1190 anaerobic/aerobic pure culture did not degrade TCE under anaerobic or aerobic conditions, while KB-1 + CB1190 anaerobic/aerobic biodegraded TCE anaerobically and its transformation product, cDCE, aerobically. cDCE was degraded by CB1190 at a rate of 0.078±0.004 /day. Error bars indicate the standard deviation of triplicates, and the shaded grey area indicates the anaerobic phase.

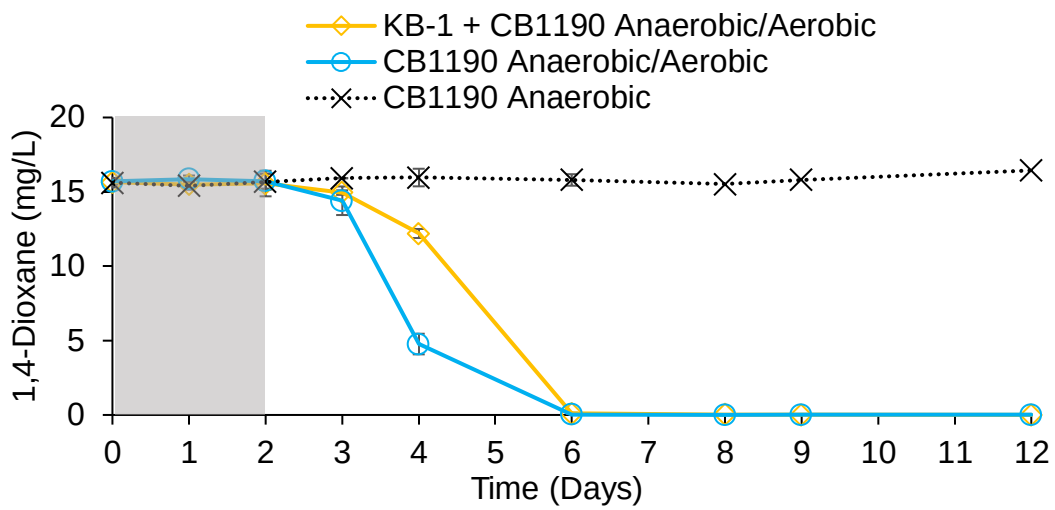

Appendix Figure A-5 1,4-Dioxane biodegradation in pure CB1190 and mixed cultures

KB-1 + CB1190 anaerobic/aerobic and CB1190 anaerobic/aerobic biodegraded 1,4-dioxane aerobically. CB1190 bottles that were not amended with oxygen did not degrade 1,4-dioxane. KB-1 + CB1190 anaerobic/aerobic degraded 15,000 µg/L of 1,4-dioxane at a rate of 0.249±0.0008 /day, and CB1190 only anaerobic/aerobic bottles at a rate of 0.250±0.00002 /day. CB1190-mediated 1,4-dioxane degradation rates were calculated using the end of the anaerobic phase and after 1,4-dioxane was degraded to below detection. Error bars indicate the standard deviation of triplicates, and the shaded grey area indicates the anaerobic phase.

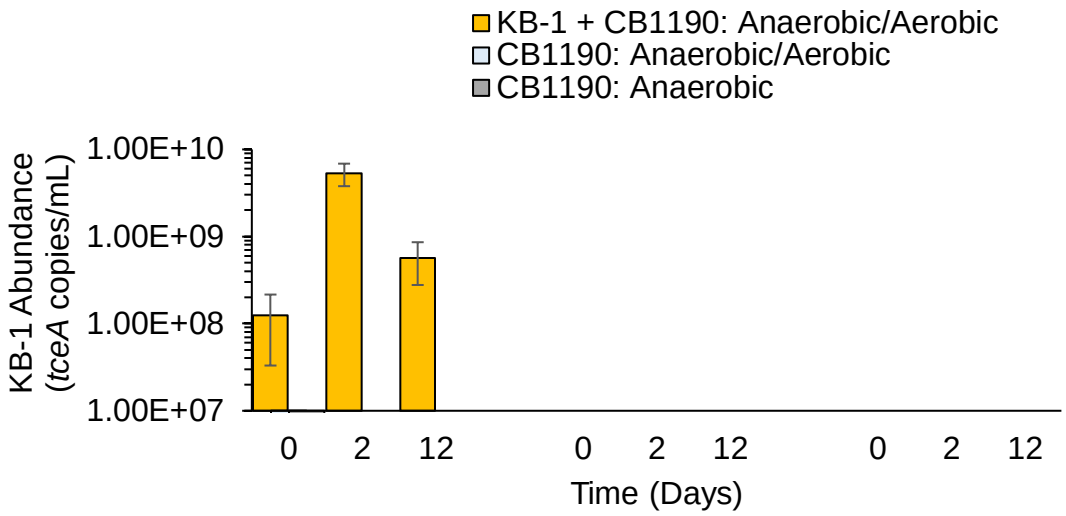

Appendix Figure A-6 KB-1 grows during anaerobic phase and does not grow during aerobic phase

Bottles contained 5,000 µg/L TCE and 15,000 µg/L 1,4-dioxane. The *tceA* gene was used to quantify cell number. Error bars indicate the standard deviation of triplicates.

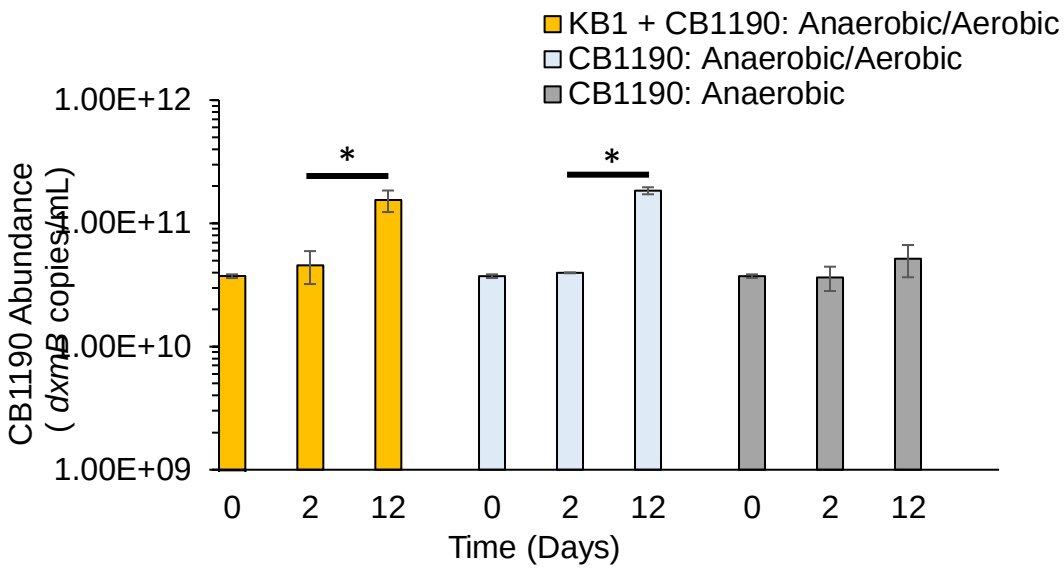

Appendix Figure A-7 CB1190 grows during aerobic phase after anaerobic incubation

Bottles contained 5,000 µg/L TCE and 15,000 µg/L 1,4-dioxane. The *dxmB* gene was used to quantify cell number. CB1190 + KB-1 anaerobic/aerobic and CB1190 anaerobic/aerobic grew after the anaerobic phase and during aerobic conditions, (* $p < 0.05$, ** $p < 0.01$). The CB1190 anaerobic bottles did not grow significantly during the anaerobic phase. Error bars represent standard deviation of triplicate samples.

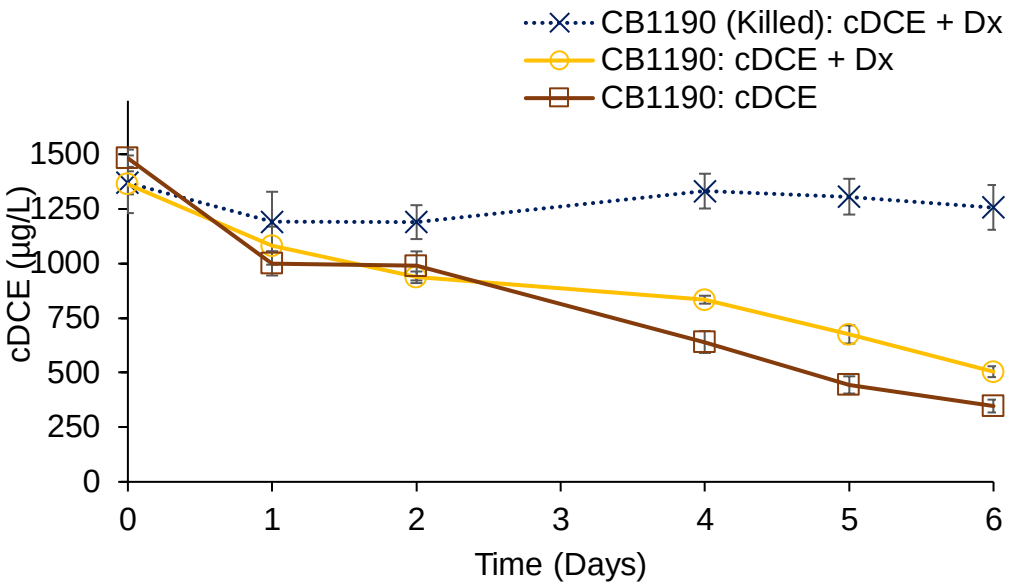

Appendix Figure A-8 CB1190 aerobically degrades cDCE with and without 1,4-dioxane

There was no significant difference in degradation rates when CB1190 was amended with and without 1,4-dioxane. Error bars indicate the standard deviation of triplicates.

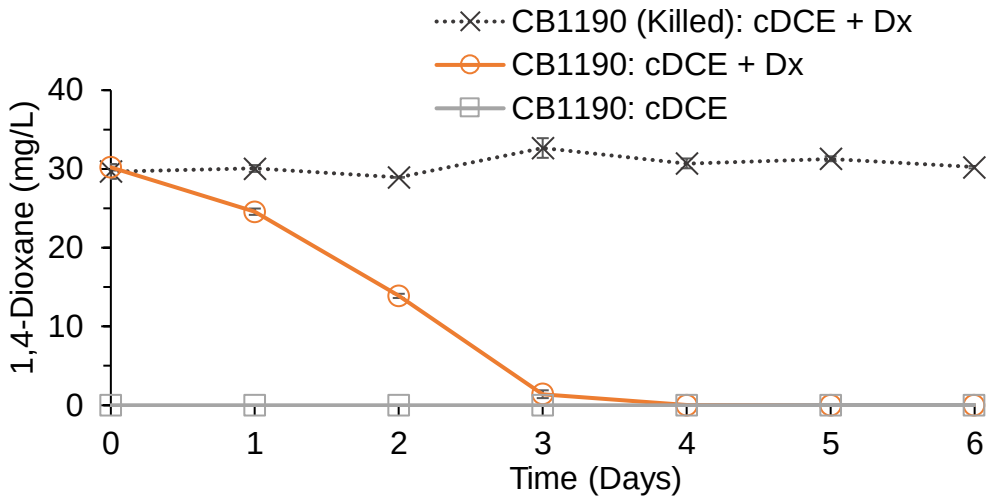

Appendix Figure A-9 CB1190 aerobically degrades 1,4-dioxane in the presence of cDCE

There was no significant 1,4-dioxane transfer from the seed culture in CB1190 amended with only cDCE. Error bars indicate the standard deviation of triplicates.

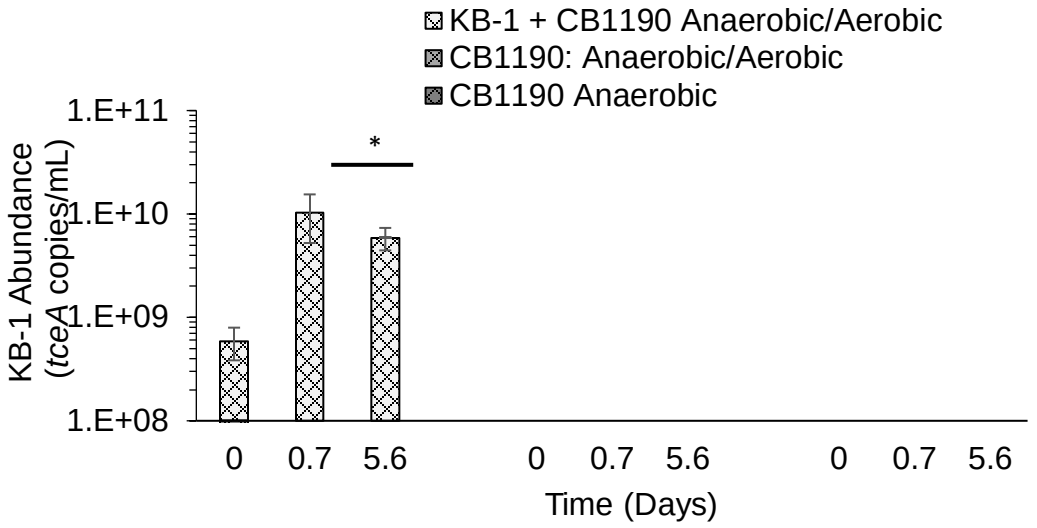

Appendix Figure A-10 KB-1 grows during anaerobic phase and does not grow during aerobic phase

Bottles contained 1,250 µg/L TCE and 3,000 µg/L 1,4-dioxane. The *tceA* gene was used to quantify cell number. KB-1 grew under anaerobic conditions in the KB-1 + CB1190 anaerobic/aerobic bottles, and did not grow under aerobic conditions (* $p < 0.05$, ** $p < 0.01$). Error bars indicate the standard deviation of triplicates.

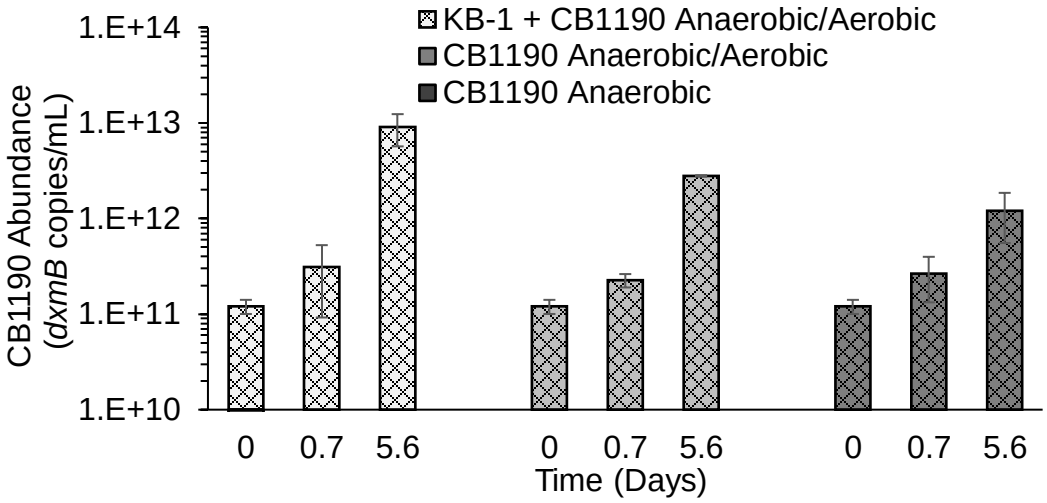

Appendix Figure A-11 CB1190 grows during aerobic phase after anaerobic incubation

Bottles contained 1,250 µg/L TCE and 3,000 µg/L 1,4-dioxane. The *dxmB* gene was used to quantify cell number. CB1190 + KB-1 anaerobic/aerobic and CB1190 anaerobic/aerobic grew after the anaerobic phase and during aerobic conditions, (* $p < 0.05$, ** $p < 0.01$). The CB1190 anaerobic bottles did not grow significantly during the anaerobic phase. Error bars indicate the standard deviation of triplicate samples.

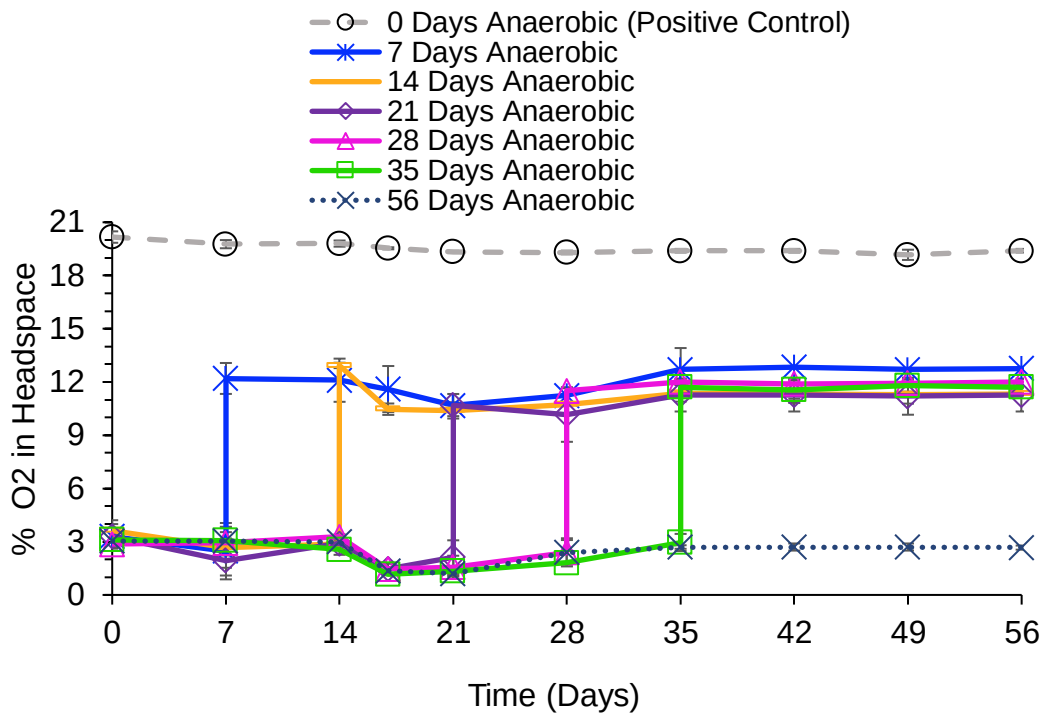

Appendix Figure A-12 Dissolved oxygen concentrations after prolonged anaerobic incubation

CB1190 was able to biodegrade 1,4-dioxane after anaerobic incubation and ~12% oxygen in the headspace. Error bars indicate standard deviation of 6 replicates.

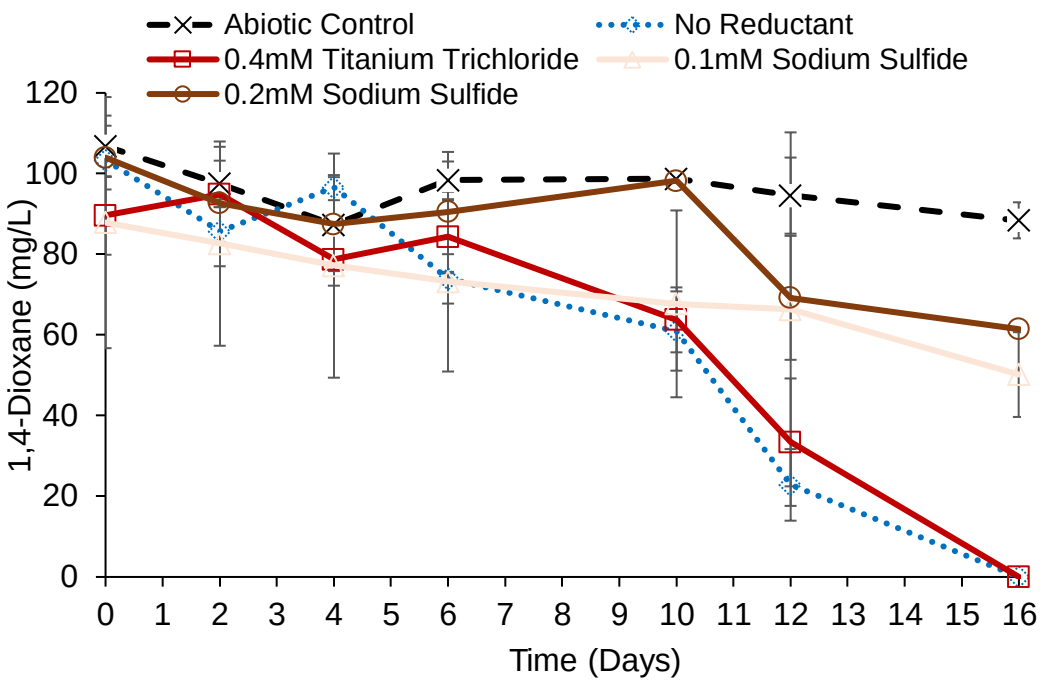

Appendix Figure A-13 Titanium trichloride has a less inhibitory effect on CB1190's ability to biodegrade 1,4-dioxane than sodium sulfide
Titanium trichloride resulted in the least inhibition and sodium sulfide resulted in the most inhibition on CB1190's ability to biodegrade 1,4-dioxane. Error bars indicate standard deviation of 6 replicates.

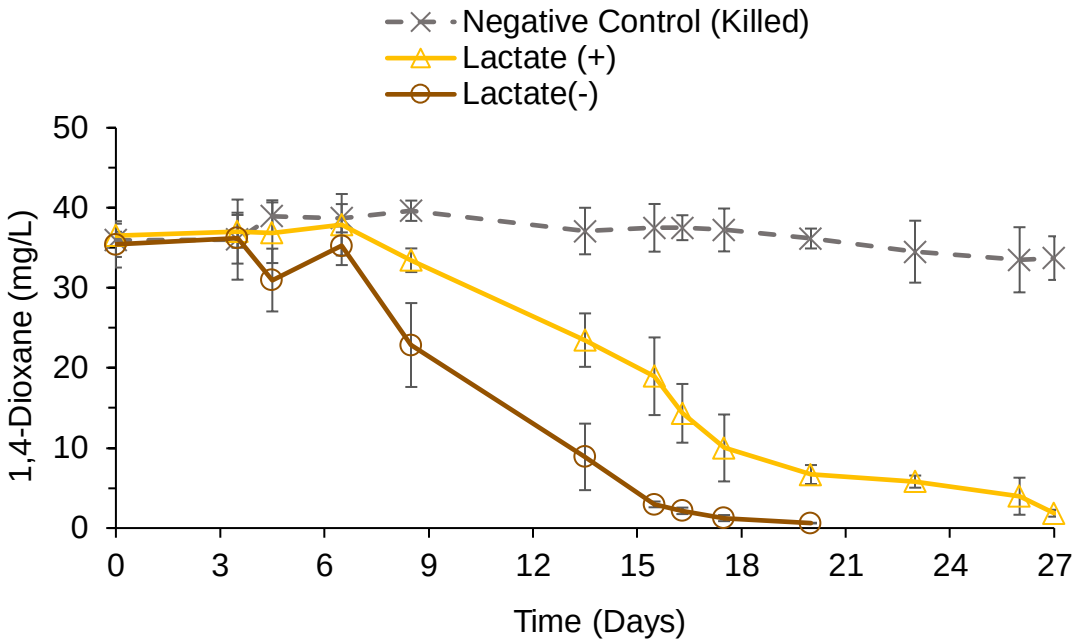

Appendix Figure A-14 CB1190 degrades 1,4-dioxane with and without lactate (1 mg/L) and an anaerobic incubation period

The anaerobic phase was 3.5 days and is indicated by the shaded grey area. 1,4-dioxane biodegradation was slightly delayed between bottles amended with lactate and those without lactate. However, 1,4-dioxane was still successfully degraded in the bottles with lactate. Error bars indicate standard deviation of 6 replicates.

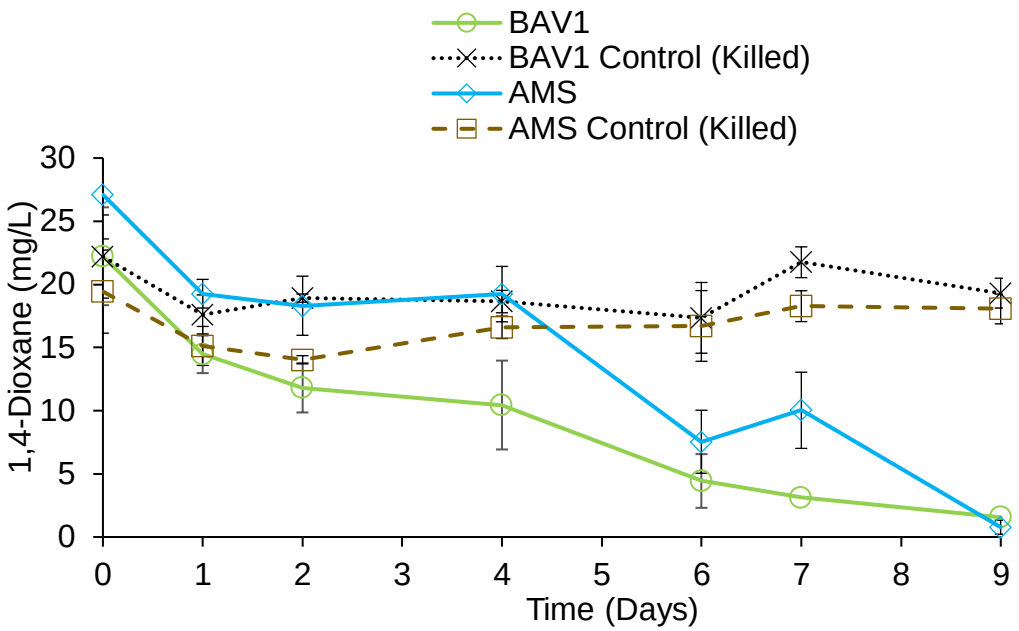

Appendix Figure A-15 1,4-Dioxane degradation by CB1190 grown in aerobic ammonium mineral salts medium (AMS) and BAV1 medium
There were no significant differences in 1,4-dioxane biodegradation when CB1190 was grown in AMS (9) or modified BAV1.(1) Error bars indicate standard deviation of 6 replicates.

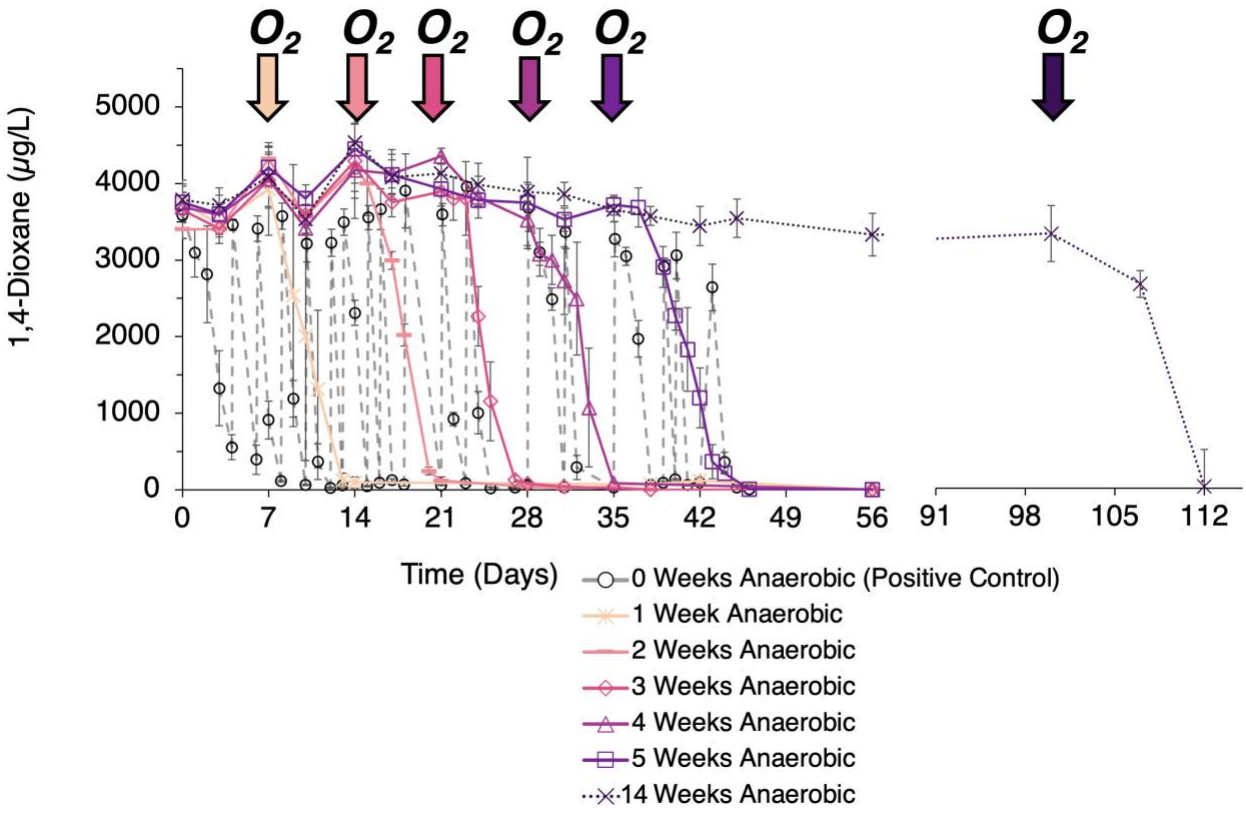

Appendix Figure A-16 CB1190 biodegrades dioxane after 100 days of anaerobic incubation
CB1190 was kept under anaerobic conditions for 100 days after which filtered high purity oxygen was amended and dioxane biodegradation was tracked. Error bars indicate the standard deviation of triplicates.

A-7 References

(1) Cole, J.R., A.L. Cascarelli, W.W. Mohn, and J.M. Tiedje. Isolation and Characterization of a Novel Bacterium Growing Via Reductive Dehalogenation of 2-Chlorophenol. Appl. Environ. Microbiol., 1994, 60, 3536-3542.

(2) Brysch, K., C. Schneider, G. Fuchs, and F. Widdel. Lithoautotrophic Growth of Sulfate-Reducing Bacteria, and Description of *Desulfobacterium autotrophicum* Gen. Nov., Sp. Nov. Arch. Microbiol., 1987, 148, 264-274.

(3) Zhang, S., P.B. Gedalanga, and S. Mahendra. Biodegradation Kinetics of 1,4-Dioxane in Chlorinated Solvent Mixtures. Environ. Sci. & Technol., 2016, 50, 9599-9607.

(4) Ritalahti, K.M., B.K. Amos, Y. Sung, Q. Wu, S.S. Koenigsberg, and F.E. Löffler. Quantitative Pcr Targeting 16s Rrna and Reductive Dehalogenase Genes Simultaneously Monitors Multiple *Dehalococcoides* Strains. Appl. Environ. Microbiol., 2006, 72, 2765-2774.

(5) Waller, A.S., R. Krajmalnik-Brown, F.E. Loffler, and E.A. Edwards. Multiple Reductive-Dehalogenase-Homologous Genes Are Simultaneously Transcribed During Dechlorination by *Dehalococcoides*-Containing Cultures. Appl. Environ. Microbiol., 2005, 71, 8257-8264.

(6) Gedalanga, P.B., P. Pornwongthong, R. Mora, S.-Y.D. Chiang, B. Baldwin, D. Ogles, and S. Mahendra. Identification of Biomarker Genes to Predict Biodegradation of 1,4-Dioxane. Appl. Environ. Microbiol., 2014, 80, 3209-3218.

(7) Alvarez-Cohen, L. and L. McCarty, P. Product Toxicity and Cometabolic Competitive Inhibition Modeling of Chloroform and Trichloroethylene Transformation by Methanotrophic Resting Cells. Appl. Environ. Microbiol., 1991, 57, 1031-1037.

(8) Gossett, J.M. Measurement of Henry's Law Constants for C_1 and C_2 Chlorinated Hydrocarbons. Environ. Sci. Technol., 1987, 21, 202-208.

(9) Parales, R.E., J.E. Adamus, N. White, and H.D. May. Dedegradation of 1,4-Dioxane by an Actinomycete in Pure Culture. Appl. Environ. Microbiol., 1994, 60, 4527-4530.

Appendix B:

B-1 Tables and Figures

Table B-1 Trace elements stock solution A for the UCLA modified medium (1 mL stock into 1L medium)

Components	MW	Stock		Final concentration in medium		
		g/l	M	g/l	M	uM
HCl (25% w/w)		10 mL		0.01 ml		
H_3BO_3	61.81	0.006	0.00010	6.00E-06	9.70E-08	0.10
NaOH	39.9	0.5	0.01253	5.00E-04	1.25E-05	12.53
$MnCl_2$-$4H_2O$	197.84	0.1	0.00051	1.00E-04	5.05E-07	0.51
$FeCl_2$-$4H_2O$	198.75	1.5	0.00755	1.50E-03	7.54E-06	7.55
$CoCl_2$-$6H_2O$	237.83	0.19	0.00080	1.90E-04	7.98E-07	0.80
$ZnCl_2$	136.28	0.07	0.00051	7.00E-05	5.13E-07	0.51
$CuCl_2$-$2H_2O$	170.48	0.002	0.00001	2.00E-06	1.17E-08	0.01
$NiCl_2$-$6H_20$	237.69	0.024	0.00010	2.40E-05	1.01E-07	0.10
Na_2MoO_4-$2H_2O$	241.94	0.036	0.00015	3.60E-05	1.49E-07	0.15

Table B-2 Selenium/tungsten stock solution B for the UCLA modified medium

Components	MW	Stock		Final concentration in medium		
		g/l	M	g/l	M	uM
Na_2SeO_4-$5H_2O$	244.94	0.006	0.00002	6.00E-06	2.45E-08	0.02
Na_2WO_4-$5H_2O$	383.88	0.008	0.00002	8.00E-06	2.08E-08	0.02

Table B-3 Sequences of oligonucleotide prime

Primers	Sequence	Reference
Universal 16S for Universal 16S rev	5'-ATGGCTGTCGTCAGCT-3' 5'-ACGGGCGGTGTGTAC-3'	(1)
dxmB for *dxmB* rev	5'-ACTTCTTAGAGGGACTATTGGCG-3' 5'-CCTTGTTACGACTTCTCCTTCCT-3'	(2)
aldH for *aldH* rev	5'-GCCGACGCTTTTAGCAGATG-3' 5'-TCATTAACGGCAGCAAACGC-3'	(2)
rpoD for *rpoD* rev	5'-GGGCGAAGAAGGAAATGGTC-3' 5'-CAGGTGGCGTAGGTGGAGAA-3'	(3)
CB-*etnA* for CB-*etnA* rev	5'-TGCCCACTGTCATGAACTCC-3' 5'-TAGTAGTGGAAGGGCCACGA-3'	This Study
CB-*etnB* for CB-*etnB* rev	5'-TCGTGGCCCTTCCACTACTA-3' 5'-ACTCCGGCGAGCAATAGAAC-3'	This Study
CB-*etnC* for CB-*entC* rev	5'-CTCCAGGTCGTCGTTGAGAC-3' 5'-TACAGAAGTGTCGCGTAGCC-3'	This Study
CB-*entD* for CB-*etnD* rev	5'-AGCAGATCATGGGCGACTAC-3' 5'-AGGATGGTGTTCGTGAAGGC-3'	This Study
CB-*dioxyA* for CB-*dioxyA* rev	5'-GAACGACTCGGCTCTCACTC-3' 5'-ATGACTTCTGGATCGGCTGC-3'	This Study
CB-*dioxyB* for CB-*dioxyB* rev	5'-CGATCATCACCCAGCCTGAA-3' 5'-GGACGAACCTGTCGAACTCA-3'	This Study
CB-*dioxyC* for CB-*dioxyC* rev	5'-CAGGAACTCAGCCAGTCACC-3' 5'-TGCTGGATCAGACGTTGTGG-3'	This Study
CB-*dioxyD* for CB-*dioxyD* rev	5'-TCACTCAGGCCTCATCGAGC-3' 5'-AGGGGAAGCTATGACCTCGT-3'	This Study
CB-*dioxyE* for CB-*dioxyE* rev	5'-ATCACTCAGGCCTCATCGAGC-3' 5'-CAGGGGAAGCTATGACCTCGT-3'	This Study

Note: CB-*etnABCD* primers were designed based on *Polaromonas* sp. Strain JS666 (4) and then aligned with CB1190's genome. Dioxygenase (CB-*dioxy*ABCDE) primers target the extradiol ring-cleavage dioxygenase class II proteins or the phthalate 3,4-dioxygenase ferredoxin subunit.

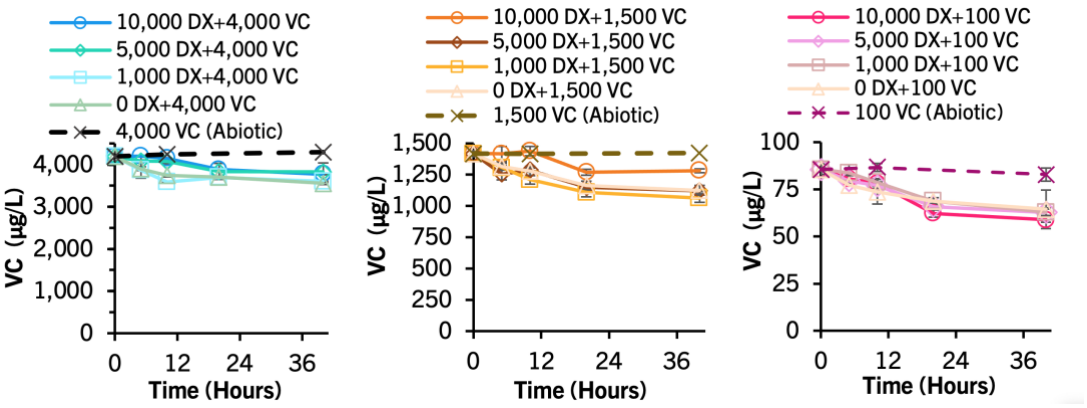

Appendix Figure B-1 VC biodegradation by CB1190 in the presence of 10,000 µg/L DX, 5,000 µg/L DX, 1,000 µg/L DX, and 0 µg/L DX
Error bars indicate the standard deviation of triplicates

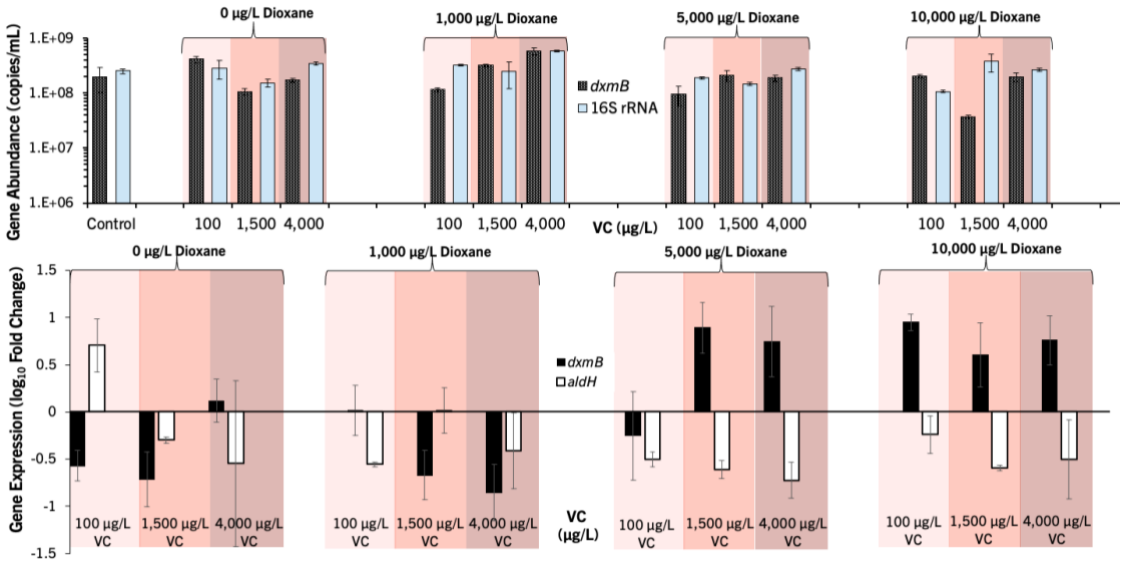

Appendix Figure B-2 CB1190 gene abundance and expression in the presence of varying VC and DX concentrations

The VC concentrations tested included: 0 µg/L, 100 µg/L, 1,500 µg/L, or 4,000 µg/L and the DX concentrations tested included: 0 µg/L, 1,000 µg/L, 5,000 µg/L, or 10,000 µg/L. 4A). CB1190 gene abundance was measured by the 16S rRNA and *dxmB* gene targets at hour 20. Compared to the control (killed), CB1190's gene abundance did not significantly decrease with increasing VC concentrations. Error bars indicate the standard deviation of triplicates. 4B). CB1190 *dxmB* and *aldH* gene expression after DX and VC exposure. *dxmB* and *aldH* regulation did not increase with increasing VC concentrations. However, *dxmB* did increase with increasing DX concentrations. The *aldH* gene target did not increase with increasing DX concentrations likely because samples were taken before sufficient DX intermediates were produced and degraded. All cDNA copy numbers were first normalized to *rpoD* housekeeping gene and then to gene target concentrations at hour 10. Error bars indicate the range of duplicates.

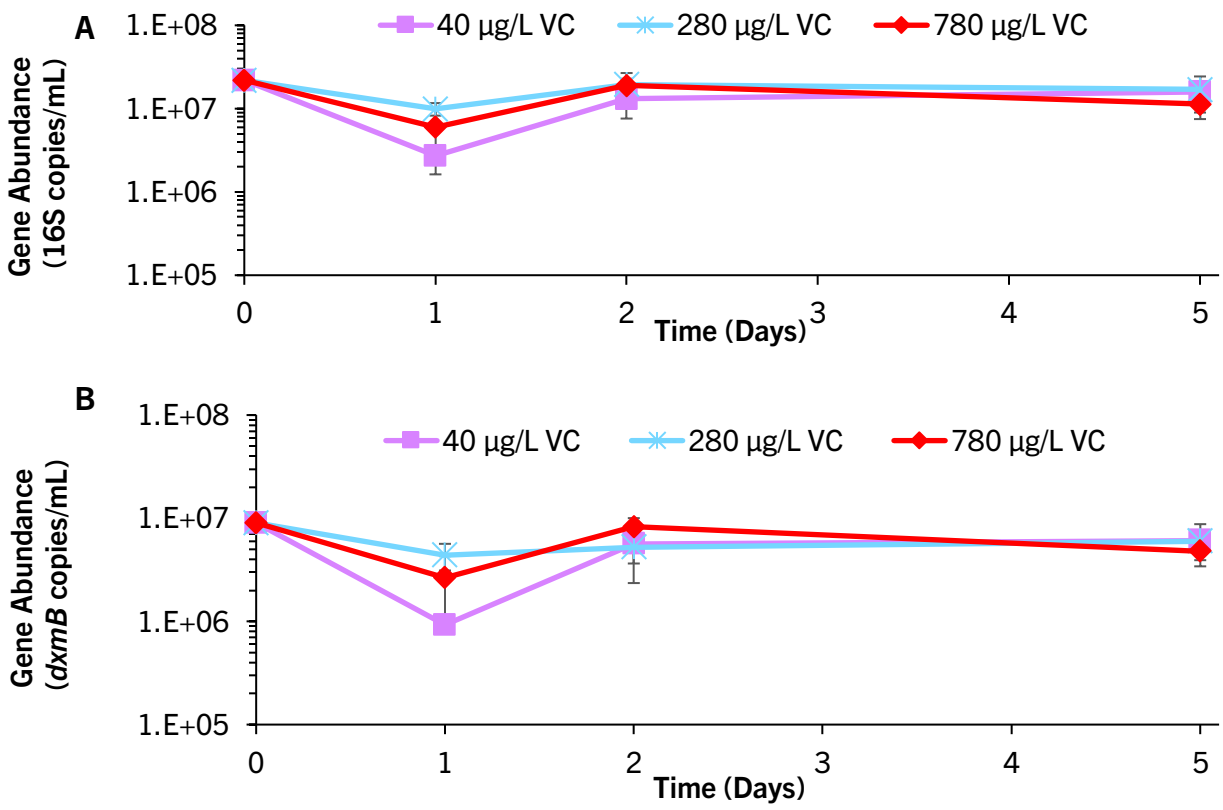

Appendix Figure B-3 CB1190 gene abundance in the presence of only VC. 3A). Gene abundance as measured by the gene target 16S rRNA during VC biodegradation. 3B). Gene abundance as measured by the dxmB gene target during VC biodegradation. Error bars indicate the standard deviation of triplicates.

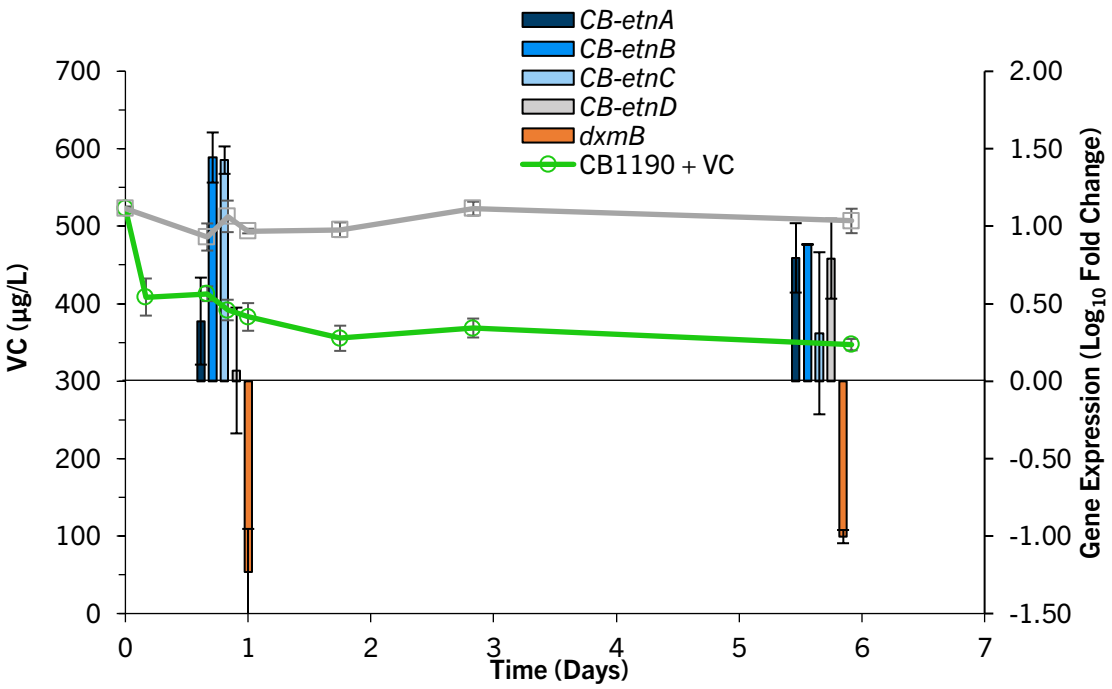

Appendix Figure B-4 VC Biodegradation by CB1190 and gene expression of alkene monooxygenase gene targets

All cDNA copy numbers were first normalized to the *rpoD* housekeeping gene and then to gene target concentrations on either day 1 or day 6. Error bars indicate the standard deviation of triplicates. During VC biodegradation CB1190 upregulated *etnA*, *etnB*, *etnC*, and *etnD* but significantly down regulated the *dxmB* gene target.

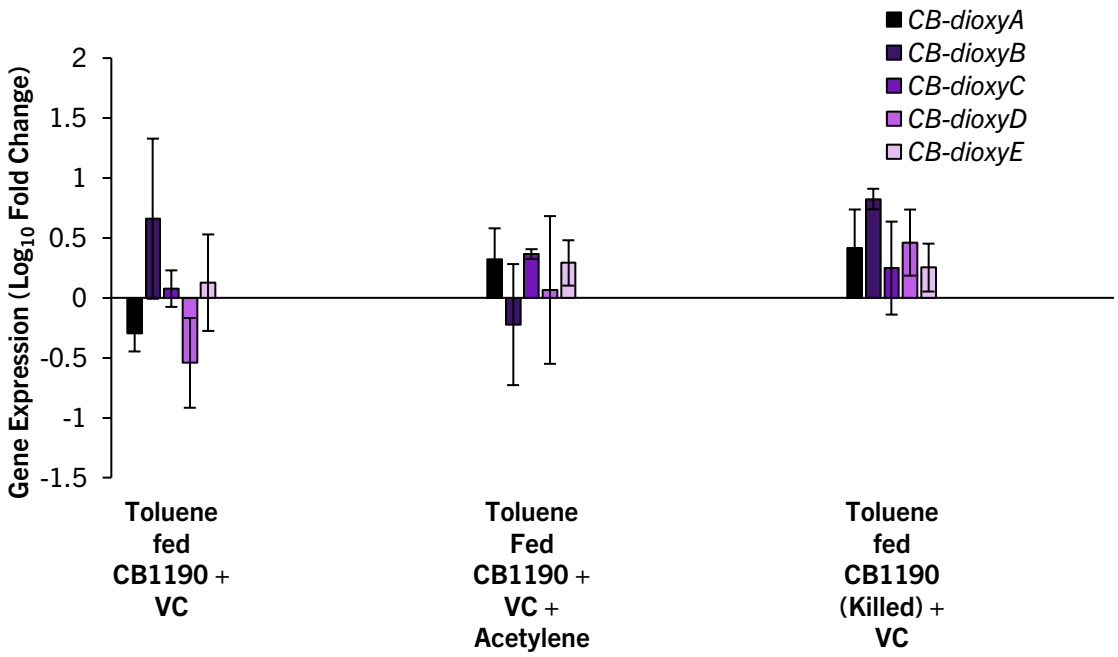

Appendix Figure B-5 Dioxygenase gene target expression in CB1190 cells grown on toluene and exposed to VC

All cDNA copy numbers were first normalized to the *rpoD* housekeeping gene and then to gene target concentrations on day 6.9. Error bars indicate the range of duplicates.

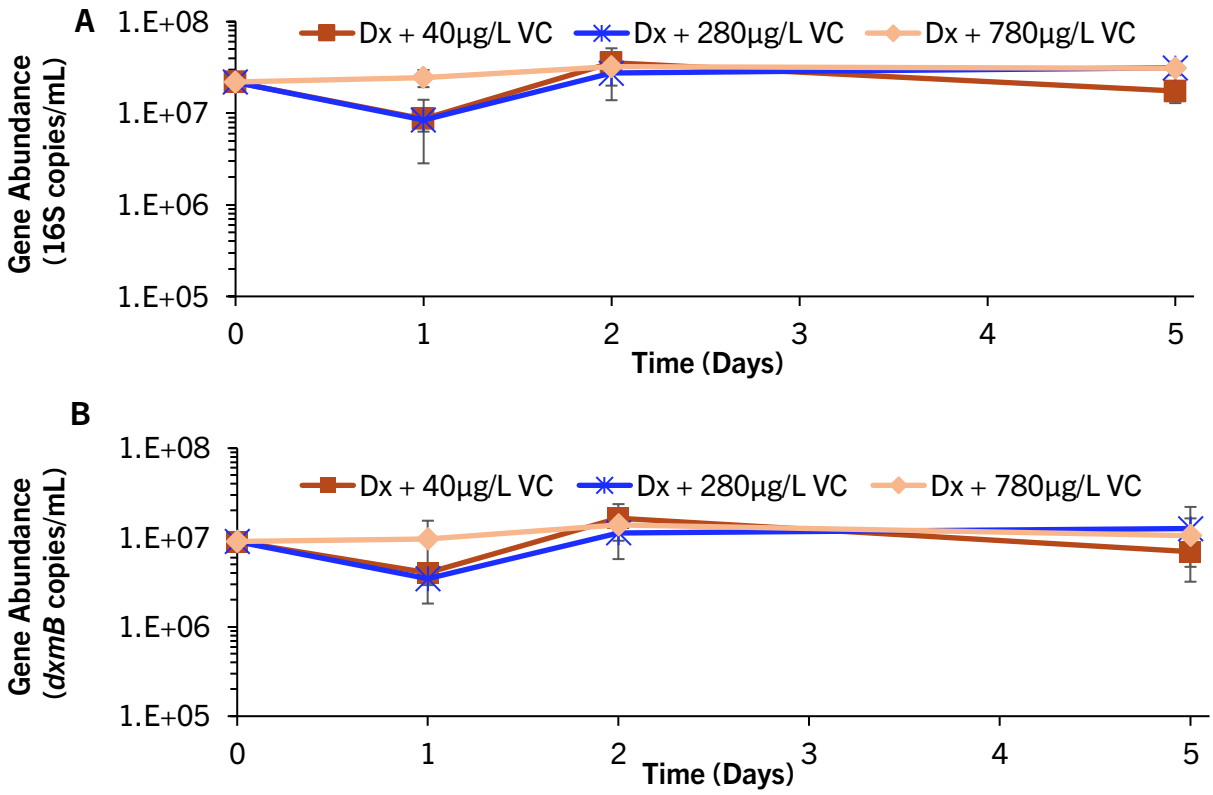

Appendix Figure B-6 CB1190 gene abundance in the presence of DX and VC. A). Gene abundance as measured by the 16S rRNA gene target during VC and DX biodegradation. B). Gene abundance as measured by the *dxmB* gene target during VC and DX biodegradation. Error bars indicate the standard deviation of triplicates

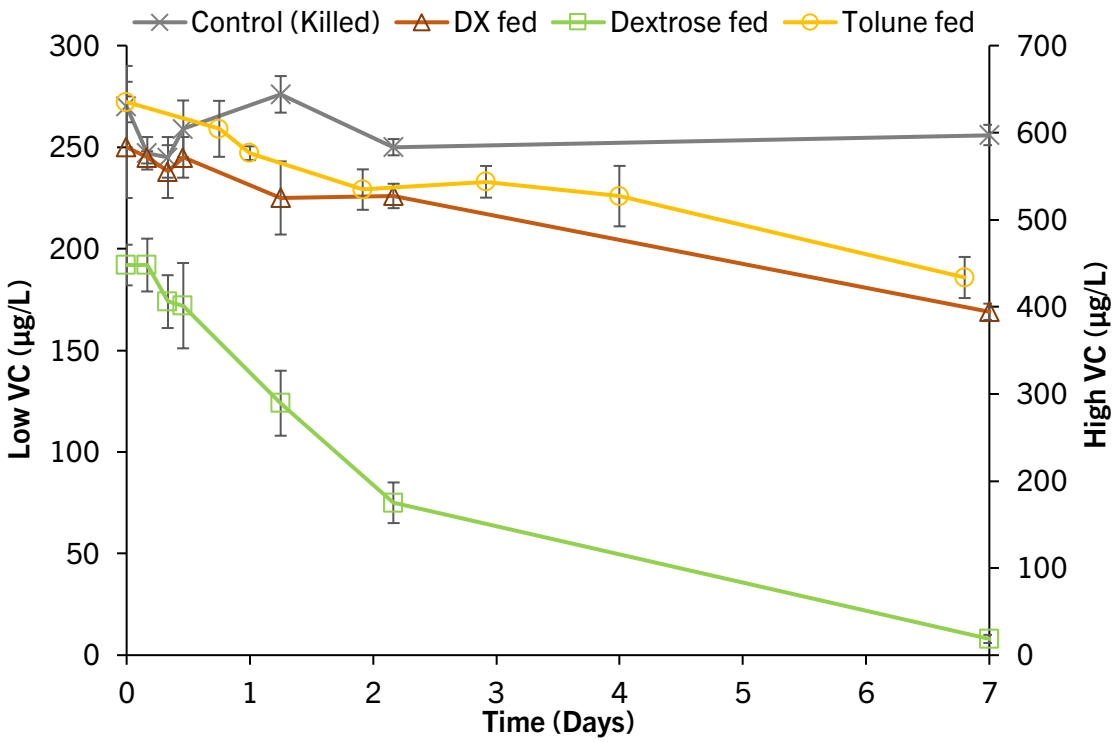

Appendix Figure B-7 Biodegradation of VC by CB1190 cells grown on DX, dextrose, or toluene

CB1190 cells grown on DX, dextrose, or toluene were able to biodegrade VC. Toluene fed cells were amended with 600 µg/L VC whereas, DX and dextrose fed cells were amended with approximately 200 µg/L VC. Error bars indicate standard deviation of triplicates.

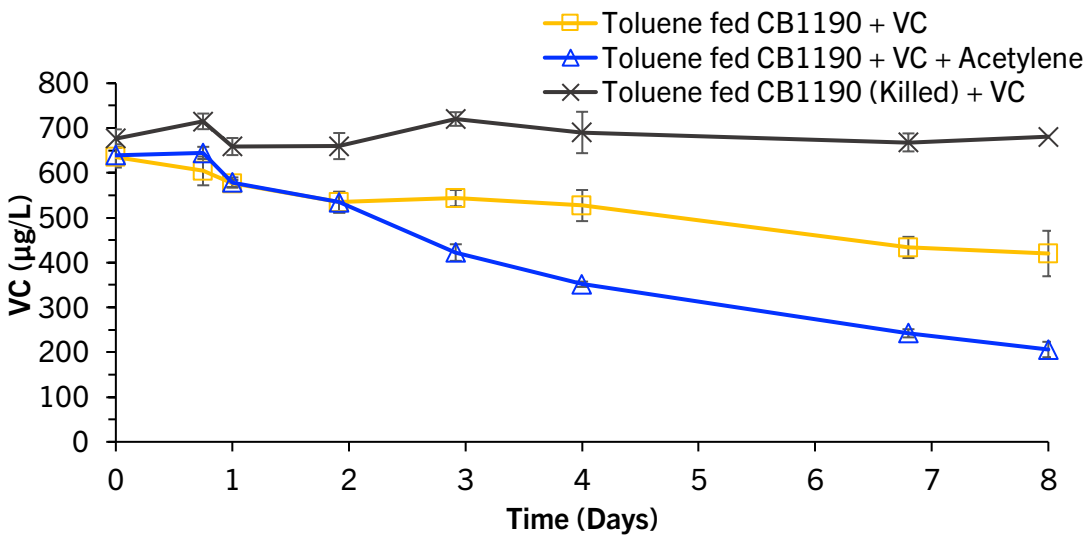

Appendix Figure B-8 CB1190 biodegrades VC after being grown on toluene Acetylene was amended to bottles containing CB1190 and incubated for 30 minutes. Subsequently, the acetylene was flushed out with filtered air and then VC was amended. Error bars indicate the standard deviation of triplicates.

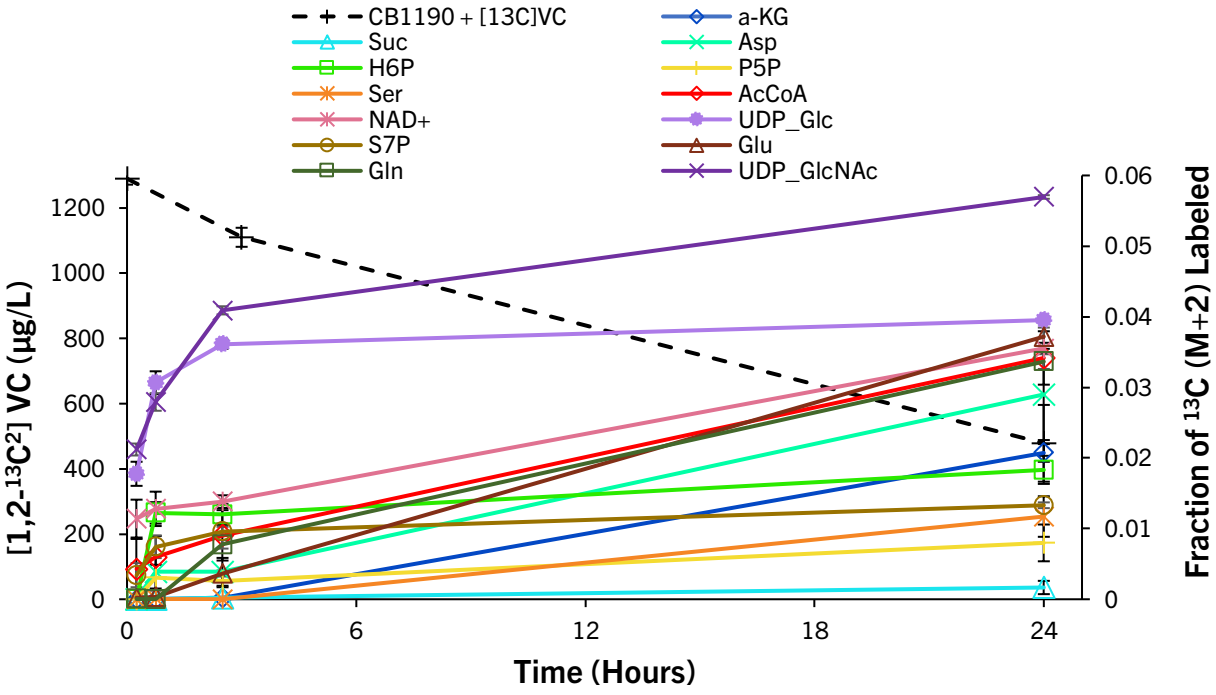

Appendix Figure B-9 Fraction of 1,2-13C2 VC (M+2) labeled in CB1190 over time. Metabolites associated with growth and containing two 13C atoms increased as CB1190 biodegraded 1,2-13C2 VC. Error bars represent standard deviation of triplicates. Metabolite abbreviations correspond to the following: a-KG = alpha-ketoglutarate; Suc = Succinate; Asp = Aspartate; H6P = Hexose-6-phosphate; P5P = Pentose-5-phosphate; Ser = Serine; AcCoA = Acetyl-CoA; NAD+ = Nicotinamide adenine dinucleotide; UDP_Glc = UDP-glucose; S7P = Sedoheptulose-7-phosphate; Glu = Glutamate; Gln = Glutamine; UDP_GlcNAc = UDP-N-acetyl-glucosamine

B-2 References

(1) Amann, R.I., W. Ludwig, and K.H. Schleifer. Phylogenetic Identification and in Situ Detection of Individual Microbial Cells without Cultivation. Microbiol Rev, 1995, 59, 143-169.

(2) Gedalanga, P.B., P. Pornwongthong, R. Mora, S.-Y.D. Chiang, B. Baldwin, D. Ogles, and S. Mahendra. Identification of Biomarker Genes to Predict Biodegradation of 1,4-Dioxane. Appl. Environ. Microbiol., 2014, 80, 3209-3218.

(3) Sales, C.M., A. Grostern, J.V. Parales, R.E. Parales, and L. Alvarez-Cohen. Oxidation of the Cyclic Ethers 1,4-Dioxane and Tetrahydrofuran by a Monooxygenase in Two *Pseudonocardia* Species. Appl. and Environ. Microbiol., 2013, 79, 7702-7708.

(4) Mattes, T.E., A.K. Alexander, P.M. Richardson, A.C. Munk, C.S. Han, P. Stothard, and N.V. Coleman. The Genome of *Polaromonas* sp. Strain JS666: Insights into the Evolution of a Hydrocarbon- and Xenobiotic-Degrading Bacterium, and Features of Relevance to Biotechnology. Appl. Environ. Microbiol., 2008, 74, 6405-6416.

Appendix C:

C-1 Description of Coated Silicone Foley Catheters

Clinical isolate experiments were carried out using 1-inch segments of silicone Foley catheters or silicone Foley catheters coated with a zwitterionic compound comprised of polysulfobetaine moieties (provided by UCLA Chemistry Department). This coating created a more hydrophilic surface, which is believed to better resist microbial adhesion as it imposes an increased energy barrier. All catheters had 16 French diameters and the drainage port and balloon were avoided due to uneven surface area and material composition (Appendix Figure C-1). The segments were cut and trimmed under sterile conditions in a biosafety cabinet with 70% ethanol.

Appendix Figure C-1 Photo of silicone catheter used in biofilm adhesion experiments

C-2 Preparation of Clinical Trials

Axenic strains were previously isolated from urine preserved in boric acid by UCLA Department of Pathology and Laboratory Medicine. Those were identified as Staphylococcus aureus, methicillin resistant-Staphylococcus aureus (MRSA), Pseudomonas aeruginosa, and Candida albicans. 1µL of the liquid urine sample was plated onto blood or MacConkey agar, incubated at 35°C for 24-48 hours and then examined for specific colonies. Isolates were sub-cultured with a 1% (v/v) transfer into LB broth at 37°C with 120 rpm shaking. Once the cultures reached early stationary phase (Approximate Optical Density (OD) measured at 600 nm = 2)), they were diluted to an OD = 0.1 and transferred to experimental vials.

C-3 Total Nucleic Acids Extraction and qPCR

For cell density measurements, 500 µL liquid samples were collected during incubation, with cells harvested via centrifugation (21,000 x g, 10 min at 4 °C) and the supernatant was discarded. Cells were lysed by adding 250 µL of lysis buffer (50 mM sodium acetate, 10 mM EDTA [pH 5.1]), 100 µL 10% sodium dodecyl sulfate, 1.0 mL pH 8.0 buffer-equilibrated phenol, and 1 g of 100 µm-diameter zirconia−silica beads (Biospec Products, Bartlesville, OK), followed by heating at 65°C for 2 min, bead beating for 2 min with a Mini-Beadbeater (Biospec Products, Bartlesville, OK), incubating for 8 min at 65°C, and bead beating again for 2 minutes. The lysate was collected by centrifugation at 13000 g for 5 min, followed by phenol−chloroform−isoamyl alcohol purification (1 volume) and chloroform−isoamyl alcohol

purification (1 volume). Precipitation of total nucleic acids was performed by the addition of 3 M sodium acetate (0.1 volume) and isopropanol (1 volume) followed by incubation at −20°C overnight. Nucleic acid pellets were collected by centrifugation at 4°C for 30 min at 20000 g. The precipitate was washed with 70% ethanol and resuspended in 100 μL DNase- and RNase-free water. The purity of DNA and RNA were determined by a Nanodrop 2000C spectrophotometer (Thermo Scientific, Wilmington, DE). All reactions were run on a StepOnePlus thermocycler (Life Technologies, Carlsbad, CA) using a total volume of 20 μL containing 1× Luminaris Color HiGreen−HiROX qPCR Master Mix (Thermo Scientific, Waltham, MA), 0.3 μM primers, and 2.5 μL of DNA (1−10 ng/μL) template. The cycling parameters to amplify the 16S rRNA gene fragment included sample holds at 95°C for 10 min, followed by 40 cycles of 95°C for 15 s and 60°C for 60 s. The cycling parameters to amplify the 18S rRNA gene fragment included sample holds at 95°C for 5 min, followed by 45 cycles of 95°C for 10 s and 56°C for 30 s and 72°C for 15 s. All reactions were accompanied by a melt curve analysis to confirm the specificity of qPCR products. Melt-curve analyses that were within the ranges of 81.7°C (16S rRNA) and 84.3°C (18S rRNA) were considered specific to each target gene. C_T values of 45 or higher were labeled as undetermined. Primer sequences are listed below in Appendix Figure C-1.

Table 6-4 Sequences of oligonucleotide primers used in this study

Primers	Sequence	Reference
Universal 16S for	5’-ATGGCTGTCGTCAGCT-3’	(1)
Universal 16S rev	5’-ACGGGCGGTGTGTAC-3’	
18S for	5’-ACTTCTTAGAGGGACTATTGGCG-3’	(2)
18S rev	5’-CCTTGTTACGACTTCTCCTTCCT-3’	

C-4 Results and Discussion

Clinical Isolate Undiluted, 10x Diluted, and 100x Diluted, qPCR Results

In order to test whether qPCR would be sufficient for samples with lower quantities of nucleic acids, samples were diluted 10-fold and 100-fold and measured via qPCR in addition to the undiluted samples. The C_T results are shown in Appendix Figure C-2.

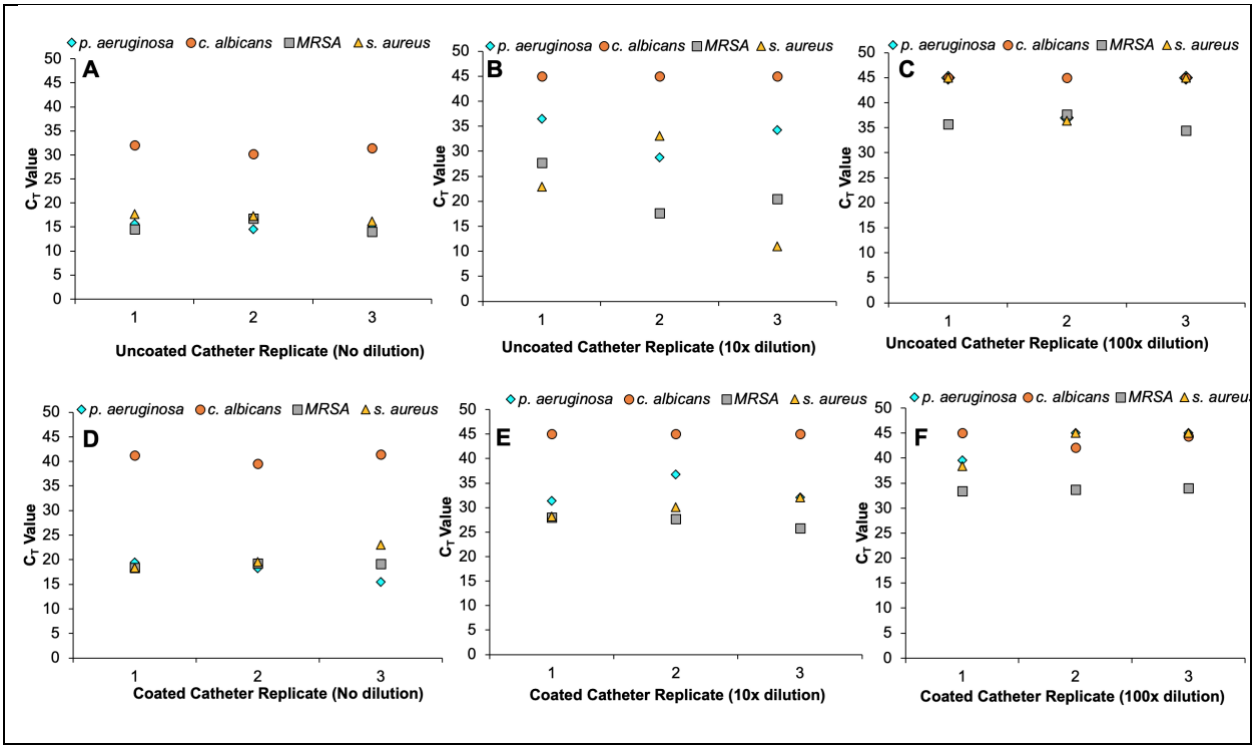

Appendix Figure C-2 Bacterial or fungal gene abundance adhered to catheters and represented as CT values
A). Uncoated catheter with no sample dilution B). Uncoated catheter with 10x sample dilution C). Uncoated catheter with 100x sample dilution D). Coated catheter with no sample dilution E). Coated catheter with 10x sample dilution F). Coated catheter with 100x sample dilution.

C-5 Overview of Biofilm Quantification Methods

In this study, four methods based on different biological and chemical parameters were evaluated in regard to their ability to quantify bacterial biofilm bound to catheter surfaces. Each method was able to detect and quantify bacterial/fungal cells, biofilm matrices and differences in catheter performance. Additionally, cost and time for each assay were taken into account as this

can be a limiting factor for many research and clinical institutions. Cost was estimated using the list prices from Thermo Fisher Scientific (Periodic Acid-Schiff, Modified Lowry Protein, qPCR) and Promega (BacTiter-Glo). Average time was based on the reaction time of the reagents for each method and did not take into account the time of labor due to the fact that this may vary depending upon experience and access to multichannel pipettors. These features are summarized in Table 6-5.

Table 6-5 Summary of biofilm quantification methods

	Measurement of		**Information on**			**Considered**		
Method	Cells	Biofilm	Ability to grow	Metabolic activity	Membrane integrity	Time (hrs) *	Costs **	Assay Target
Modified Lowry Protein Assay	✓	✓	No	No	No	0.7	$0.08	Protein
BacTiter-Glo™	✓		Yes	Yes	No	0.1	$0.36	ATP
Periodic-Schiff Assay		✓	No	No	No	24	$0.33	Poly-sacchrides
qPCR	✓	✓	No	No	No	2	$0.81	Nucleic Acids
Notes:	*Time calculated based on reaction time for reagents until results are obtained. Time for instrumental analysis also included for 96-well plate. **Material cost based on list price from vendor for reagents and are calculated as cost per well.							

C-6 Raw Values from Biofilm Quantification Assays

The averages and standard deviations for each assay are provided below (Table 6-6).

Table 6-6 Summary of raw data from biofilm quantification methods

qPCR (undiluted)				
	Average (16S or 18S copies/mL)	**Standard Deviation (16S or 18S copies/mL)**	**Average (16S or 18S C_T value)**	**Standard Deviation (16S or 18S C_T value**
P. aeruginosa Uncoated	1.64E+11	5.40E+10	15.13	0.22
P. aeruginosa Coated	1.48E+10	4.84E+09	17.73	2.70
C. albicans Uncoated	1.34E+08	7.54E+07	31.12	0.90
C. albicans Coated	2.18E+06	1.77E+06	40.72	1.02
MRSA Uncoated	1.93E+11	1.02E+11	15.10	1.49
MRSA Coated	1.42E+10	3.58E+09	18.90	0.13
S. aureus Uncoated	5.10E+10	2.28E+10	17.04	0.44
S. aureus Coated	1.03E+10	7.94E+09	20.29	4.04

Modified Lowry Total Protein Assay		
	Average total protein (mg/L)	**Standard Deviation (mg/L)**
P. aeruginosa Uncoated	148	14.8
P. aeruginosa Coated	99	21.6
C. albicans Uncoated	152	39.4
C. albicans Coated	124	23.4
MRSA Uncoated	109	11.9
MRSA Coated	98	6.8
S. aureus Uncoated	176	19.6
S. aureus Coated	152	20.9

ATP Assay		
	Average ATP (mg/L)	**Standard Deviation (mg/L)**
P. aeruginosa Uncoated	6.88	2.44
P. aeruginosa Coated	2.87	1.22
C. albicans Uncoated	1.77	0.45
C. albicans Coated	0.81	0.13
MRSA Uncoated	2.93	0.70
MRSA Coated	1.41	0.61
S. aureus Uncoated	4.68	2.40
S. aureus Coated	1.27	1.11

Periodic Acid-Schiff Carbohydrate Assay		
	Average (mg equivalent dextran/L)	**Standard Deviation (mg equivalent dextran/L)**
P. aeruginosa Uncoated	3,411	505
P. aeruginosa Coated	2,511	417
C. albicans Uncoated	2,189	386
C. albicans Coated	667	352
MRSA Uncoated	1,122	135
MRSA Coated	411	126
S. aureus Uncoated	3,022	839
S. aureus Coated	1,333	252

Values reported as averages and standard deviation of experimental triplicates.

C-7 References

(1) Amann, R.I., W. Ludwig, and K.H. Schleifer. Phylogenetic Identification and in Situ Detection of Individual Microbial Cells without Cultivation. Microbiol. Rev., **1995**, 59, 143-169.

(2) Fu, L., X. Cui, Y. Li, L. Xu, C. Zhang, R. Xiong, D. Zhou, and J.C. Crittenden. Excessive Phosphorus Enhances *Chlorella regularis* Lipid Production under Nitrogen Starvation Stress During Glucose Heterotrophic Cultivation. Chem. Eng. J., **2017**, 330, 566-572.